

For Reference

NOT TO BE TAKEN FROM THIS ROOM

Ex LIBRIS
UNIVERSITATIS
ALBERTAENSIS





Digitized by the Internet Archive
in 2019 with funding from
University of Alberta Libraries

<https://archive.org/details/Lee1977>

THE UNIVERSITY OF ALBERTA

RELEASE FORM

NAME OF AUTHOR: SHU KAY JOSEPH LEE

TITLE OF THESIS: MULTILAYER GRAVITY INVERSION

USING FOURIER TRANSFORMS

DEGREE FOR WHICH THESIS WAS PRESENTED: Master of Science

YEAR THIS DEGREE GRANTED: 1977

Permission is hereby granted to the UNIVERSITY OF ALBERTA LIBRARY to reproduce single copies of this thesis and to lend or sell such copies for private, scholarly or scientific research purposes only.

The author reserves other publication rights, and neither the thesis nor extensive extracts from it may be printed or otherwise reproduced without the author's written permission.

THE UNIVERSITY OF ALBERTA

MULTILAYER GRAVITY INVERSION
USING FOURIER TRANSFORMS

by



SHU KAY JOSEPH LEE

A THESIS

SUBMITTED TO THE FACULTY OF GRADUATE STUDIES AND RESEARCH
IN PARTIAL FULFILMENT OF THE REQUIREMENTS FOR THE DEGREE
OF MASTER OF SCIENCE

DEPARTMENT OF PHYSICS

EDMONTON, ALBERTA

FALL, 1977

THE UNIVERSITY OF ALBERTA
FACULTY OF GRADUATE STUDIES AND RESEARCH

The undersigned certify that they have read, and recommend to the Faculty of Graduate Studies and Research, for acceptance, a thesis entitled MULTILAYER GRAVITY INVERSION USING FOURIER TRANSFORMS submitted by SHU KAY JOSEPH LEE in partial fulfilment of the requirements for the degree of Master of Science in Physics.

DEDICATION

This thesis is dedicated to my mother, Yee-mui Lee, and my wife, Julia.

ABSTRACT

A Fourier transform technique for inverting gravity data has been developed to yield a two dimensional multilayer density profile. The method extends an algorithm originally developed by Parker (1972) and Oldenburg (1974). This multilayer inversion scheme requires an initial starting model from a seismically determined model and allows for lateral variation of density and thickness within each stratum. The inversion procedure is used to study the crustal structure of the southern plains of Western Canada and the resulting inversion models are in reasonable agreement with additional independant seismic models. It is shown that the algorithm may be rearranged to find the density distribution of a near surface slab in order to fit the residual gravity anomaly. This appears to be a valuable tool for interpreting shallow features responsible for the short wavelength components in the Fourier transform of a gravity profile. The density distribution at the top of the Precambrian crustal basement across the Churchill-Superior provinces has been computed and it appears to be useful in interpreting the position of the boundary.

ACKNOWLEDGMENTS

With sincere appreciation, I wish to thank Dr. E.R. Kanasewich who initially proposed the project to me. His counsel, work and encouragement have been indispensable throughout the entire programme.

Dr. G.L. Cumming was very kind to allow me to take part in the gravity survey. I am indebted to him for many useful suggestions.

Dr. D.W. Oldenburg was very generous to allow me to use his computer programs. His advice has been very helpful and is much appreciated.

Mr. McCloughan did an exceptionally fine job in making the gravity survey and the data reduction.

Dominion Observatory, Department of Energy, Mines and Resources, provided us with the LaCoste and Romberg gravimeter. Their cooperation is gratefully acknowledged.

I also wish to thank the Gulf Research and Development Company to allow us to access its confidential magnetic maps.

During the course of his research, the author was supported by a Graduate Teaching Assistantship from the Department of Physics, University of Alberta.

TABLE OF CONTENTS

	<u>Page</u>
ABSTRACT	iv
ACKNOWLEDGMENTS	v
TABLE OF CONTENTS	vi
LIST OF TABLES	vii
LIST OF FIGURES	viii
CHAPTER 1. Introduction	1
1.1 Previous Work	1
1.2 Parker-Oldenburg Algorithm	3
1.3 Filtering	6
CHAPTER 2. Multilayer Gravity Inversion Method	9
2.1 Extension of Oldenburg Inversion Algorithm	9
2.2 The Multilayer Inversion Scheme	13
2.3 Oldenburg's Cosine Model	16
2.4 Multilayer Numerical Example	23
CHAPTER 3. Geology and Geophysics of The Area	27
3.1 Geological Background	27
3.2 Regional Geology and Geophysics	29
3.3 Seismic Data	33
CHAPTER 4. Inversion Models of Western Canada	38
4.1 Source of Data	38
4.2 Crustal Models	41
4.3 Inversion of Profile (1)	45
4.4 Inversion of Profile (2)	76
4.5 Inversion of Residual Gravity for Density .	89
4.6 Interpretation	93
4.7 Conclusions	100
BIBLIOGRAPHY	103
APPENDIX A Derivation of Parker Algorithm	107
APPENDIX B Convergence criteria of the Parker- Oldenburg Algorithm	112
APPENDIX C Magnetic Map of Southern Saskatchewan	117
APPENDIX D Computer Programs	118

LIST OF TABLES

Table	Description	Page
I	Crustal Model of Suffield-Swift Current	35
II	Crustal Model around Winnipeg area	36
III	Inversion parameters of Suffield-Swift Current gravity profile	47
IV	Inversion parameters of Swift Current- Winnipeg gravity profile	62
V	Inversion parameters of Elbow-Lake Winnipeg gravity profile	78

LIST OF FIGURES

Figure		Page
1.1	Subsurface configuration	5
2.1	Schematic representation of the multilayer inversion procedure.	15
2.2	Two-dimensional cosine model and its gravity anomaly.	17
2.3	Inversion model obtained from the offset gravity anomaly (-84 mgal) of the Cosine model.	22
2.4	Inversion model obtained from the offset gravity anomaly (-126 mgal) of the Cosine model.	22
2.5	Inversion model obtained from the offset gravity anomaly (-126 mgal) of the Cosine model; with $k = 0.125$ and $k = 0.25$.	22
2.6	Difference between observed gravity and gravity calculated from inversion models shown in Fig. 2.3, Fig. 2.4, and Fig. 2.5.	22
2.7	Four-layer numerical model, composed of three concentric triangular prisms.	25
2.8	Original gravity and gravity computed from the inversion model of the four-layer numerical model.	25
2.9	Comparison of the inverted shape and the original shape of the four-layer model.	25
2.10	Difference between observed gravity and inverted gravity of the four-layer model.	25
2.11	Difference between inverted topography and original topography of the four-layer model.	26
3.1	Gravity map of the southern plains of Saskatchewan and Manitoba; showing locations of the two gravity profiles, and area of detail gravity survey.	28
4.1	Detail gravity map of southern Saskatchewan	40

Figure		Page
4.2	Crustal Models I, II, III and IV.	43
4.3	Gravitational observations of the Swift Current-Suffield profile.	49
4.4	Reduced gravitational observations of the Swift Current-Suffield profile.	50
4.5	Inversion model of Swift Current-Suffield profile assuming crustal Model I.	51
4.6	Comparison between observed gravity and gravity calculated from inversion model of Fig. 4.5..	52
4.7	Inversion model of Swift Current-Suffield profile assuming crustal Model II.	53
4.8	Comparison between observed gravity and gravity calculated from inversion model of Figure 4.7.	54
4.9	Inversion model of Swift Current-Suffield profile assuming crustal Model III.	55
4.10	Comparison between observed gravity and gravity calculated from inversion model of Figure 4.9.	56
4.11	Inversion model of Swift Current-Suffield profile assuming crustal Model IV.	57
4.12	Comparison between observed gravity and gravity calculated from inversion model of Figure 4.11.	58
4.13	Gravitational observation of the Swift Current-Winnipeg profile.	64
4.14	Reduced gravitational observations of the Swift Current-Winnipeg profile.	65
4.15	Inversion model of Swift Current-Winnipeg profile assuming crustal Model I.	66
4.16	Comparison between observed gravity and gravity calculated from inversion of Figure 4.15.	67
4.17	Inversion model of Swift Current-Winnipeg profile assuming crustal Model II.	68

Figure		Page
4.18	Comparison between observed gravity and gravity calculated from inversion model of Figure 4.17.	69
4.19	Inversion model of Swift Current-Winnipeg profile assuming crustal Model III.	70
4.20	Comparison between observed gravity and gravity calculated from inversion model of Figure 4.19.	71
4.21	Inversion model of Swift Current-Winnipeg profile assuming crustal Model IV.	72
4.22	Comparison between observed gravity and gravity calculated from inversion model of Figure 4.21.	73
4.23	Gravitational observation of the Elbow-Lake Winnipeg profile.	79
4.24	Reduced gravitational observations of the Elbow-Lake Winnipeg profile.	80
4.25	Inversion model of Elbow-Lake Winnipeg profile assuming crustal Model I.	81
4.26	Comparison between observed gravity and gravity calculated from inversion model of Figure 4.25.	82
4.27	Inversion model of Elbow-Lake Winnipeg profile assuming crustal Model II.	83
4.28	Comparison between observed gravity and gravity calculated from inversion model of Figure 4.27.	84
4.29	Inversion model of Elbow-Lake Winnipeg profile assuming crustal Model III.	85
4.30	Comparison between observed gravity and gravity calculated from inversion model of Figure 4.29.	86
4.31	Inversion model of Elbow-Lake Winnipeg profile assuming crustal Model IV.	87
4.32	Comparison between observed gravity and gravity calculated from inversion model of Figure 4.31.	88

Figure		Page
4.33	Density profile from inversion of residual gravity of the Swift Current-Winnipeg profile, and comparison of original residual gravity and gravity calculated from the inverted density profile.	92
4.34	Density profile from inversion of residual gravity of the Elbow-Lake Winnipeg profile; and comparison of original residual gravity and gravity calculated from the inverted density profile.	94
4.35	Gravity map of the southern plains of Saskatchewan and Manitoba showing possible loactions of the western limit of the Superior province and the eastern limit of the Churchill province.	103

CHAPTER 1 INTRODUCTION

1.1. Previous work

Many methods have been developed to determine the shape, density distribution and depth of a subsurface body from a measured gravity anomaly. In the thirties and forties with the introduction of use of graticules, dot charts and other similar graphical aids to compute gravitational attraction, attempts were made to perturb an initial starting structure until the gravity calculated matched the observed field. (Skeels, 1947) In theory these methods can be made as precise as one pleases, merely by increasing the scale to which the graticule is constructed, however, in actual practice this may be difficult, if not impossible.

Talwani et al (1959) devised the line-integral method to compute the gravity of a perturbing body. Talwani's inversion scheme involves approximating the cross-sectional shape of the perturbing body by polygons. The residuals between the calculated and observed fields are used to adjust the model parameters: density contrast, shape, and depth. By choosing a sufficient large number of sides for each polygon, the cross-sectional shape of the body can be approximated to any desired accuracy. The main drawback of this method is that the interpreter has to decide what changes to make for the shape of the model. As the shape of most perturbing masses is not known, such changes will bias the final interpretation.

Vening Meinesz and others (1934) proposed the use of rectangular blocks of variable size for the computation of gravity of any irregularly shaped bodies. Bott (1960), Corbato (1965), Tanner (1967), Negi and Garde (1969) approximated the initial model by a set of rectangular prisms of constant density, and calculated its gravitational field. The differences between the calculated and observed fields are used to readjust the heights of these rectangles (Corbato, 1965). This method can be made as precise as one pleases by using a sufficiently large number of small blocks. However, as the number of blocks is increased the computations become increasingly tedious, and the iteration scheme become unstable and converge slowly.

Parker (1972) derived an algorithm to compute gravitational attraction of a three-dimensional source using Fourier transform method. The use of the Fast Fourier Transform or FFT (special issue of IEEE, 1967) resulted in a saving in computation time compared with other methods in the analysis of three-dimensional gravity sources. Parker's three-dimensional scheme can be simplified to obtain two-dimensional gravity profiles.

Oldenburg (1974) rearranged Parker's two-dimensional formula to obtain an iterative procedure to calculate the shape of the surface between two constant density media.

The purpose of this thesis is to expand the Parker-Oldenburg inversion algorithm to many layers, allowing

densities to vary along the length of the gravity profile.

The inversion of two gravity profiles in the southern parts of Manitoba and Saskatchewan is offered as a practical application of this multi-layer inversion scheme (Fig 3.1).

This modified version of the Parker-Oldenburg inversion algorithm is later rearranged to find the density variation of a near surface slab in order to fit the difference between the original gravity and the gravity computed from the inverted topography.

1.2. Parker-Oldenburg Algorithm

The derivation of Parker's (1972) formula was fully discussed in his original paper and subsequently by Hinson (1976). A full discussion of the derivation is presented in Appendix A.

Parker's algorithm for a three-dimensional source with constant density is:

$$F[\Delta g] = -2\pi G d \exp(-|\vec{K}| Z_0) \sum_{n=1}^{\infty} (|\vec{K}|^{n-1}/n!) F[h^n(\vec{r})] \quad (1)$$

where $F[\Delta g]$ is the Fourier transform of the gravitational anomaly, G is the universal gravitational constant, \vec{K} is the wavenumber vector on the x-y plane, \vec{r} is the position vector on the x-y plane from the origin to the source element, d is the density, Z_0 is the distance from the origin to the observation datum plane, and $h(\vec{r})$ is the upper boundary of

the perturbing mass measured from the x-y plane. (See Figure 1.1)

For a two-dimensional source the gravity Δg is now a function of x not \vec{r} , and K is now a scalar not a vector. To obtain Oldenburg's inversion scheme the first term of the infinite sum is transposed and rearranged.

$$F[h(x)] = -\exp(KZ_0) F[\Delta g(x)] / 2\pi G d - \sum_{n=2}^{\infty} (K^{n-1}/n!) F[h^n(x)] \quad (2)$$

Assuming Z_0 and d are known, and $\Delta g(x)$ is given, this expression can be used iteratively to obtain the topography $h(x)$ of the perturbing body. An initial guess of $h(x)$ (even for $h(x)=0$ is satisfactory) is input to the right hand side of the equation (2). The infinite sum is computed until convergence criterion is met. An updated value of $h(x)$ is obtained by taking the inverse Fourier transform of the right hand side of equation (2). This updated version of $h(x)$ is then put back in the right hand side of equation (2) and the iterative procedure is continued until some convergence requirement is met or a maximum number of iterations has been performed.

The conditions necessary for convergence and the convergence criteria of the infinite series and the iterative procedure were both discussed in detail by Parker (1972) and Oldenburg (1974). They are not going to be repeated here. However, a summary is presented in appendix B.

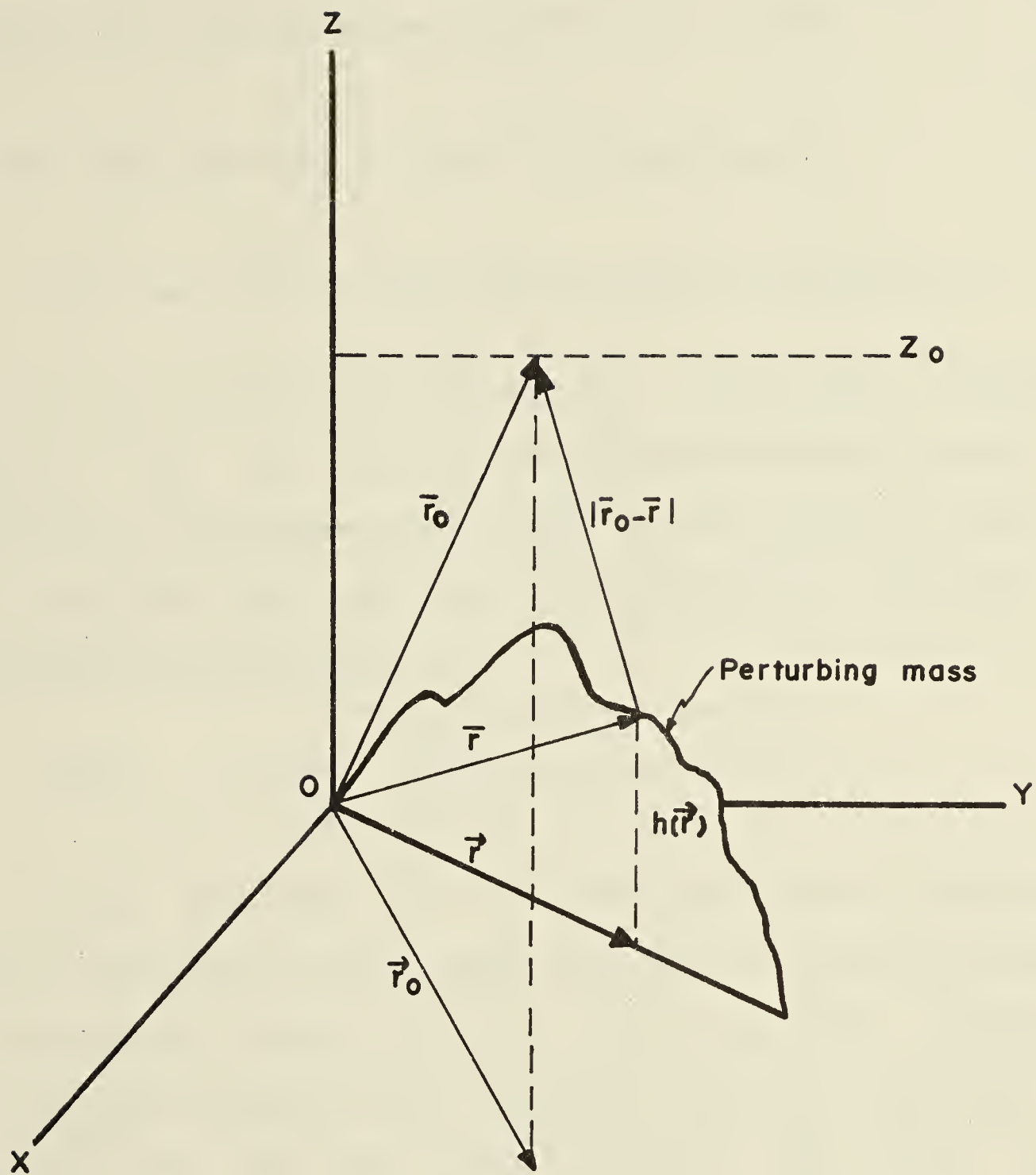


Figure 1.1: Subsurface configuration.

The convergence criteria of the infinite sum of Oldenburg (1974) algorithm was $S_n/S_2 < 5E-3$ while that of Parker (1972) algorithm was $R_n/R_1 < 10E-6$, where:

$$S_n = \max \text{ over all } K \mid (|K|^{n-1}/n!) F[h^n(x)] \mid \quad (3)$$

and

$$R_n = \max \text{ over all } K \mid \exp(-|K|Z_0) (|K|^{n-1}/n!) F[h^n(x)] \mid \quad (4)$$

As for the iterative method the convergence criterion required that the mean-root-squared difference between two consecutive approximations of $h(x)$ be less than 0.5 metre or ten iterations were run. The mean-root-squared error can be expressed mathematically as

$$\text{Error} = 1/N \sqrt{\sum_{i=1}^N [h_i(x) - h_{i+1}(x)]^2} \quad (5)$$

Parker has shown that for $Z_0 > 0$ the rate of convergence of the algorithm is most rapid if H/Z_0 is a minimum; where H is the maximum value of $|h(x)|$. However, if H/Z_0 approaches 1 or greater than one the algorithm may still converge, but at a slow rate. To make H/Z_0 minimum, the origin plane should be placed at the median of $h(x)$. Since the initial placement of the origin plane is entirely arbitrary, a displacement of the origin plane does not affect the validity of equation (1), but it does alter the numerical values of Z_0 and $h(x)$ and thereby H .

1.3. Filtering

It was indicated that straight forward application of the iterative procedure usually resulted in divergence, especially when the relief of $h(x)$ was high. To solve this problem, the standard technique of filtering downward continued data was applied to the iterative procedure. Since most short wavelength anomalies are caused by shallow features, it's therefore justified to remove the high frequency components. To remove these high wavenumber oscillations the right hand side of equation (2) is multiplied by a low pass filter $B(K)$ which cuts off all spatial frequencies above $k(WH)$ and passes all spatial frequencies up to $k(SH)$. The filter used by Oldenburg (1974) was:

$$B(K) = \begin{cases} 1 & ; |K/2\pi| < k(WH) \\ 1/2 \{1 + \cos[(K - 2\pi k(WH))/2(k(SH) - k(WH))]\} & ; k(WH) \leq |K/2\pi| \leq k(SH) \\ 0 & ; |K/2\pi| > k(SH) \end{cases} \quad (6)$$

Wavenumber K is related to spatial frequency by: $K = 2\pi k$. This filter was chosen over several other possible filters because it reduces Gibb's phenomenon.

It was also indicated that judicious choice of $k(WH)$ and $k(SH)$ could be very critical. For any gravitational profile the filter parameters $k(WH)$ and $k(SH)$ can be adjusted to ensure convergence of the iterative process. A decrease in the value of $k(WH)$ and $k(SH)$ will result in faster convergence. However, if $k(WH)$ and

$k(SH)$ are too low, the filtering effect will be severe and the inverted topography will lose most of its detail. In the extreme case the gravity anomaly computed from the inverted model might not necessarily agree with the observed gravity. On the other hand, if $k(WH)$ and $k(SH)$ are too high, divergence of the iterative process might occur.

Judicious choice of Z_0 and d is vital to convergence as well. If Z_0 is fixed, the number of iterations will increase when d decreases. Likewise, if d is fixed increasing Z_0 will require more iterations to achieve convergence. Actually there exists a minimum value, $d(\min.)$, and a maximum value, $Z(\max.)$, beyond which the iterative procedure no longer converges.

CHAPTER 2 MULTILAYER GRAVITY INVERSION METHOD

2.1. Extension of Oldenburg Inversion Algorithm

Oldenburg's inversion scheme is based on the assumption that the observed gravitational anomaly is caused by a single surface between two constant density media. Such an inversion solely attributes the variation of the gravity attraction to the change of topography of one interface only. Examples that will satisfy these conditions are rare.

As most geological examples consist of many layers, any variation of shape, bedthickness, density, etc., of beds overlying the inversion boundary can explain the same gravitational anomaly as that explained by the shape of a single surface alone. Thus the inverted topography of a given profile obtained by attributing all the variation in mass completely to a single interface between two constant density media will be very different from the topography that takes into account of the effect of the overlying layers.

The problem we are going to study is as follows: Given a two-dimensional gravity anomaly resulting from a multi-layered medium and assuming that the thickness and density of each layer, obtained from seismic information at a limited number of points along the profiles, varies in a known way or else linearly along the profile and that each interface takes on the same shape as the bottom-most

interface (called the inversion interface or boundary throughout this thesis), what is the shape of the inversion boundary?

To extend Oldenburg's inversion procedure to allow for variation of bedthickness and density of beds overlying an inversion interface, we revert to Parker's (1972) original theory. For a three-dimensional source with variable density Parker's (1972) equation is:

$$F[\Delta g] = -2\pi G \exp(-|\vec{K}| z_0) \sum_{n=1}^{\infty} (|\vec{K}|^{n-1}/n!) F[d(\vec{r}) h^n(\vec{r})] \quad (7)$$

If the perturbing body is two-dimensional, equation (7) becomes:

$$F[\Delta g] = -2\pi G \exp(-|K| z_0) \sum_{n=1}^{\infty} (|K|^{n-1}/n!) F[d(x) h^n(x)] \quad (8)$$

To compute the total gravitational effect of a medium of many layers equation (8) takes the following form:

(z_0 is replaced by z for the rest of this thesis)

$$F[g(\text{total})] = -2\pi G \sum_{j=1}^{j=M} \exp(-|K| z_j) \sum_{n=1}^{\infty} (|K|^{n-1}/n!) F[d_j(x) h_j^n(x)] \quad (9)$$

M is the number of layers in the medium. The gravity of the bottom-most layer (inversion interface) is designated as $g(\text{inv})$, and that of the overlying layers as $g(\text{sum})$. $g(\text{total})$ is the summation of $g(\text{sum})$ and $g(\text{inv})$.

To evaluate $g(\text{inv})$ M is set equal to 1 in equation (9), that is:

$$F[\Delta g(\text{inv})] = -2\pi G \exp(-|K|Z_1) \sum_{n=1}^{\infty} (|K|^{n-1}/n!) F[d_1(x) h_1^n(x)] \quad (10)$$

Transposing the $n=1$ term from the infinite sum and rearranging,

$$F[d_1(x) h_1(x)] = -(F[\Delta g(\text{inv})]/2\pi G) \exp(|K|Z_1) - \sum_{n=2}^{\infty} (|K|^{n-1}/n!) F[d_1(x) h_1^n(x)] \quad (11)$$

Since $\Delta g(\text{inv}) = g(\text{total}) - g(\text{sum})$,

$$F[d_1(x) h_1(x)] = -F\{[g(\text{total}) - g(\text{sum})]/2\pi G\} \exp(|K|Z_1) - \sum_{n=2}^{\infty} (|K|^{n-1}/n!) F[d_1(x) h_1^n(x)] \quad (11A)$$

where

$$F[g(\text{sum})] = -2\pi G \sum_{j=2}^{j=M} \exp(-|K|Z_j) \sum_{n=1}^{\infty} (|K|^{n-1}/n!) F[d_1(x) h_1^n(x)].$$

Equation (11) and (11A) is the multilayer inversion scheme.

Essentially equation (11) is similar to equation (2) except the densities at various locations are allowed to vary.

Knowing the densities at various locations, the most recent determination of $h(x)$ is multiplied by $d(x)$ and the infinite sum is computed until convergence is met. Division of the inverse Fourier transform of the right hand side of equation (11) by $d(x)$ will generate an updated version of

$h(x)$. This revised value for the topography is substituted back into equation (11) and the whole iterative procedure is continued in the same manner as previously described.

It is most unlikely that densities at all locations along the gravity profile are known. However, if densities at two or more positions are known, either from seismology or from borehole data, and if densities can be assumed to vary linearly, or as some known functions, a series of digitised densities can be produced to satisfy the requirement of equation (11). To remove the gravitational effect of beds overlying the inversion surface ($g(\text{sum})$) to obtain a reduced gravitational anomaly ($g(\text{inv})$) for inversion we have to strip off the gravity of the overlying layers. To do this the variations of bedthickness, density, depth and shape of these beds have to be known. Information regarding the shape of these beds is difficult to obtain unless detailed seismic surveying has been done. However, the topography of these beds can be assumed to change in the same manner as the boundary we want to invert. This assumption is justified on the basis that the earth is radially homogeneous to a first approximation. In the absence of other pertinent information it is the best assumption we can make. Data concerning the variation of bedthickness of each bed at all locations is not often available either. However, often seismic survey or borehole data will furnish enough information about the average bedthickness and density of each bed at two or more

locations to allow for linear interpolation. Knowing the average bedthickness and density of different layers, and assuming the topography of overlying layers to vary in the same manner as the inversion interface we can now proceed to strip off the gravitational effect of all overlying beds, and do the inversion.

2.2. The Multilayer Inversion Scheme

The inversion procedure is illustrated schematically by the flowchart in Figure 2.1. The flowchart itself is self explanatory, however, it is necessary to elaborate on a few points.

Only a fraction of the observed gravity is used for the first inversion because the inversion horizon only accounts for a fraction of the observed gravity. The choice of this fraction is critical to the number of iterations needed to achieve convergence. If it is too large or too low, more iterations are required to reach convergence. A good estimation of this fraction can be obtained by dividing the density of the perturbing mass by the summation of the densities of all layers.

To calculate the gravitational anomaly of beds overlying the inversion boundary it is necessary to compute a new Z for every bed. If Z is the value of Z for the inversion horizon the value of $Z(i+1)$ for the overlying layers is given by equation (10):

$$Z(i+1) = Z(i) - BTK(i+1) \quad (10)$$

where $i = 1, 2, 3, \dots$, is the total number of beds overlying the inversion horizon, and $BTK(i+1)$ is the bed thickness of $(i+1)$ th layer.

After the gravitational anomaly of all layers above the inversion horizon are calculated and summed ($g(\text{sum})$ of flowchart), the difference between the observed gravity ($g(\text{total})$ of flowchart) and the gravity $g(\text{sum})$ will give a new version of the gravity $g(\text{inv})$ which can be used for subsequent iterations. But, if the initial value used for the first iteration is too low the inverted $h(x)$ will be too small. Since $g(\text{sum})$ depends heavily on $h(x)$, keeping other factors unchanged, too small a $h(x)$ will generate too low a gravity $g(\text{sum})$. Thus the difference between $g(\text{total})$ and $g(\text{sum})$ will be too high, and the inverted $h(x)$ of subsequent iteration will be too high as well. Hence, $h(x)$ will either be too low or too high and never converge. Likewise, if the initial value is too high, $h(x)$ will never converge. To avoid this the mean of $g(\text{res})$, which is $(g(\text{total}) - g(\text{sum}))$, and the gravity $g(\text{inv})$ employed for the last iteration is used instead. This avoids dependence on a judicious choice of FRACTION, but also avoids the problem of divergence resulting from a wrong choice of FRACTION. Since the gravity used for every iteration is not exactly the same, at least for the first few iterations, the rate of convergence will be slower than that using a

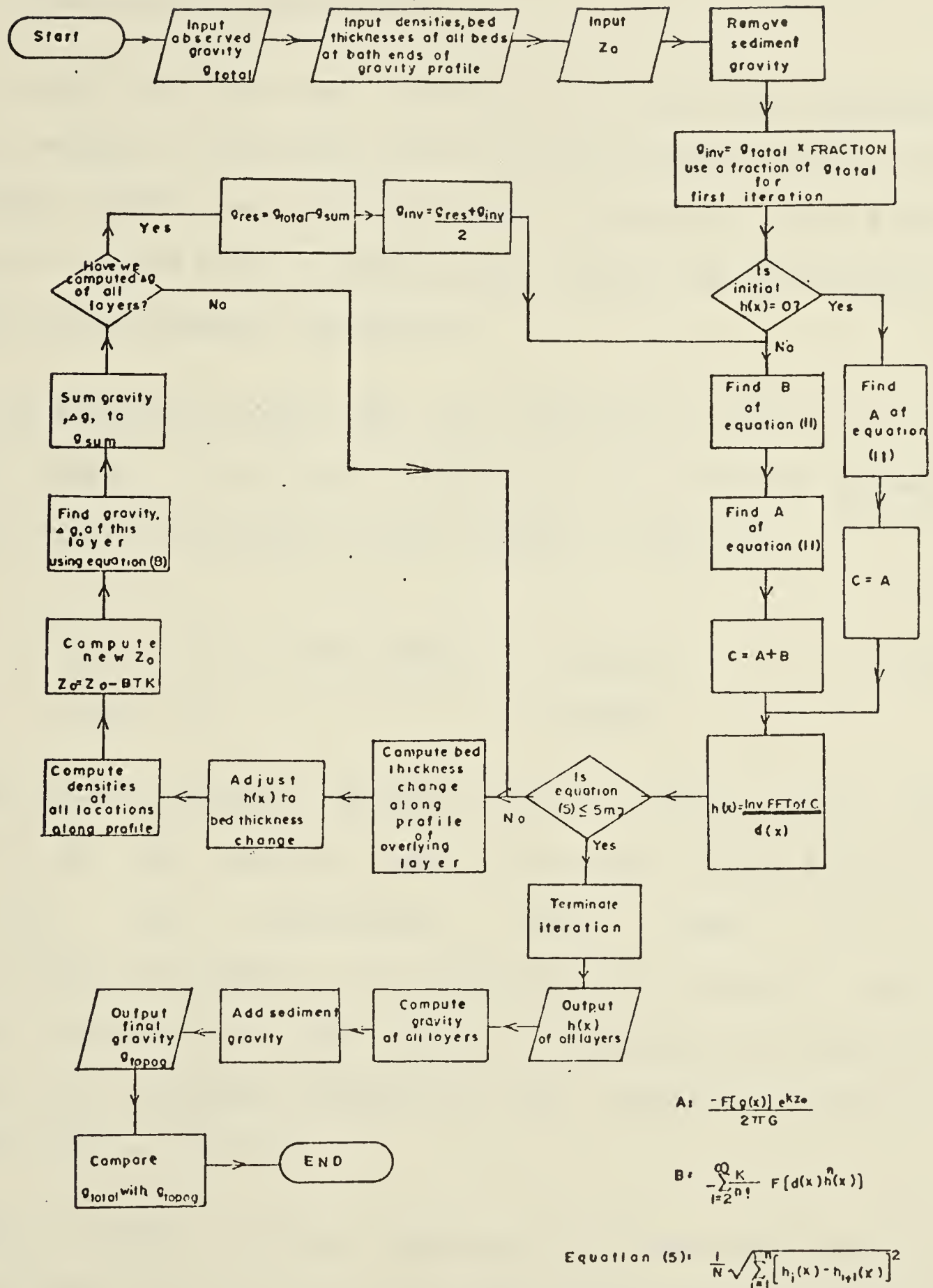


Figure 2-1 Schematic representation of the multilayer inversion procedure.

constant gravity, and more iterations are needed to reach convergence.

2.3. Oldenburg's Cosine Model

To test the one layer algorithm of Parker and Oldenburg it was decided to reproduce some of the results obtained by Oldenburg (1974). As a further check, Talwani's (1959) line-integral method for two-dimensional bodies was also used to compute gravitational attraction.

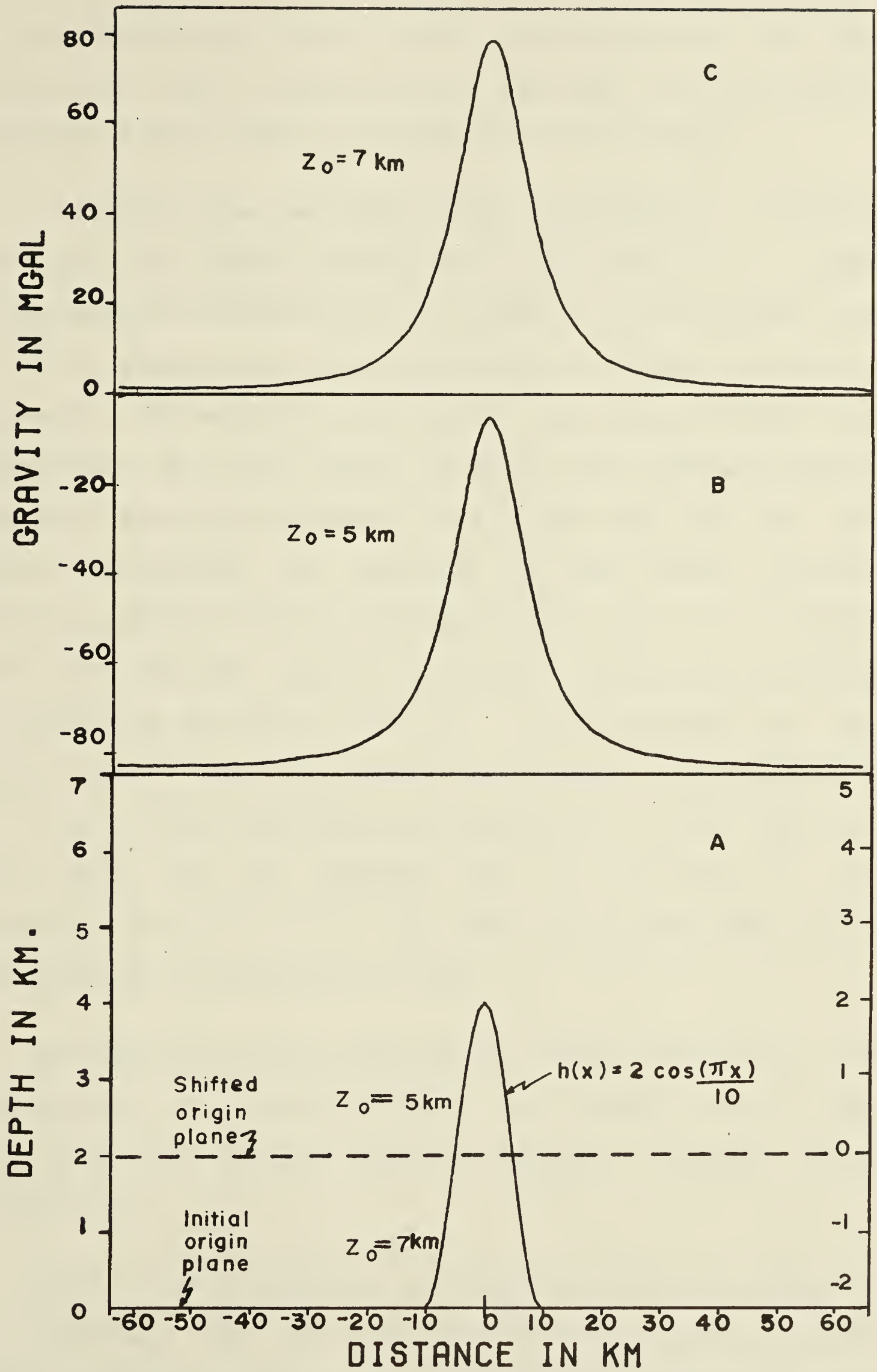
The numerical model used by Oldenburg (1974) was a cosine model, 4 km high, 20 km wide, and floored 7 km deep (Figure 2.2A). The shape of this model is given by:

$$\begin{aligned} h(x) &= 2 + 2 \cos(\pi x/10) & -10 \leq x \leq 10 \\ h(x) &= 0 & |x| > 10 \end{aligned} \quad (11)$$

The gravity anomaly (Figure 2.2C) of this model was computed at 128 points, each 1 km apart, using Parker's algorithm. The parameters used were $Z = 7$ km, $d = 1$ gm/cc and $H/Z_0 = 4/7$ which is 0.57. Talwain's line-integral method was also used to calculate the gravity anomaly. The difference between the two resultant profiles was less than a milligal.

This gravity profile (Figure 2.2C) was then used to find the shape of the inversion model. Convergence criteria were the same as that used by Oldenburg. The inversion parameters were $d = 1$ gm/cc, $k(WH) = 0.075$, $k(SH) = 0.125$ and

Figure 2.2: Two-dimensional cosine model and its gravity anomaly. Fig 2.2A shows the normal position of the origin plane, $z = 7$ km, and the position for optimum convergence, $z = 5$ km. Fig 2.2B and Fig 2.2C are the gravity profiles computed with $z = 5$ km and 7 km respectively. Note that the vertical axis is doubly valued to indicate vertical distances relative to the initial and shifted origins.



Z was varied from 2 km to 7 km at an increment of 1 km. The frequencies were chosen because they were the ones used by Oldenburg (1974, p533) to reproduce the topography.

Inversion with the above stated parameters or similar ones did not produce convergence at any level of z . Later investigation indicated that an offset of -84 milligals was actually added to the gravity anomaly in Figure 2.2C before inversion. The reason for the offset was that during his computation of the gravity anomaly of the cosine model Oldenburg actually subtracted 2 km from each of the 128 points describing the elevation of the model. Such an operation merely shifts the origin plane up 2 km (Figure 2.2A) and does not change the physical relationship between the model and the datum plane Z . A displacement of the origin plane does not affect the validity of equation (1) but it does alter the numerical values of Z , $h(x)$, and H as well. Thus $h(x)$ is negative for $5 < |x| < 10$, Z is decreased from 7 km to 5 km, and H/Z changes from $4/7$ to $2/5$, because $H = \max|h(x)| = 2 \text{ km}$

To shift the origin plane up by 2 km is equivalent to subtracting the gravity effect of a Bouguer slab of 2 km thick from the initial gravity waveform (Hinson, 1976. Appendix C).

Each of the 128 gravity stations was therefore offset -84 milligals, and the resulting gravity profile (Figure 2.2B) was used for inversion. The inversion parameters used

were $d = 1 \text{ gm/cc}$, $k(\text{WH}) = 0.075$, $k(\text{SH}) = 0.125$ and Z was varied from 2 km to 7 km at an increment of 1 km. Convergence occurred at all levels of Z , except for $Z = 6$ km and 7 km. For $Z = 6$ km and 7 km, the scheme diverged after three iterations. The right inversion model ($Z = 5$ km), shown in Figure 2.3, took four iterations to converge.

To see why initial inversion with the gravity of Figure 2.2C diverged, and why an offset gravity (Figure 2.2B) produced convergence, it is necessary to understand how different parameters control convergence. Convergence of Parker's algorithm is governed by d , Z and H/Z . For the inversion scheme convergence is also controlled by the filter parameters.

The ratio H/Z only affects the infinite sum of the Parker-Oldenburg algorithm. As long as H/Z_0 is less than 1 or not much greater than 1 convergence of the infinite sum is assured. In our present situation d has no effect upon convergence because the value used for inversion was the same as that used in the computation of the gravity profile. As already indicated, for any given gravity profile there exists a maximum value for Z , $Z(\text{max})$, for every set of inversion parameters being used; beyond which the iterative procedure no longer converges. If $Z(\text{max})$ is high enough to enclose the appropriate value of Z needed to produce a successful inversion model there is no problem. However, if $Z(\text{max})$ is small enough to exclude the proper value of Z the inversion algorithm will never converge even when the right

Z is used.

It appears that for the gravity profile in Figure 2.2C, and using $k(WH) = 0.075$ and $k(SH) = 0.125$, the value of $Z(max)$ was 2 km. This is because the inversion scheme only tended to converge at $Z = 2$ km. With $k(SH)$ reduced from 0.125 to 0.100 the inversion algorithm not only converged at $Z = 2$ km, but also tended to converge at $Z = 3$ km. Thus $Z(max)$ was then 3 km. Since the right value of Z to produce the proper inversion model is 7 km, which is off the above stated ranges of $Z(max)$, the initial inversion procedure therefore diverged.

It can be observed that the effect of increased filtering is twofold. Firstly, for any given Z increased filtering decreases the number of iterations required to deliver convergence. Secondly, increased filtering raises the value of $Z(max)$. In theory the values of $k(WH)$ and $k(SH)$ can be decreased to such an extent as to raise the magnitude of $Z(max)$ to enclose the Z necessary to produce the right inversion model. However, in practice, severe filtering is most undesirable. Severe filtering cuts off high frequency components necessary to form sharp discontinuities, and the inversion model loses most of its detail. The gravity computed from the inversion model might not agree with the observed gravity.

Instead of reducing the magnitudes of $k(WH)$ and $k(SH)$ to increase the range of $Z(max)$ it was found that the

same effect can be achieved by adding an appropriate amount of offset to the initial waveform. This was evidenced by the inversion using the gravity profile shown in Figure 2.2B. Using this gravity waveform the iterative scheme converged at all levels of Z except at $Z = 6$ km and 7 km. $Z(\text{max})$ was extended to 5 km.

By introducing an appropriate amount of gravity offset the value of Z needed to produce the right inversion model is also reduced. With the cosine model at a base of 7 km (no offset applied to the initial gravity) Z has to be equal to 7 km to produce the right shape. However, with the cosine model based at 2 km below the origin plane Z only has to be equal to 5 km to reproduce the input shape. As already indicated decreasing Z increases the rate of convergence. Hence, fewer iterations are needed.

The introduction of a proper amount of gravity displacement also has the effect of reducing the amount of filtering needed to produce convergence. To decrease filtering will mean allowing high wavenumber oscillations to pass. This is especially important when we are inverting bodies with sharp discontinuities, because high wavenumbers are needed to form sharp curves. To achieve fast convergence of the inversion scheme it is most desirable if Z and H/Z are as small as possible. However, decreasing the value of Z also increases the ratio H/Z . Hence, the infinite sum takes more terms to converge. If Z is so small that H/Z is close to one or greater than one, the infinite sum will

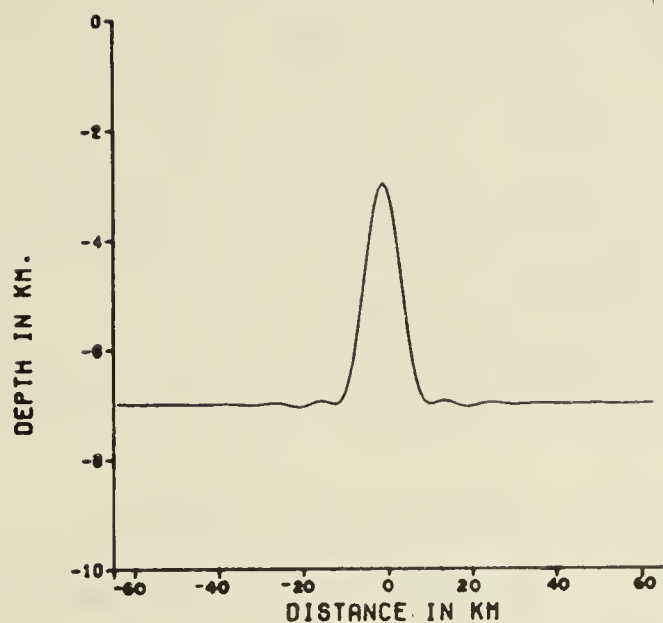


Figure 2.4: Inversion model obtained from the offset gravity anomaly (-126 mgal) of the cosine model. Inversion parameters used were $z_0 = 4$ km, $d = 1$ gm/cc, $k_{WH} = 0.075$, $k_{SH} = 0.125$. 4 iterations were used.

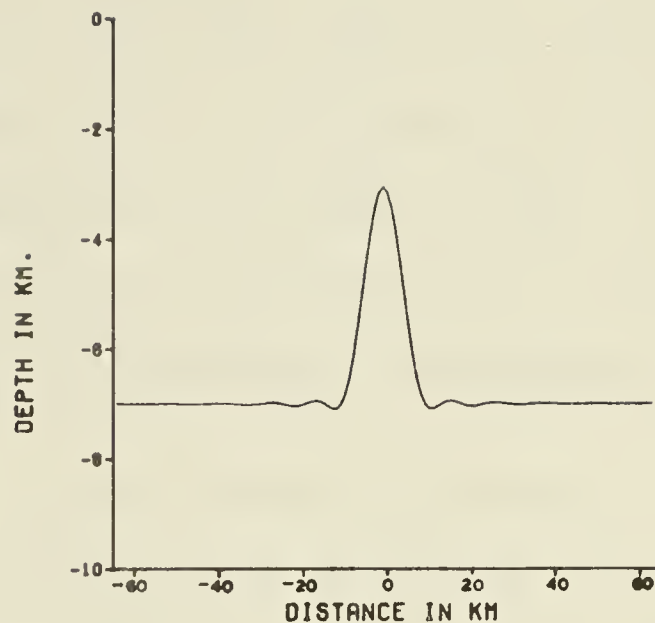


Figure 2.3: Inversion model obtained from the offset gravity anomaly (-84 mgal) of the cosine model. Inversion parameters used were $z_0 = 5$ km, $d = 1$ gm/cc, $k_{WH} = 0.075$, $k_{SH} = 0.125$. 4 iterations were used.

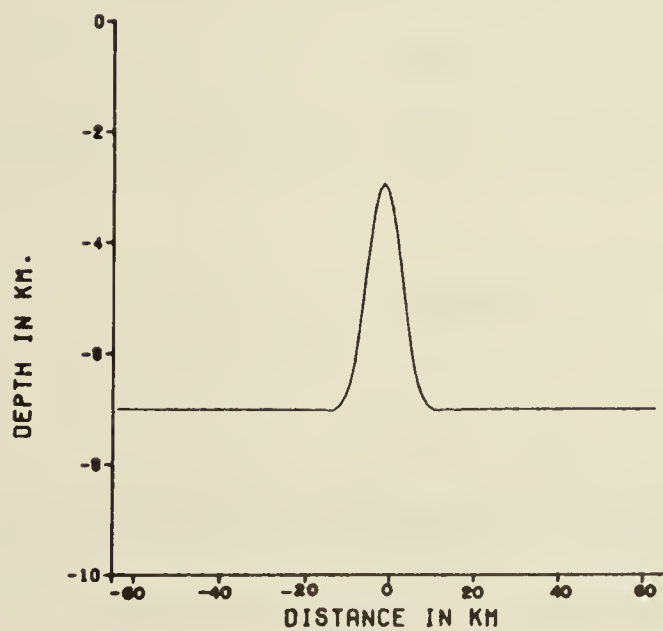


Figure 2.5: Inversion model obtained from the offset gravity anomaly (-126 mgal) of the cosine model. Inversion parameters were the same as those used in Fig 2.4 except $k_{WH} = 0.125$, $k_{SH} = 0.25$, 4 iterations were used.

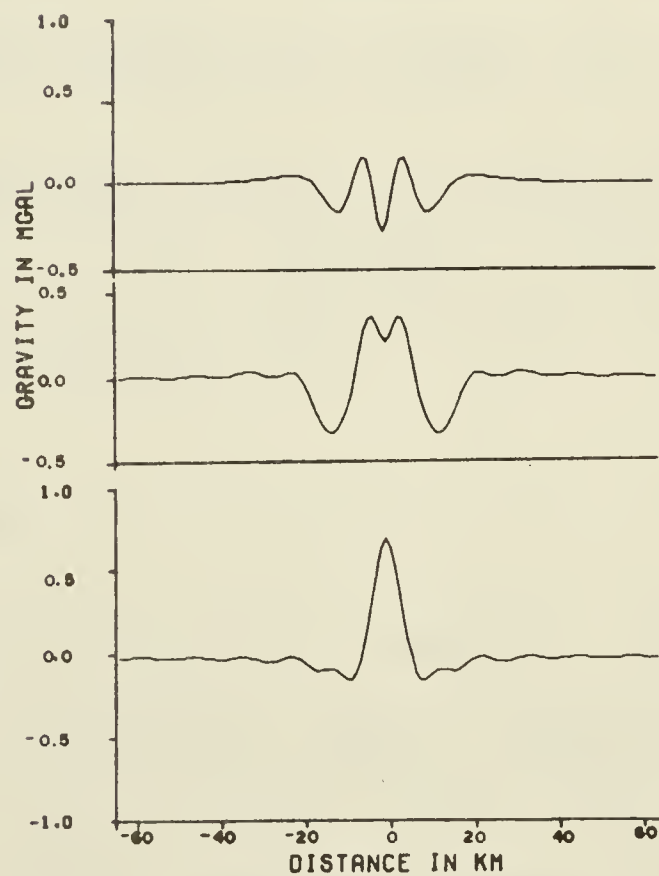


Figure 2.6: Difference between observed gravity and gravity calculated from the inversion models shown in Fig 2.3, Fig 2.4, and 2.5.

either converge very slowly or diverge. On the other hand, if Z is large H/Z will be small. A large Z will mean more iterations. The amount of computer time that might have been saved by using a small Z could well be cancelled by the increase of computer time in calculating the extra terms of the infinite sum. A compromise between the values of Z and the ratio H/Z is therefore needed to facilitate convergence.

Figure 2.4 is the inversion model produced by adding - 126 mgals (3 km Bouguer Slab) to the gravity in Figure 2.2C. With $Z = 4$ km and using the same filter ($k(WH) = 0.075$ and $k(SH) = 0.125$) it took three iterations to deliver convergence. When the filter parameters were changed to $k(WH) = 0.15$, $k(SH) = 0.25$ it took four iterations to converge. Notice the shape is less oscillatory (Figure 2.5).

Figure 2.6 shows the difference between the observed gravity and the gravity obtained from the inversion models shown in Figure 2.3, Figure 2.4 and Figure 2.5.

2.4. Multilayer Numerical Example

To test out the multilayer inversion program the gravitational anomaly caused by a four-layer model composed of three concentric triangular prisms (Figure 2.7) is used. Each triangular prism has a base 40 km wide, a height of 4 km, and a density contrast of 0.5 gm/cm^3 . The lower triangular model is based at 8 km, while each of the overlying layers is vertically displaced by 1 km.

The gravity of this four-layer model was computed for 128 points, each 1 km apart, using the equation for triangular prisms in Heiland (p151, 1940, 1963). The gravity waveform is shown in Figure 2.8. To optimize convergence - 251 milligals were added to each of the 128 gravity stations. The resultant gravity profile was then used for inversion. The parameters used for inversion were: $d = 0.5 \text{ gm/cm}^3$, $Z = 4 \text{ km.}$, $\text{FRACTION} = 1/3$, $k(\text{WH}) = 0.075$, $k(\text{SH}) = 0.125$. Six iterations were used to produce convergence. It is to be noted that by adding -251 milligals to the original gravity waveform we are merely introducing a Bouguer Slab of 4 km thick, because only one-third of the offset gravity is used for inversion. The inversion model, Figure 2.9, agrees well with the input model. Difference between the observed gravity and the inverted gravity is shown in Figure 2.10. Figure 2.11 shows the difference between the topography of the input model and that of the inversion model.

As can be seen in Figure 2.10 (also in Figure 2.11) the major discrepancies between original gravity profile (or topography) and inverted gravity waveform (or topography) occur at locations with sharp discontinuity. This is because the high frequency components which are needed to form sharp curves were filtered.

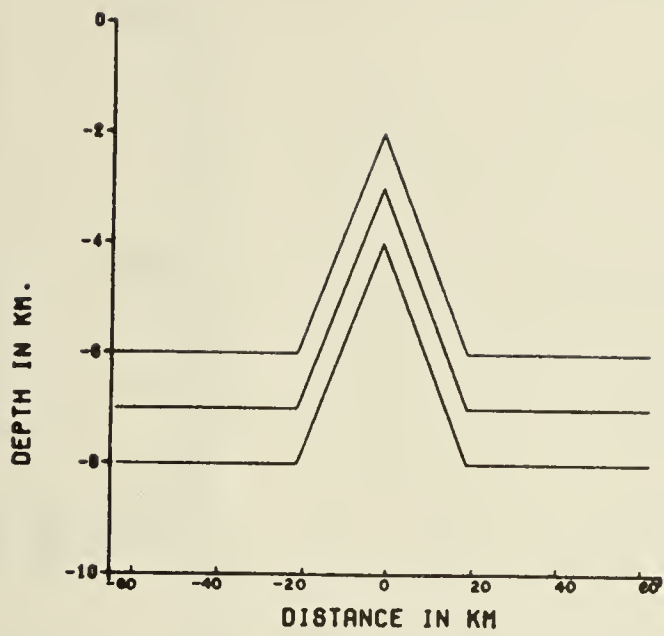


Figure 2.7: Four-layer numerical model, composed of three concentric triangular prisms.

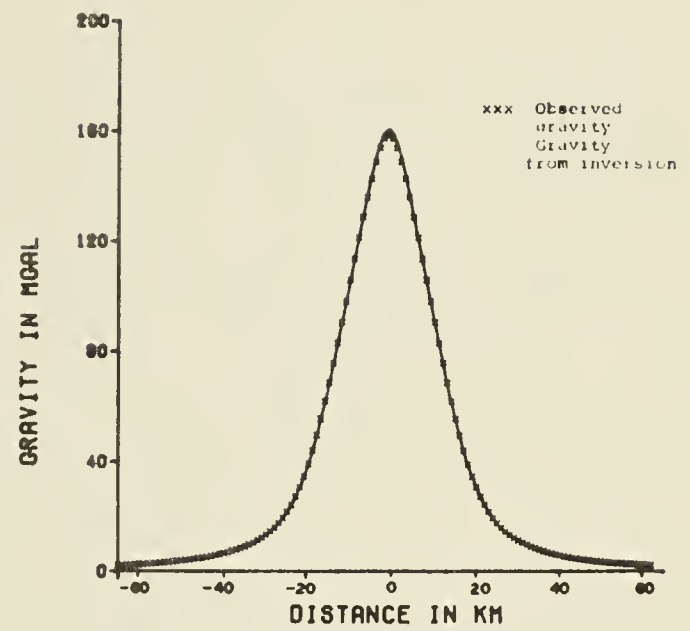


Figure 2.8: Original gravity and gravity computed from the inversion model of the four-layer numerical model.

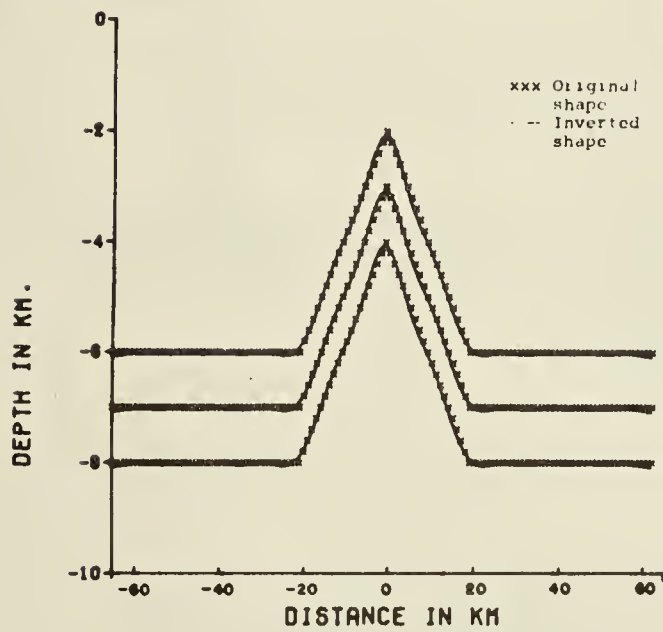


Figure 2.9: Comparison of the inverted shape and the original shape of the four-layer model.

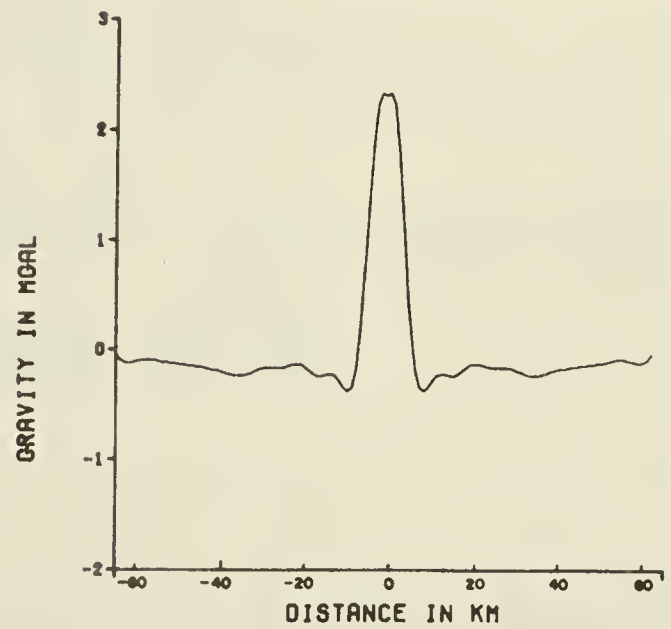


Figure 2.10: Difference between observed gravity and inverted gravity of the four-layer model.

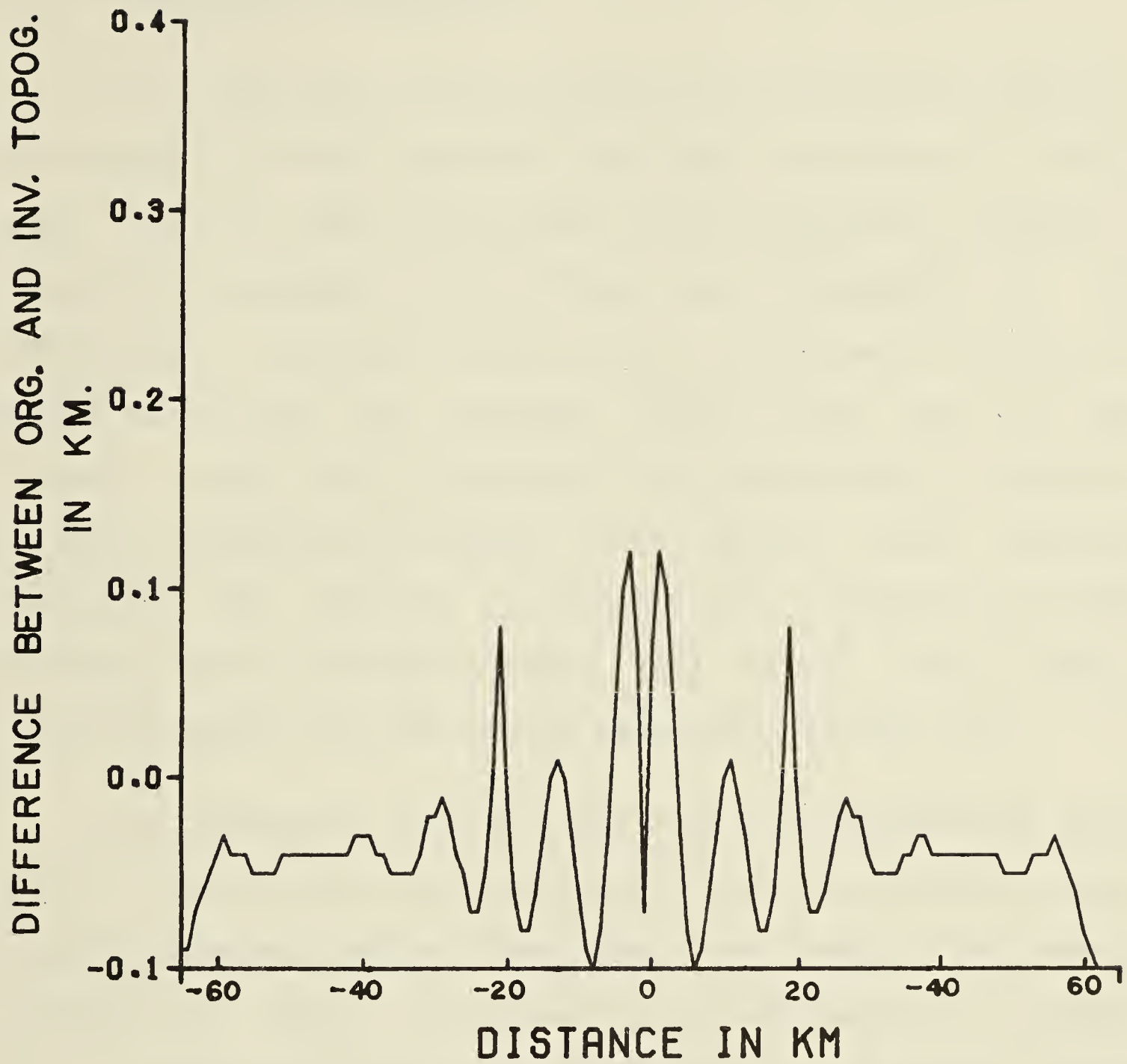


Figure 2.11: Difference between the inverted topography and the original topography of the four-layer model.

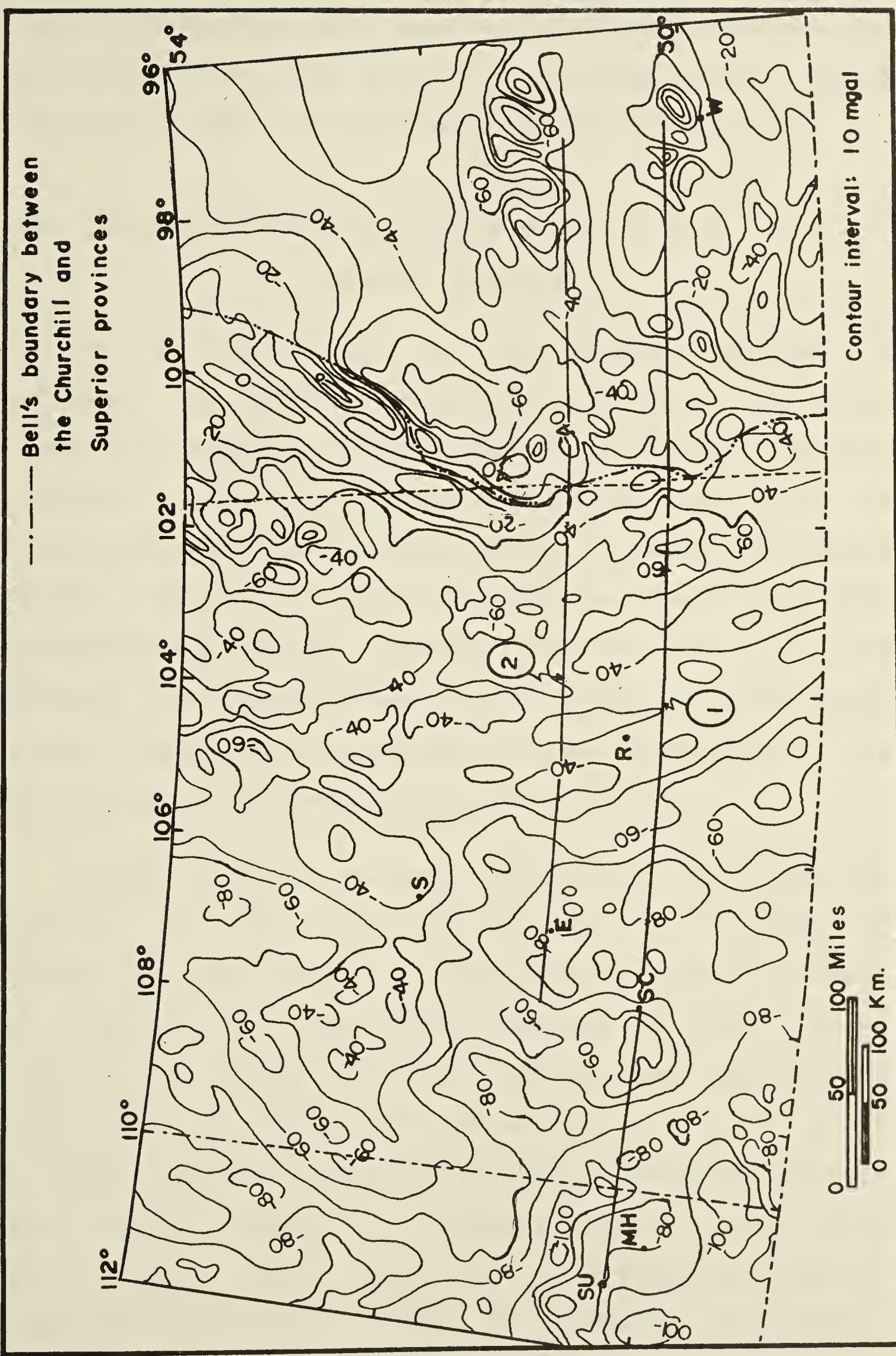
CHAPTER 3 GEOLOGY AND GEOPHYSICS OF THE AREA

3.1. Geological Background

The locations of the two gravity profiles for which we are going to do the inversion are shown in Figure 3.1. This area is of great economical and geological interest. Significant amounts of oil and gas have accumulated in the Phanerozoic sediments that overlie the basement. Nickel is being mined from the Thompson nickel belt, one of the world's major nickel deposits. The area is also of tectonic interest because the boundary zone (Bell, 1971b) between Churchill and Superior provinces which outcrops in the northern part of Manitoba might well extend south (Bell, 1971b) beneath the Phanerozoic sediments (Figure 3.1).

The southern plains of Manitoba and Saskatchewan form part of the Interior Platform. Phanerozoic sedimentary rocks thin out towards eastern Manitoba. The nearly horizontal sedimentary rocks are covered by a thick mantle of glacial drift to form the plains and plateaux of the Interior Plains physiographical province. Beneath the Phanerozoic strata are Precambrian sedimentary and crystalline rocks, the latter forming the basement of this area. To the north of the plains the Precambrian rocks are exposed on the Canadian Shield. The Precambrian rocks of northern Saskatchewan and northwest Manitoba form part of the Churchill structural province, while those of north-east Manitoba compose a portion of the Superior structural province. Part of the

Figure 3.1: Gravity map of the southern plains of Saskatchewan and Manitoba, showing locations of the two gravity profiles, and area of detail gravity survey. SU=Suffield, SC=Swift Current, MH=Medicine Hat, E=Elbow, R=Regina, and W=Winnipeg.



Superior Province is also exposed in southeast Manitoba. The Superior and Churchill provinces are partially separated by a transition zone: the Pikwitonei province (Bell, 1971b).

3.2. Regional Geology and Geophysics of the Area

Superior Province

The Manitoba portion of the Superior province is dominated by east-west trending structures. Its rocks consists of belts of calc-alkaline and calcic volcanic sequences with interlayered sediments, and belts of sedimentary gneiss interlaminated with granitic intrusions (Wilson, 1971). The volcanic-sedimentary belts have been extensively intruded by granitic plutons, and have been deformed and metamorphosed to the greenschist metamorphic facies. The sedimentary gneisses have been metamorphosed to amphibolite and occasionally granulite facies.

Strong east-west magnetic and gravitational trends are observed. The two types of belt are characterised by distinct magnetic patterns. On the whole it appears as belts of magnetically high areas composed of broad linear anomalies of moderate relief, and narrow linear anomalies of high relief. The volcanic-sedimentary belts occur in areas of lower magnetic intensity than the surrounding gneissic areas which are broad E-W trending magnetic highs with little relief. Local sharp and intense magnetic highs are registered across the volcanics and ironstone formations. Granitic bodies are characterised by elliptical high

amplitude anomalies (Kornick, 1971; Kornick and Maclaren, 1966; Hall, 1968, 1971, 1976).

The Boundary Zone

There is much controversy concerning the exact location and the extent of the boundary between the Churchill and Superior structural provinces. For the past several decades, earth scientists have tried to use both geological and geophysical data to infer the exact location and extent of this boundary, however, the boundary enigma is still unsolved. A transition zone, rather than a sharp boundary, was proposed to separate the Churchill and Superior provinces (Burwash et al. 1962; Peterman and Hedge, 1964; Bell, 1971b). Geochronological data from bottom-hole samples indicated that the Churchill and Superior provinces of the Canadian Shield not only extend into southern Saskatchewan and Manitoba but also into the Williston basin of North Dakota (Burwash et al. 1962; Peterman, 1962; Peterman and Hedge, 1964). On the basis of gravity data (Innes, 1960; Wilson and Brisbin, 1961) and K-Ar ages of subsurface samples (Burwash et al. 1962; Peterman and Hedge, 1964), it was indicated that the boundary zone in the subsurface extends from the Nelson River gneissic zone southwest into eastern Saskatchewan and hence into north-central North Dakota, following the Nelson River gravity low. North of Lake Winnipeg, Bell (1971b) defined the boundary zone as the Pikwitonei province, which can be traced intermittently from the foot of Lake Winnipeg, northeast, then east, under the

Hudson Bay Lowland and the flat-lying Aphebian rocks that outcrop west of James Bay (Bell, 1971b, p32, Figure 8). The rocks north and northwest of the Pikwitonei province - the Waboden subprovince, were initially included by Bell as part of the Churchill province. However, recent geological field work and Rb-Sr radiometric dating by Cranstone and Turek (1976) have shown that the Wabowden subprovince is best described either as a separate entity or as part of the Pikwitonei province.

The Pikwitonei province is a zone of early Precambrian, retrograded, granulite to amphibolite facies gneisses that lie unconformably beneath 'type' Archean greenstone-belt rocks - Cross Lake Group (Bell 1971). It's rocks have a NE-SW fabric which abruptly truncated the E-W trends of the Superior Province.

Like the Pikwitonei province, the Waboden subprovince is NE-SW trending. Its rock types are predominantly migmatic gneisses which enclose a belt of sedimentary and volcanic rocks of significantly lower metamorphic grade. In general, the metasedimentary and metavolcanic rocks appear to be greenschist to lower amphibolite facies, whereas the layered migmatic gneisses are generally upper amphibolite facies (Bell, 1971b). The vast nickel deposits of the 'Thompson Nickel Belt' occur in the west edge of this subprovince. The boundary between the Wabowden subprovince and the Pikwitonei province is a major fault zone (Assean Lake fault zone) in the north (Bell, 1971b) and a metamorphic transition zone in

the south and central regions (Cranstone and Turnek, 1976). The definition of the boundary in the south is not well established as similar gneisses occur in both provinces.

Aeromagnetic and gravity studies indicated that there is a remarkable correlation of surface geology with gravity and magnetic anomalies (Bell, 1971b) in the Pikwitonei province. The Pikwitonei province granulite facies gneisses are reflected as small ovoid high and low magnetic anomalies of relatively high amplitude (Bell, 1971b; Kornik and Maclaren, 1966; Kornik, 1969). In contrast with the Pikwitonei gneisses the Waboden migmatic gneisses is characterised by elongated, high intensity magnetic anomalies; parallel to the trend of the belt. The Pikwitonei province and the Waboden subprovince are marked by a prominent gravity high and low respectively, of similar magnitude and dimensions (Wilson and Brisbin, 1961, 1962; Gibb 1968b). It was on the basis of these regional geophysical trends that Bell extrapolated the boundary zone into the areas covered by Paleozoic and Pleistocene deposits (Bell, 1971b, p32, Figure 8).

The eastern limit of the Churchill province proposed by Bell (1971b) is on the east flank of the Nelson River gravity high, while that of Innes (1960), Wilson and Brisbin (1961), Burwash (1962) and Peterman (1964) is along the Nelson River gravity low.

Churchill Province

Churchill province rocks consist of mainly metasediments and migmatites, plus minor metamorphosed intermediate to mafic volcanic rocks. Bodies of massive to weakly foliated granitic rocks are also present. The volcanic-sedimentary areas in the Churchill province are different magnetically from the volcanic-sedimentary areas in the Superior province. The Churchill volcanic-sedimentary areas do not contain the large gneissic belts which produce the large magnetic highs present in the Superior province. Instead it is dominated by local intrusive features which have smaller and discontinuous magnetic anomalies. Like the magnetic anomalies, the gravity anomalies are isolated and closed and do not show any strong trends.

3.3. Seismic Data

Much seismic work have been done to determine the crustal structure of Western Canada. Seismic surveys carried out by G.L. Cumming and E.R. Kanasewich et al (1966) in the plains of southern Alberta and Saskatchewan indicated a crustal thickness of about 47 km in eastern Alberta, and 43 km in western Saskatchewan. Their derived crustal model from Swift Current, Saskatchewan to Suffield, Alberta is summarized in Table I. Similar surveys were done in the southern part of eastern Manitoba (Hall and Hajnal, 1969; Gurbuz, 1969, 1970). Their derived crustal thickness is about 34 km. The crustal model adopted by Gurbuz, (1969, 1970) is shown in Table II. It is based on the data present

in these two tables, together with the seismic data (Hall, 1969) concerning the structure of the crust around central-south Lake Winnipeg that the parameters (e.g. depth of interface, density and thickness) necessary for the multilayer inversion scheme are derived.

Table I

Discontinuity	SUFFIELD		SWIFT CURRENT	
	Depth (Km)	P-Wave Velocity (Km/sec)	Density (Gm/cc)	Depth (Km)
Surface	0.0	_____		0.0
Basement	2.24	_____		2.02
		6.16	2.73	
Man. Riel	12.5	_____		10.4
		6.5	2.8	
Alta. Riel	35.5	_____		33.4
		7.15	3.17	
Mohorovicic	46.9	_____		43.2
		8.08	3.4	

Crustal model from Suffield, Alberta to Swift Current, Saskatchewan. All depths are measured relative to the surface. The Table is not drawn to scale.

Density values are calculated from the density-compressional velocity curve given by Nafe and Drake (1957).

Table II

Discontinuity	Depth (Km)	P-Wave Velocity (Km/sec)	Density (Gm/cc)
Surface	0	_____	
		6.11±0.01	2.73
Man. Riel	18±3.0	_____	
		6.81±0.08	2.96
Alta. Riel	25.5±3.5	_____	
		7.10±0.04	3.17
Mohorovicic	34±3	_____	
		7.90±0.05	3.36

Crustal model of the southern portion of eastern Manitoba, as derived by Gurbuz (1969, p970). All depths are measured relative to the surface. All density values are computed from the density-compressional velocity curve given by Nafe and Drake (1957).

It is to be noted that there is ambiguity in the usage of the term "Riel discontinuity" (R.D.). Previously Kanasewich and Cumming et al (1959) termed the discontinuity just above the Mohovicic discontinuity (Moho) the "Conrad Discontinuity". This nomenclature was criticized because it implied a stratigraphic or petrologic correlation with the European Conrad discontinuity which represents an interface with velocity changing from about 5.6 to 6.2 km/sec. (Conrad, 1925; Jeffreys, 1926). In southern Alberta, the refracting and reflecting intermediate layer represents a change in velocity from 6.5 to 7.2 km/sec. To avoid the implication of an intercontinental correlation, Kanasewich and Cumming et al (1968) subsequently replaced the term "Conrad" with "Riel". In Manitoba the term "Riel discontinuity" was used to refer to the discontinuity which represents a velocity change from 6.1 to 6.8 km/sec.

To avoid any confusion in the future we designate the Alberta R.D. (ARD) as the discontinuity just above the intermediate layer with velocity 7.1 ± 0.15 km/sec; and Manitoba R.D. (MRD) as the interface just above the layer with velocity 6.72 ± 0.23 km/sec.

CHAPTER 4

4.1. Source of Data

The gravity data used for inversion were obtained from the Dominion Observatory. Additional data were obtained by C. McCloughan and the author during a gravity field program in the summer 1976. The gravity values of stations marked along the two profiles were used as the gravity observations.

The Gravity Survey (Figure 4.1)

In the summer of 1976, Mr. McCloughan and the author, under the direct supervision of Professor G.L. Cumming of the University of Alberta, undertook a gravity survey in the southern plains of Saskatchewan and Manitoba. The survey was intended to add more details to the Dominion Observatory Gravity Map Series. Observations were carried out with a Lacoste and Romberg gravimeter, supplied by the Dept. of Energy, Mines and Resources (E.M.R.). The survey area is bounded by $50^{\circ}30'N$ and $52^{\circ}N$ latitudes and $101^{\circ}W$ and $104^{\circ}W$ longitudes. About 690 observations were made. Readings were taken at 1 or 2 miles intervals, depending on the density of gravity stations already present in the area. Observations were taken along highways, railway stations and crossings and grid roads. Elevation control was provided by known elevations at section corners, railway crossings, benchmarks, lake levels and by the use of two altimeters.

Readings were taken at gravity control stations every 2 hours and at points of known elevation every hour.

The station positions were marked on 4-mile topographic maps, from which their latitudes and longitudes were scaled. The updated version of the Potsdam Standard gravity base was used in data reduction. The free air and Bouguer correction amounts to 0.1968 milligals per meter above sea level. A density of 2.67 gms. per c.c. was used in correcting for the attraction of material between the station and sea level. Topographic correction was not applied to the data because there is not much variation in terrain in the area. The elevation of most of the stations obtained are believed accurate within 5 feet. The estimated uncertainty of the final Bouguer anomalies is ± 0.3 mgal.

It is to be noted that the gravity values appeared in the above stated gravity map series were obtained using the old version of the Potsdam Standard for gravity. An analysis of the Dominion gravity data and our data at the same locations indicated that our gravity values are 7 mgals lower than that of the Dominion Observatory. To bring all Dominion data to the new Potsdam Standard we subtract 7 mgals from all Dominion gravity stations.

Location (Figure 3.1)

Profile (1) runs from Suffield ($111^{\circ}00'W$) Alberta, along $50^{\circ}20'N$ latitude, to the northern part of Winnipeg ($96^{\circ}00'W$). Profile (2) is 50.5 minutes north of Profile (1)

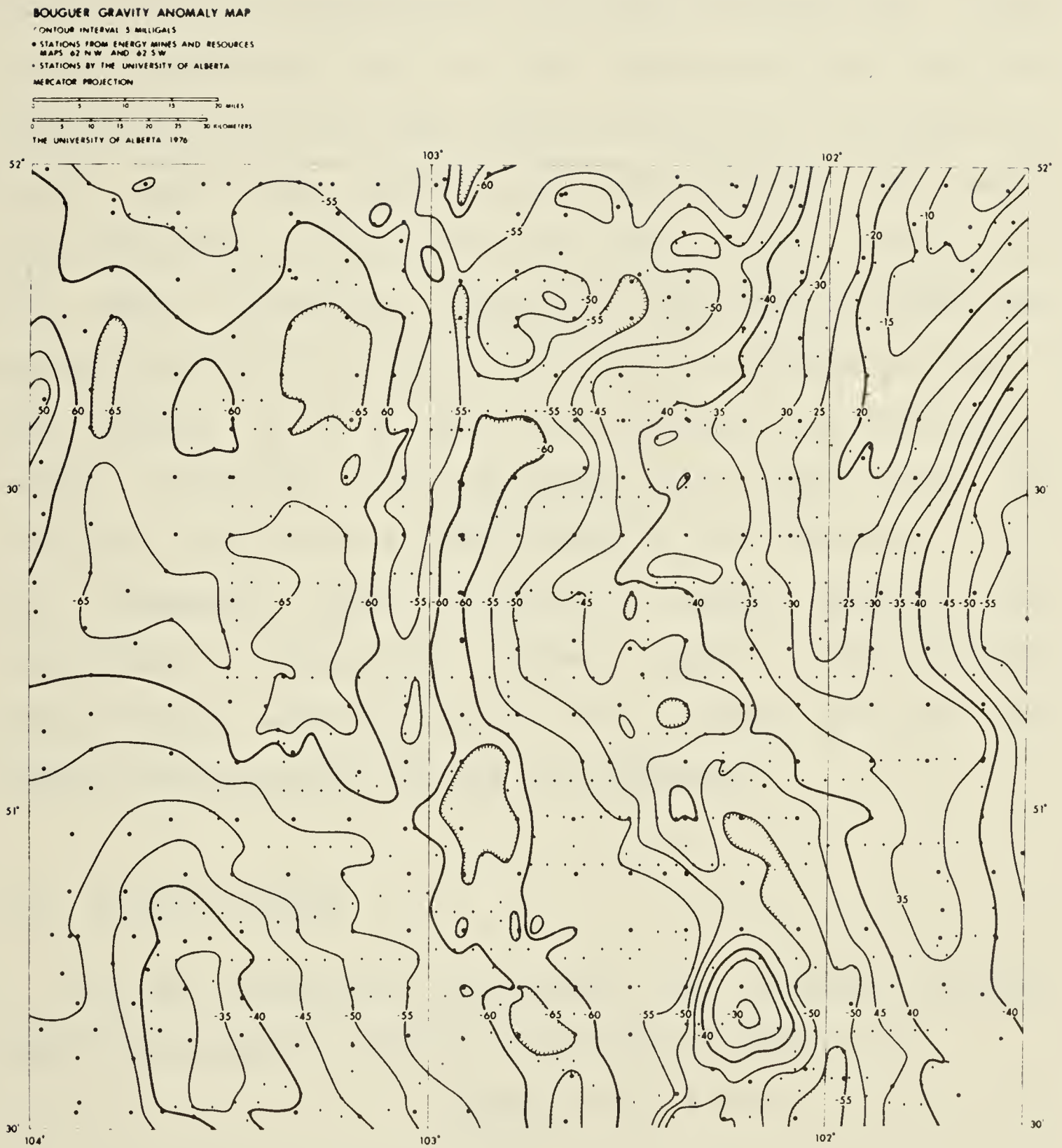


Figure 4.1: Detail gravity map of southern Saskatchewan.

and runs along latitude $51^{\circ}10.5'N$.

Correction for the Sediment Layer

The sedimentary basin of the southern plains of Saskatchewan and Manitoba can be roughly divided into three groups. Sediments with a mean density of 2.42 gm/cc are considered to be the first group, and they are composed of shale, shaly sand, sandstone and some limestone. The second group consists of evaporites which have a mean density of 2.16 gm/cc . Dolomites, limestones, high velocity sands and shales form the third group, and they are assumed to have a mean density of 2.67 gm/cc . The thickness and altitude of various formations were determined from isopach maps¹. The resultant gravitational contribution of the sediments, which were computed using Talwani's (1959) method, was subsequently subtracted from their corresponding gravitational observations on the profile to give the reduced gravitational profile for inversion.

4.2. Crustal Models

In the following inversions four different crustal models are assumed, and they are shown in Figure 4.2.

Model I (Fig. 4.2-A)

Model I consists of a sedimentary layer underlain by three crustal layers, A, B and C with a discrete

¹ From Geological History of Western Canada, ASPG, Calgary, Alberta.

compressional velocity.

Model II (Fig. 4.2-B)

In this model, ARD is assumed non-existent and the material between MRD and the Moho is represented by a layer (BC) whose density is the mean of the densities of layers B and C in Model I. The expression used to find the mean density is:

$$\sum_{i=1}^{i=n} d(i)h(i) / \sum_{i=1}^{i=n} h(i) \quad \begin{array}{l} n = 1, 2, 3, \dots \\ \text{= total number of layers} \end{array}$$

where $d(i)$ and $h(i)$ is the density and thickness of the i th layer respectively.

Model III (Fig. 4.2-C)

This model is similar to Model II except MRD is assumed non-existent instead of ARD. The mean of the densities of layers A and B of Model I is used as the density of the layer (AB) between ARD and the basement.

Model IV (Fig. 4.2-D)

In this model, layers A, B and C of Model I is combined to form one single layer (ABC) whose density is the mean of the densities of layers A, B and C.

4.3. Inversion of Profile (1)

Profile (1) is divided into two segments: east of Swift Current, and west of Swift Current. To see how the various inversion models produced by the multilayer inversion scheme

MODEL I

SEDIMENT	
LAYER A	MRD
LAYER B	ARD
LAYER C	Moho
LAYER D	

FIGURE 4.2-A

MODEL II

SEDIMENT	
LAYER A	MRD
LAYER BC	Moho
LAYER D	

FIGURE 4.2-B

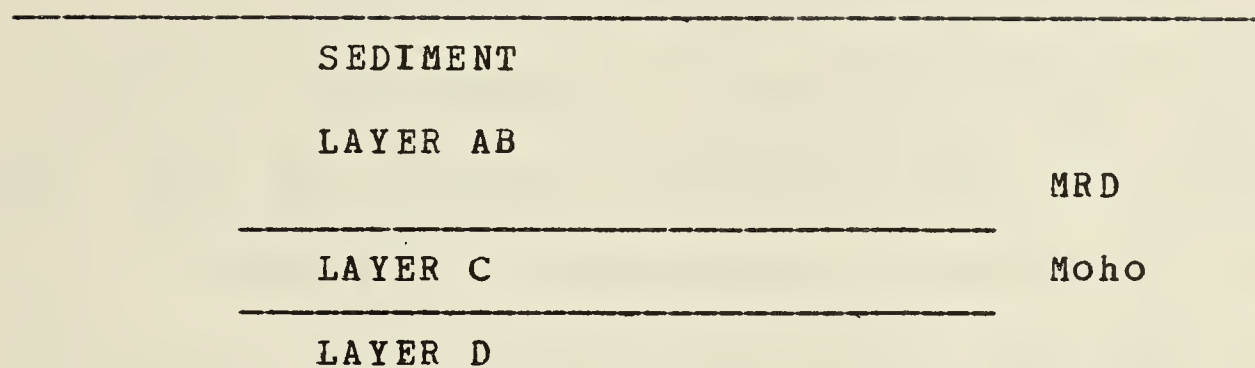
MODEL III

FIGURE 4.2-C

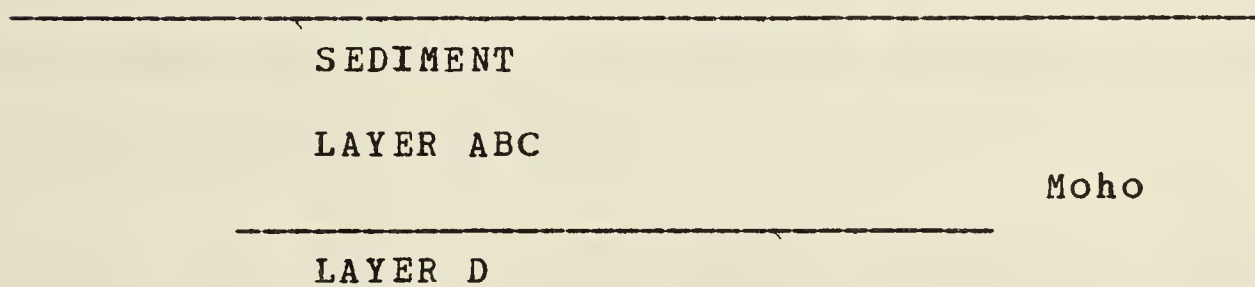
MODEL IV

FIGURE 4.2-D

compared with the Suffield - Swift Current crustal model put forward by Cumming and Kanasewich et al (1966), inversion was first performed on the western segment.

Suffield - Swift Current

We used as gravitational observations the first 35 stations east of $111^{\circ}58'N$ longitude (Fig. 4.3). Sediment gravity at corresponding locations was computed and removed to obtain the reduced gravitation profile. In order to meet the requirement that for finite transform the data series has to be infinitely replicated, a "mirror image" of the reduced gravitational profile was generated. A spline routine was used to interpolate these stations. The resulting profile was then digitised at intervals of 5 km yielding a series 128 points long (Fig. 4.4). Convergence criteria were the same as the numerical examples. A maximum of 15 iterations were allowed.

Table III shows the thicknesses, densities and depths of each layer at Swift Current and Suffield (Cumming and Kanasewich 1966). It is to be noted that these figures are the average values around Swift Current and Suffield. However, during the process of inversion, these values were used as the values of the corresponding layer at Swift Current and Suffield. It was assumed that the thickness (or density) of a layer vary linearly along the profile if the thickness (or density) of the stratum is not the same at both ends of the profile.

The total number of iterations required for convergence, and the inversion parameters used for the four different models are also shown in Table III. The depth of the Moho at Swift Current provides the constraints required for the proper choice of Z . It was assumed that the depths of the Moho, ARD, and MRD at Swift Current are at 43.2, 33.4 and 10.4 km respectively.

The above described procedure and assumptions also apply to the inversions that follow.

Table III

MODEL I

INVERSION PARAMETERS		Z =33.5 km	FRACTION=0.3
		k =0.087	OFFSET=-250.0 mgal
		k =0.057	ITER=7
LOCATION		SUFFIELD	SWIFT CURRENT
Average	A	10.26	8.38
Thickness of	B	23.00	23.00
Layer (km)	C	11.40	9.80
Average	A	2.73	2.73
Density	B	2.80	2.80
of	C	3.17	3.17
Layer (gm/c.c.)	D	3.40	3.40

MODEL II

INVERSION PARAMETERS		Z =32.7km	FRACTION=0.3
		k =0.087	OFFSET=-250.0 mgal
		k =0.057	ITER=6
LOCATION		SUFFIELD	SWIFT CURRENT
Average Thickness	A	10.26	8.38
of Layer (km)	BC	34.40	32.80
Average Density	A	2.73	2.73
of	BC	2.92	2.92
Layer (gm/c.c.)	D	3.4	3.4

MODEL III

INVERSION PARAMETERS		Z =32.7 km k =0.087 k =0.057	FRACTION=0.3 OFFSET=-250.0 mgal ITER=6
LOCATION		SUFFIELD	SWIFT CURRENT
Average Thickness of Layer (km)	AB	33.26	31.38
	C	11.40	9.80
Average Density of Layer (gm/c.c.)	AB	2.78	2.78
	B	3.17	3.17
	D	3.40	3.40

MODEL IV

INVERSION PARAMETERS		Z =27.7 km k =0.087 k =0.057	FRACTION=1.0 OFFSET=-250.0 mgal ITER=7
LOCATION		SUFFIELD	SWIFT CURRENT
Average Thickness of Layer (km)	ABC	44.66	41.18
Average Density of Layer (gm/c.c.)	ABC	2.87	2.87
	D	3.4	3.40

DEPTH OF INTERFACES

	LOCATION DISCONTINUITY	SUFFIELD	SWIFT CURRENT
Average Depth of (km)	MRD	12.5	10.4
	ARD	35.5	33.4
	Moho	46.9	43.2

Table III. Suffield - Swift Current inversion parameters.
ITER = number of iterations required for convergence.

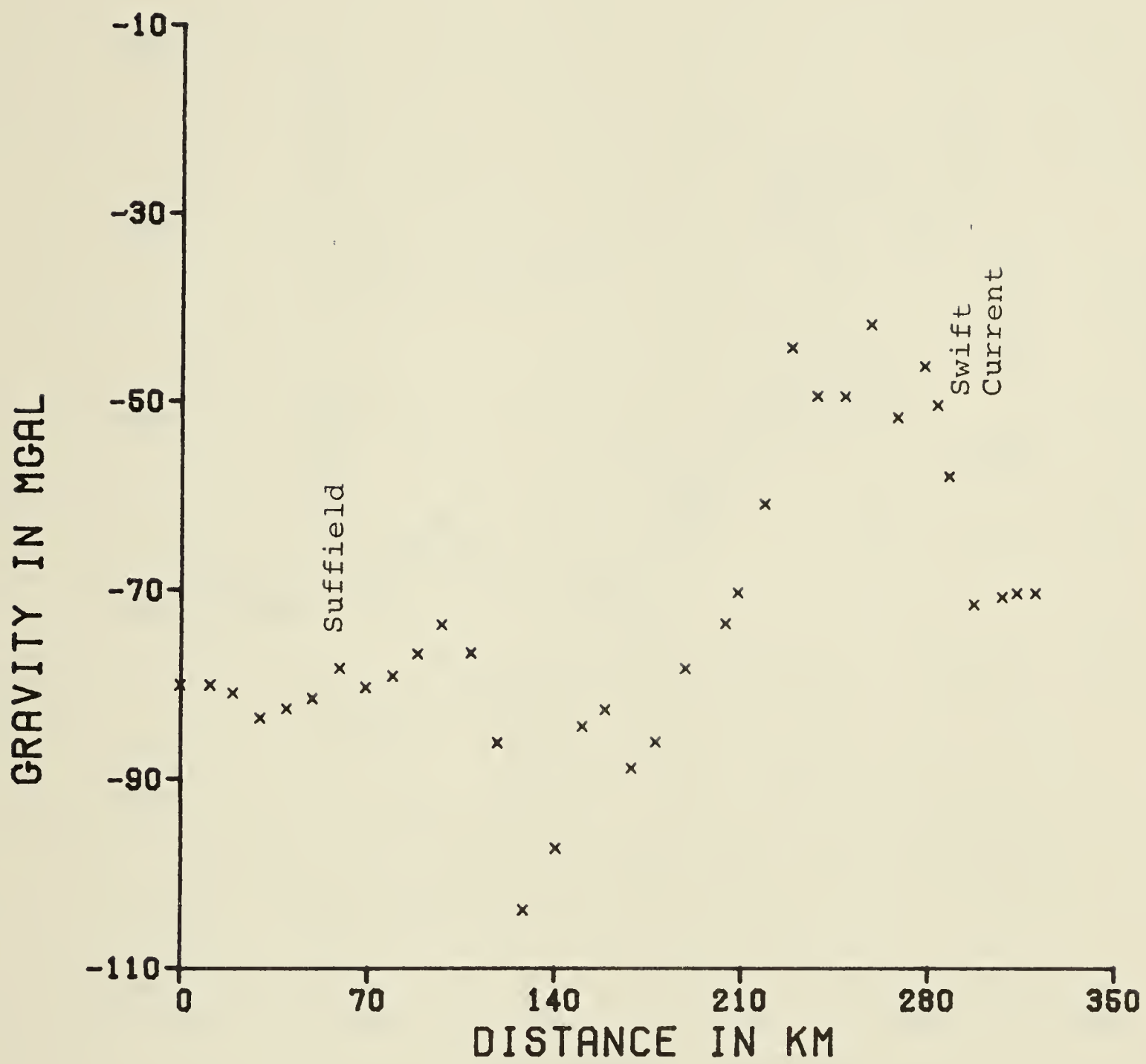


Figure 4.3: Gravitational observations of the Swift Current-Suffield profile.

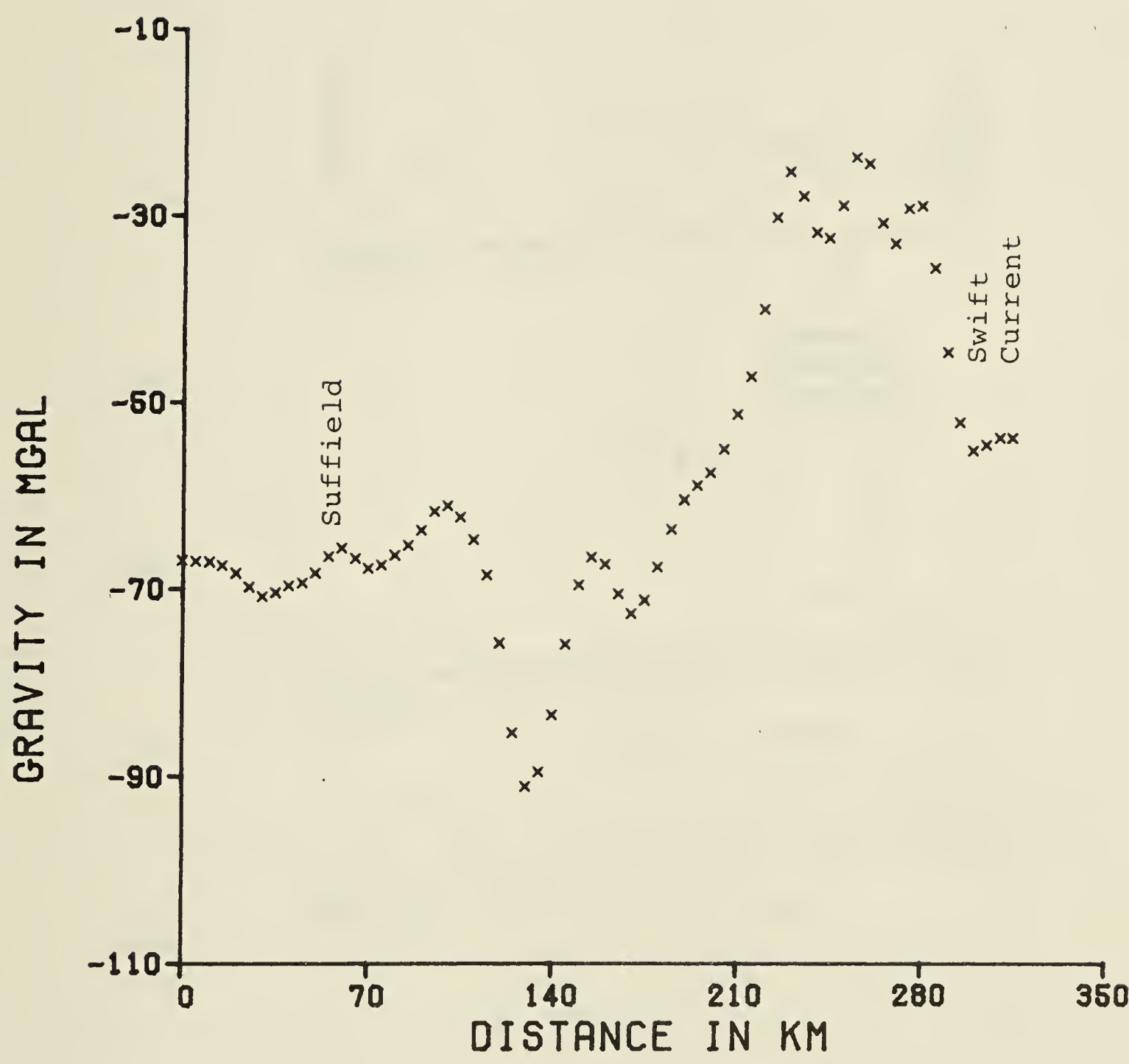


Figure 4.4: Reduced gravitational observations of the Swift Current-Suffield profile.

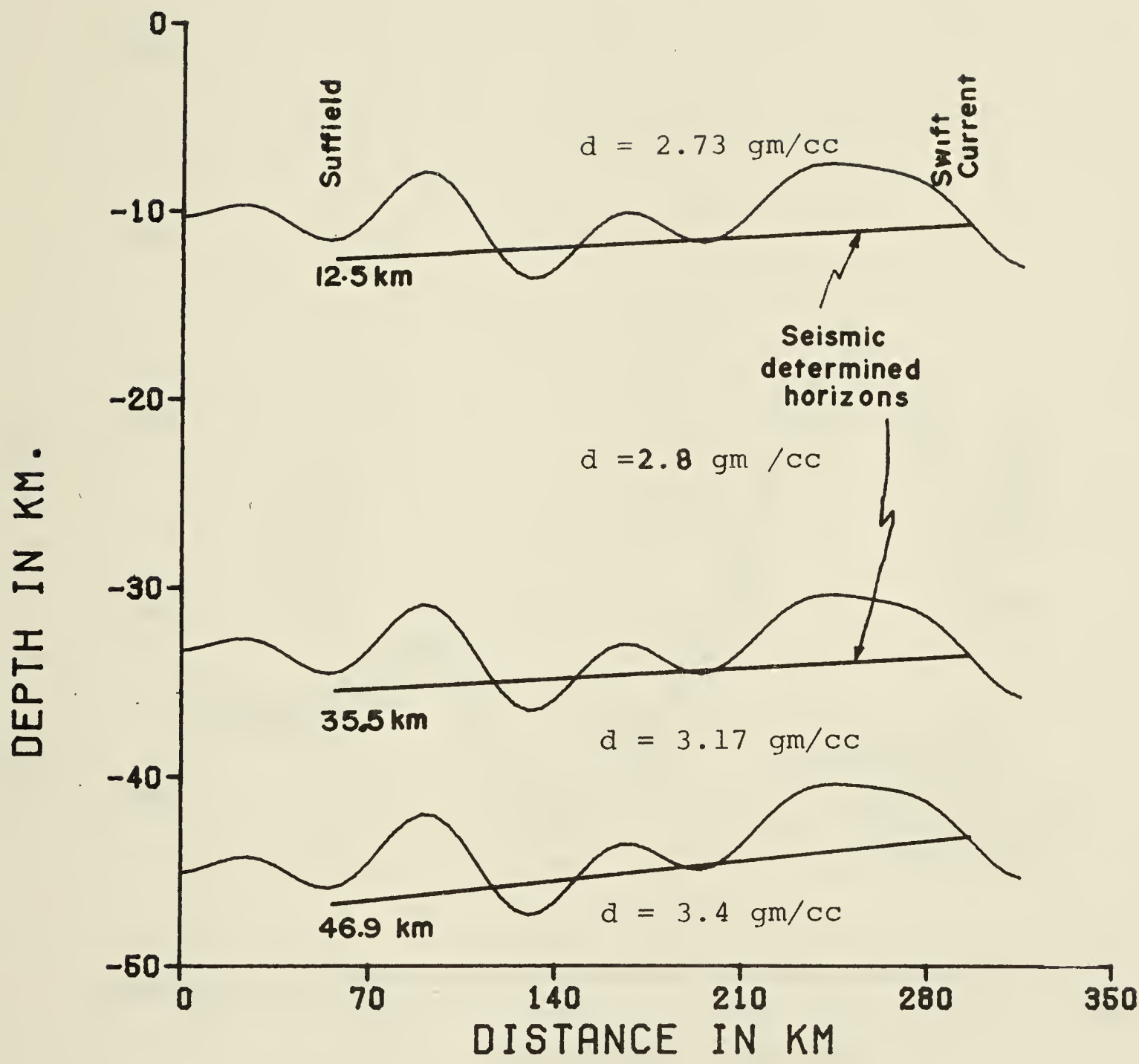


Figure 4.5: Inversion model of Swift Current-Suffield profile assuming crustal model I. Vertical exaggeration = 7.

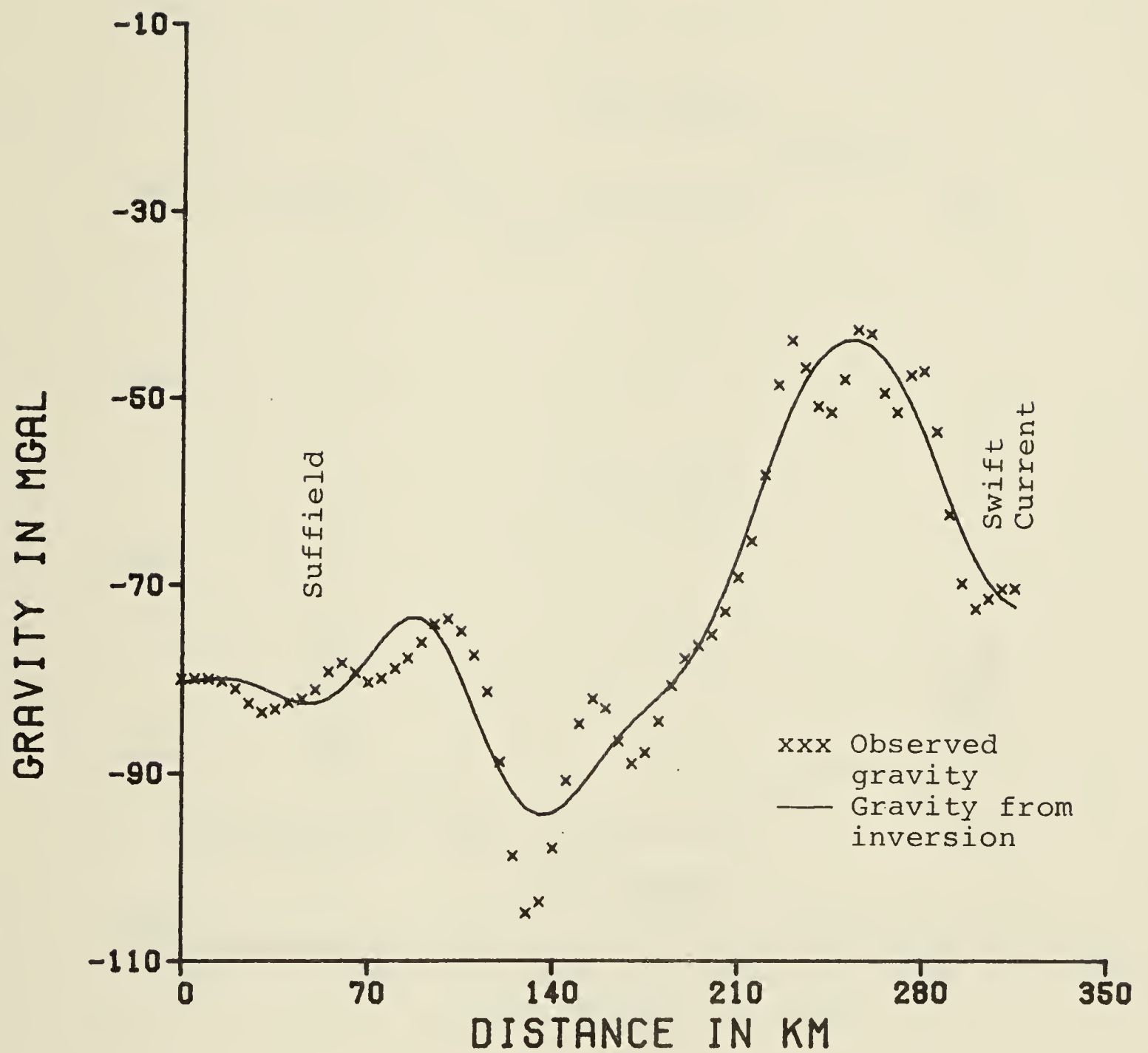


Figure 4.6: Comparison between observed gravity and gravity calculated from inversion model of Fig 4.5.

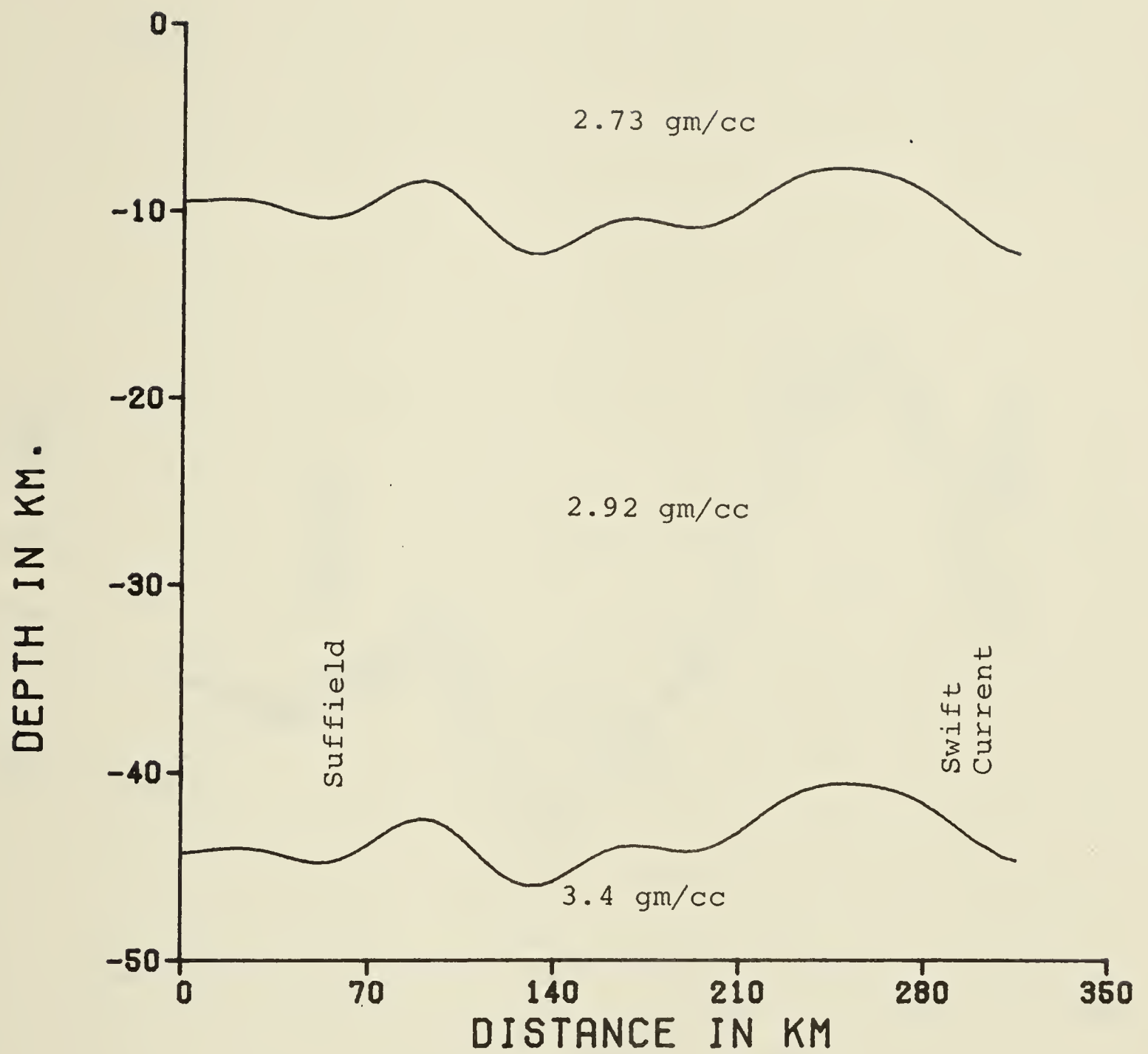


Figure 4.7: Inversion model of Swift Current-Suffield profile assuming model II.

INVERTED AND ORIGINAL GRAVITY ANOMALIES

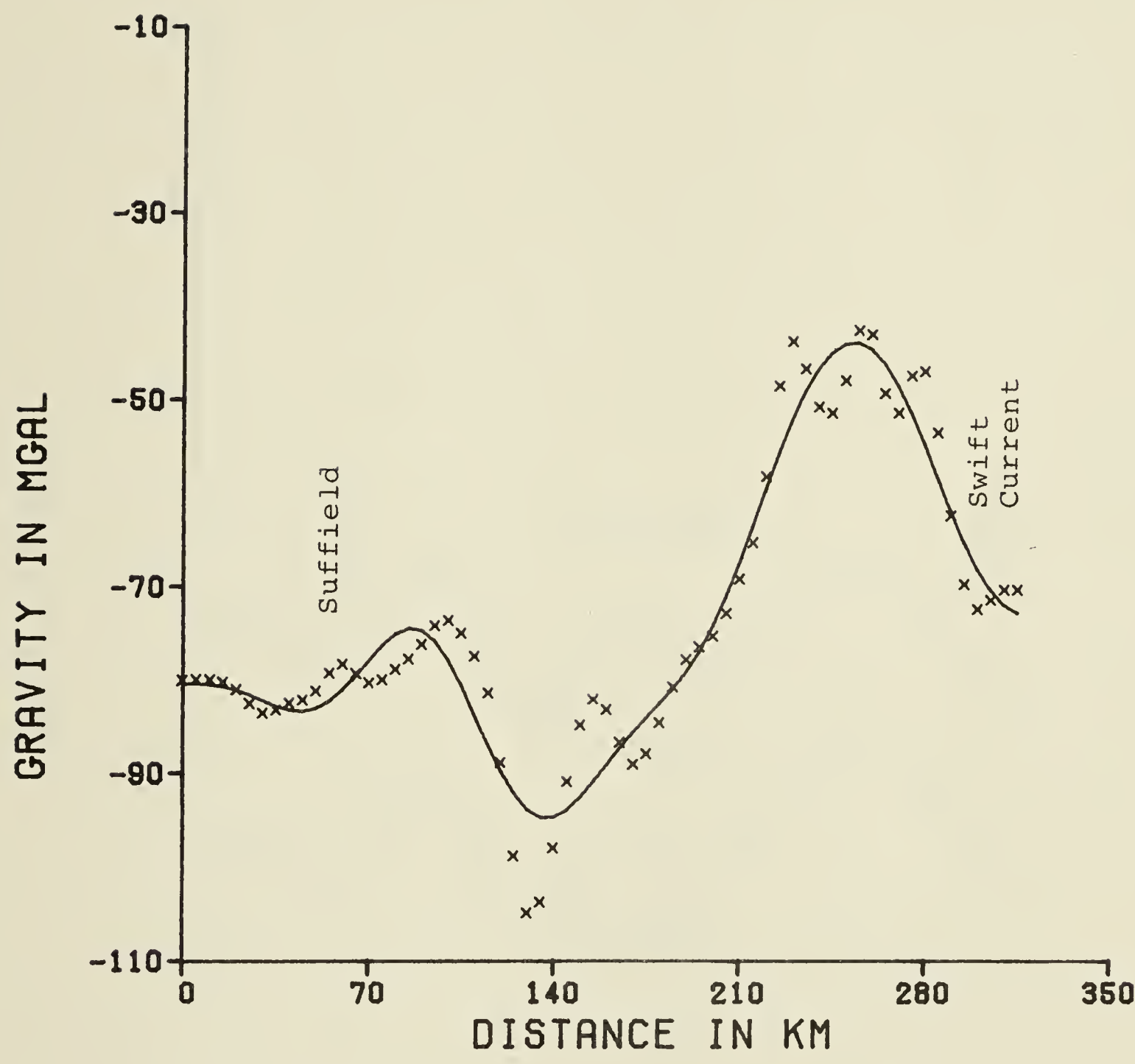


Figure 4.8: Comparson between observed gravity and gravity calculated from inversion model of Fig 4.7.

INVERTED TOPOGRAPHY

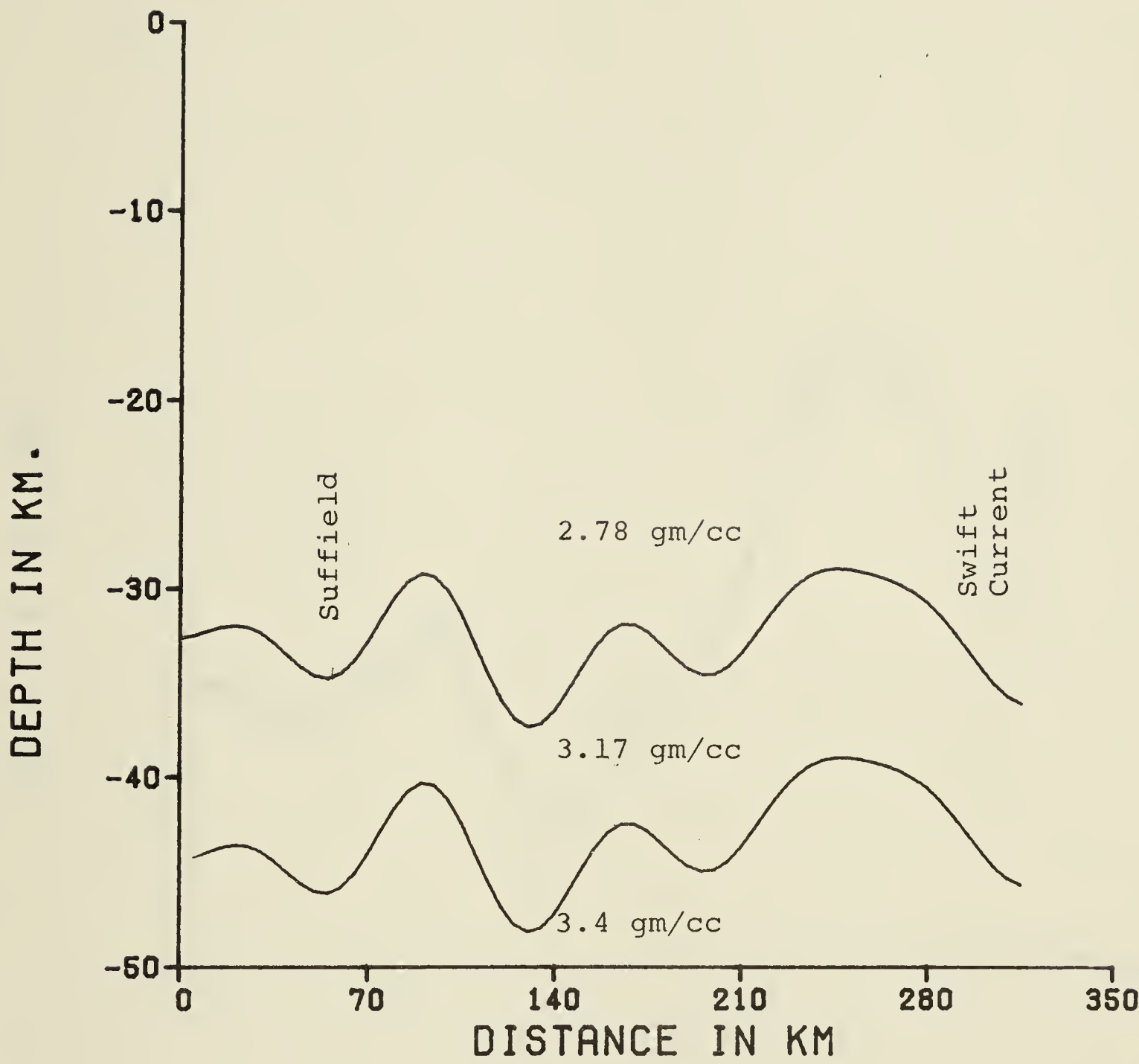


Figure 4.9: Inversion model of Swift Current-Suffield profile assuming crustal model III.

INVERTED AND ORIGINAL GRAVITY ANOMALIES

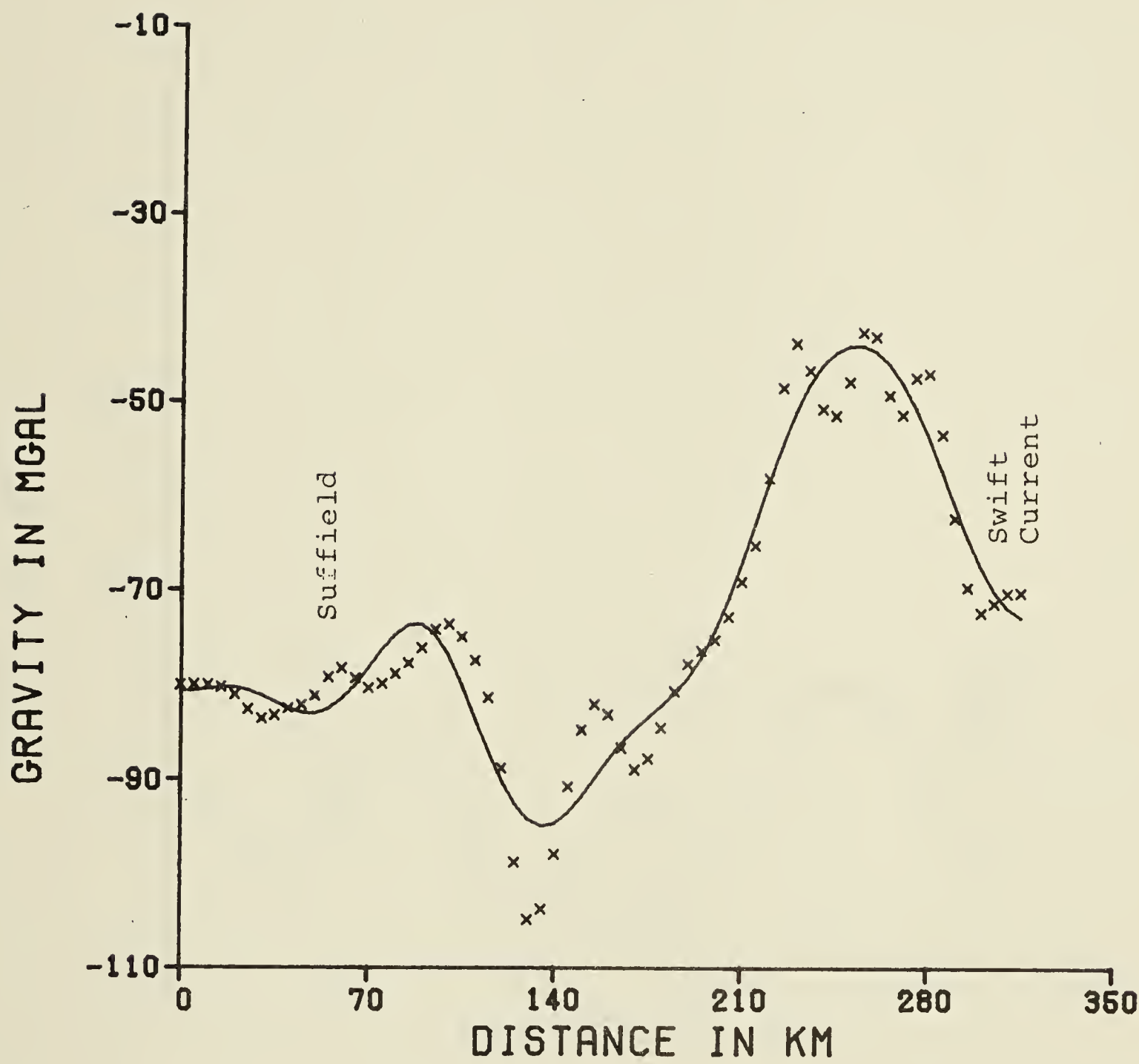


Figure 4.10: Comparison between observed gravity and gravity calculated from inversion model of Fig 4.9.

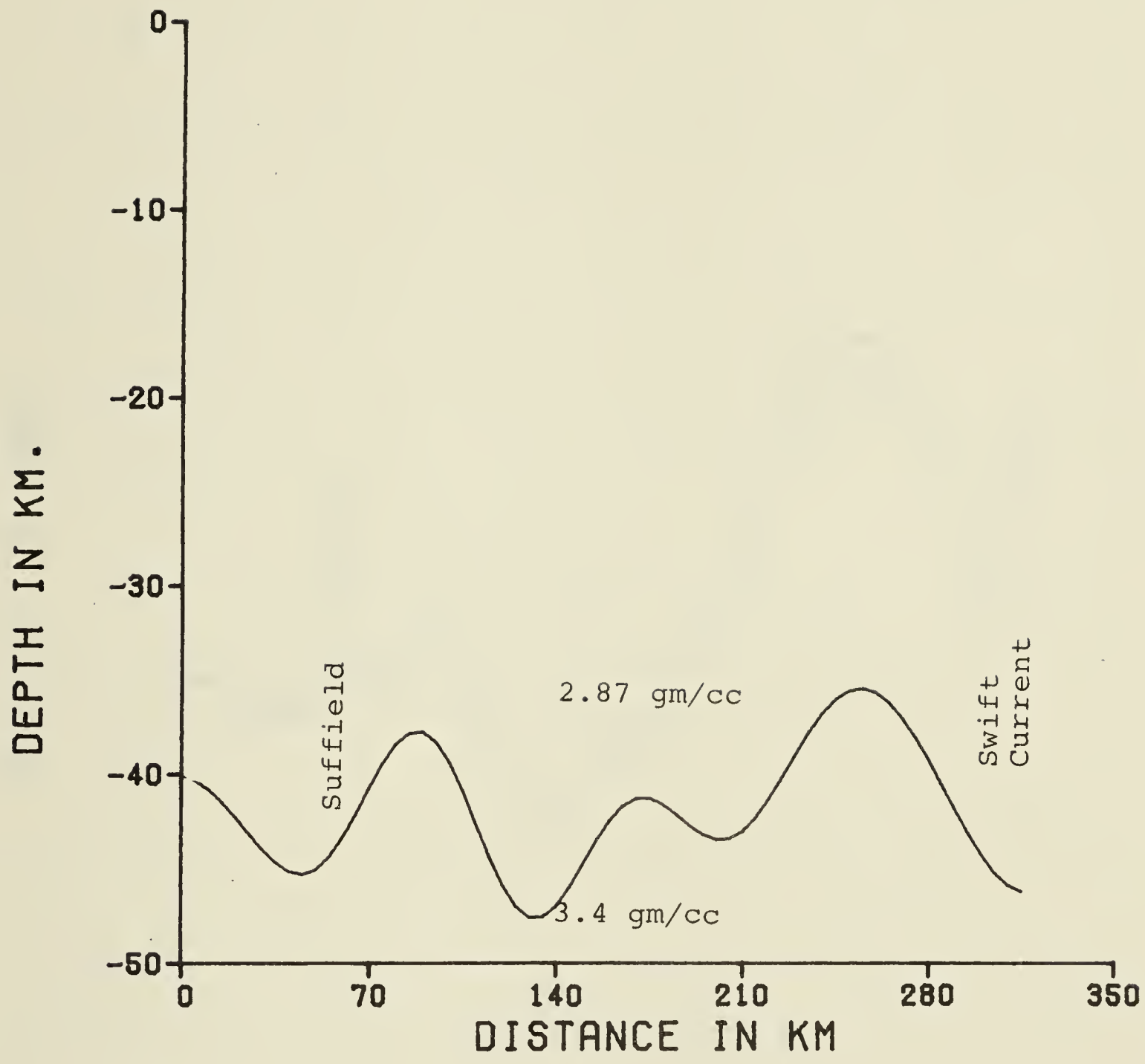


Figure 4.11: Inversion model of Swift Current-Suffield profile assuming crustal model IV.

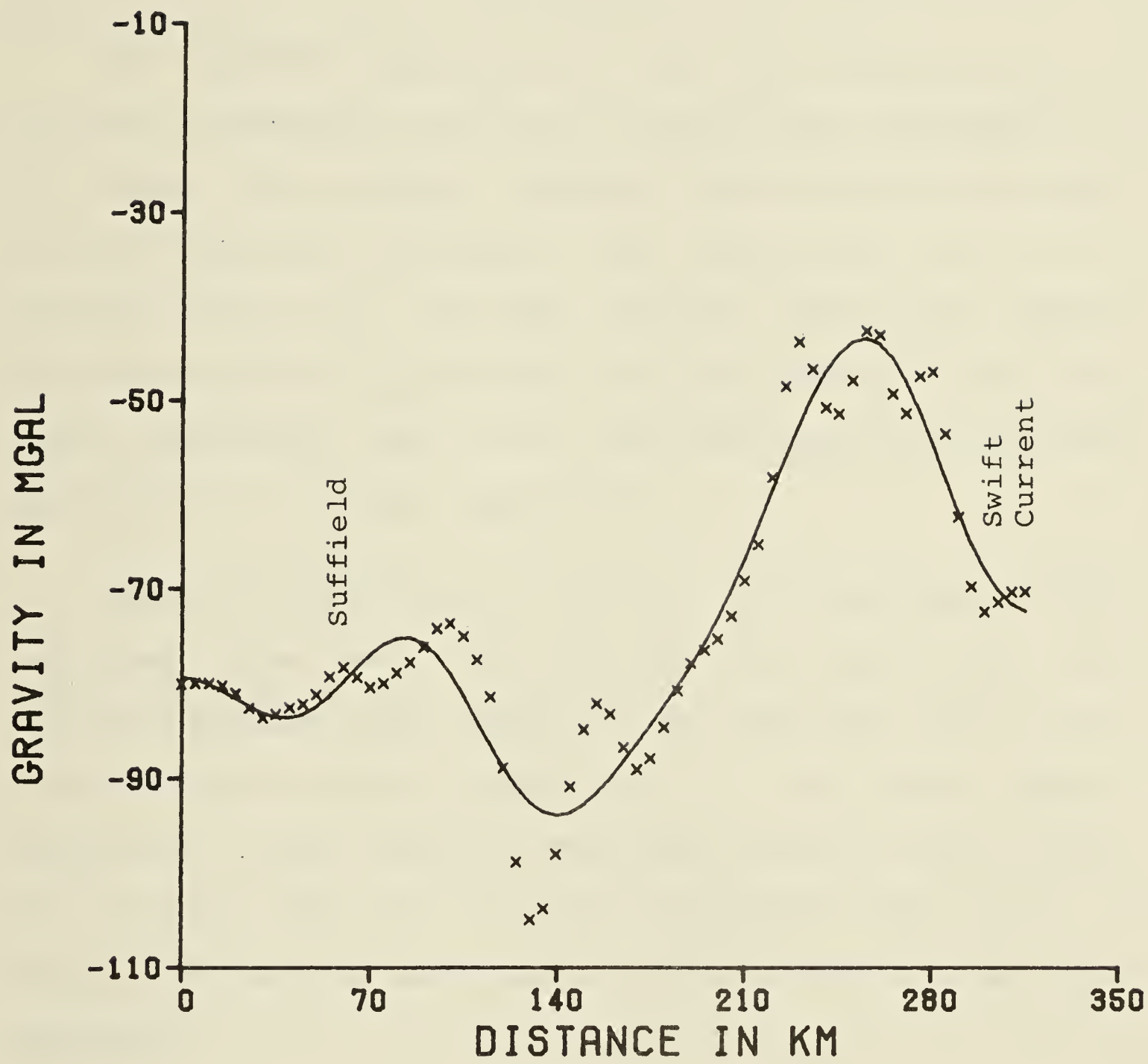


Figure 4.12: Comparision between observed gravity and gravity calculated from inversion model of Fig 4.11.

The inversion models and the gravity profiles from inversion for the four different crustal models are shown in Fig. 4.5, 4.6, 4.7, 4.8, 4.9, 4.10, 4.11 and 4.12.

Model I (Fig. 4.5 and Fig. 4.6)

The inverted topography of this model appears to be in reasonable agreement with that of Cumming and Kanasewich et al (1966). The average inverted depth of the Moho around Suffield (from 45 to 60 km in the figure) is 45.7 km , compared with 46.9 km from seismic data. The average inverted depths of the ARD (34.5 km) and MRD (11.5 km) also agree reasonably well with those obtained by Cumming and Kanasewich et al (1966, Table III).

Seismic determinations (Cumming and Kanasewich 1966) indicated that east of Suffield the crust thins out gradually towards Swift Current. Such trend can also be seen in the inversion model. Though there is no clear seismic indication of the relief of the Moho between 70 and 140 km, this does not mean the inverted topography of this area is unreal. It is just that there was insufficient seismic data available.

The agreement between the observed and the anomaly calculated from the inversion model is shown in Figure 4.6.

Models II, III and IV (Fig. 4.7, 4.8, 4.9, 4.10, 4.11 and 4.12)

Generally speaking, the inverted topography of the Moho of these models is of similar shape as that of Model I; and all 3 models show crustal thinning towards Swift Current.

The inverted depths of the Moho and MRD around Suffield of Model II appear to be in reasonable agreement with that obtained from seismic determination (Cumming and Kanasewich, 1966). The same is true for the inverted depths of the Moho and ARD of Model III and the Moho of Model IV.

A comparison of the inverted shape of the Moho of the 4 models shows that Models I and II, which exhibit similar relief, have the lowest relief of all models; followed by Models III and IV in ascending order. The reason why Model IV and III have relatively higher relief is obvious: to account for a given gravity profile the topographic relief of a structure at greater depth has to be higher than that of a shallow structure. The agreement between the observed gravity and the anomalies calculated from the 3 inversion models is shown in Fig. 4.8, 4.10 and 4.12.

On the whole, the anomalies computed from all 4 inversion models fit the original observations quite well. The short wavelength anomalies probably arise from error in using isopach maps to compute the sediment gravity; the non-two-dimensionality of the sediment-crustal boundary and the effect of possible additional shallow geological features, may also contribute significantly to these anomalies.

Swift Current - Winnipeg

The observed gravity of this segment of Profile (1) is shown in Figure 4.13; while the reduced gravitational profile is shown in Figure 4.14. Procedure similar to that

used on the western segment was employed here as well. The data series had 256 points; at a sampling interval of 7 km Inversion parameters, together with densities, depths and thicknesses of each layer, used for the four different models are shown in Table IV.

It can be observed from Table IV that the density of layer B, and the thicknesses of various layers at Swift Current are different from those at Winnipeg. Linear interpolation was employed to find the densities and thicknesses of intermediate stations. Again the depth of the Moho at Swift Current provides the necessary constraint required for choosing the right Z . The depths of the Moho ARD, and MRD at Swift Current are assumed at 43.2, 33.4 and 10.4 km respectively.

Table IV

MODEL I

INVERSION PARAMETERS		Z =32.5 km	FRACTION=0.3
		k =0.087	OFFSET=-250.0 mgal
		k =0.057	ITER=9
LOCATION		SWIFT CURRENT	WINNIPEG
Average	A	8.38	18.0
Thickness of	B	23.00	7.5
Layer (km)	C	9.80	8.5
Average	A	2.73	2.73
Density	B	2.80	2.96
of	C	3.17	3.17
Layer (gm/c.c.)	D	3.40	3.40

MODEL II

INVERSION PARAMETERS		Z =32.2km	FRACTION=0.3
		k =0.087	OFFSET=-250.0 mgal
		k =0.057	ITER=5
LOCATION		SWIFT CURRENT	WINNIPEG
Average Thickness	A	8.38	18.0
of Layer (km)	BC	32.80	16.0
Average Density	A	2.73	2.73
of	BC	2.92	3.07
Layer (gm/c.c.)	D	3.40	3.40

MODEL III

INVERSION PARAMETERS		Z =32.1km k =0.087 k =0.057	FRACTION=0.3 OFFSET=-250.0 mgal ITER=6
LOCATION		SWIFT CURRENT	WINNIPEG
Average Thickness of Layer (km)	AB	31.38	25.5
	C	9.80	8.5
Average Density of Layer (gm/c.c.)	AB	2.78	2.79
	B	3.17	3.17
	D	3.40	3.40

MODEL IV

INVERSION PARAMETERS		Z =30.0 km k =0.086 k =0.057	FRACTION=1.0 OFFSET=-250.0 mgal ITER=7
LOCATION		SWIFT CURRENT	WINNIPEG
Average Thickness of Layer (km)	ABC	41.18	34.0
Average Density of Layer (gm/c.c.)	ABC	2.87	2.89
	D	3.40	3.40

DEPTH OF INTERFACES

	LOCATION DISCONTINUITY	SWIFT CURRENT	WINNIPEG
Average Depth of (km)	M.R.	10.40	18.0 ± 3.0
	A.R.	33.40	25.5 ± 3.5
	Moho.	43.20	34.0 ± 3.0

Table IV. Swift Current - Winnipeg Inversion Parameters.

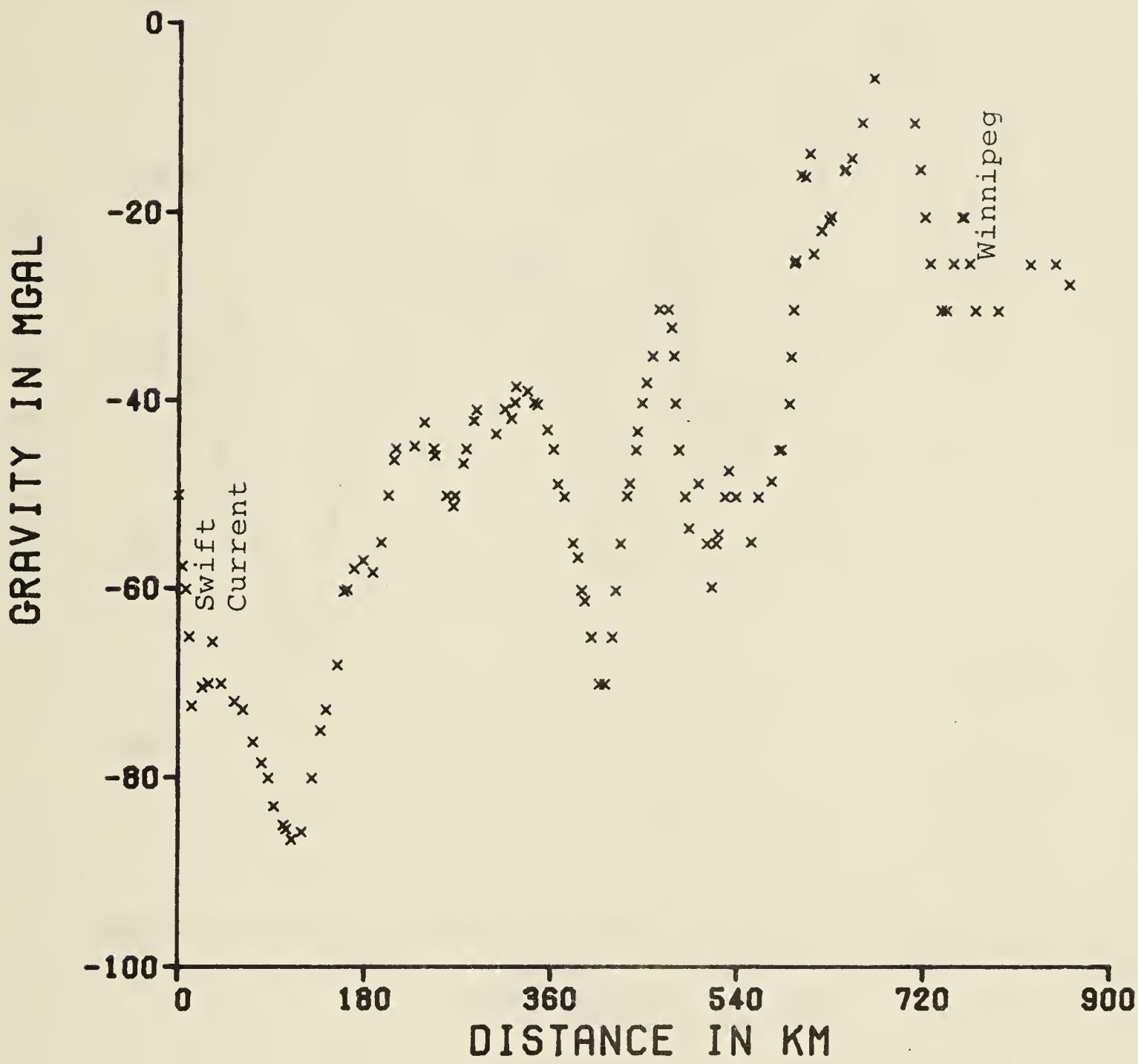


Figure 4.13: Gravitational observation of the Swift Current-Winnipeg profile.

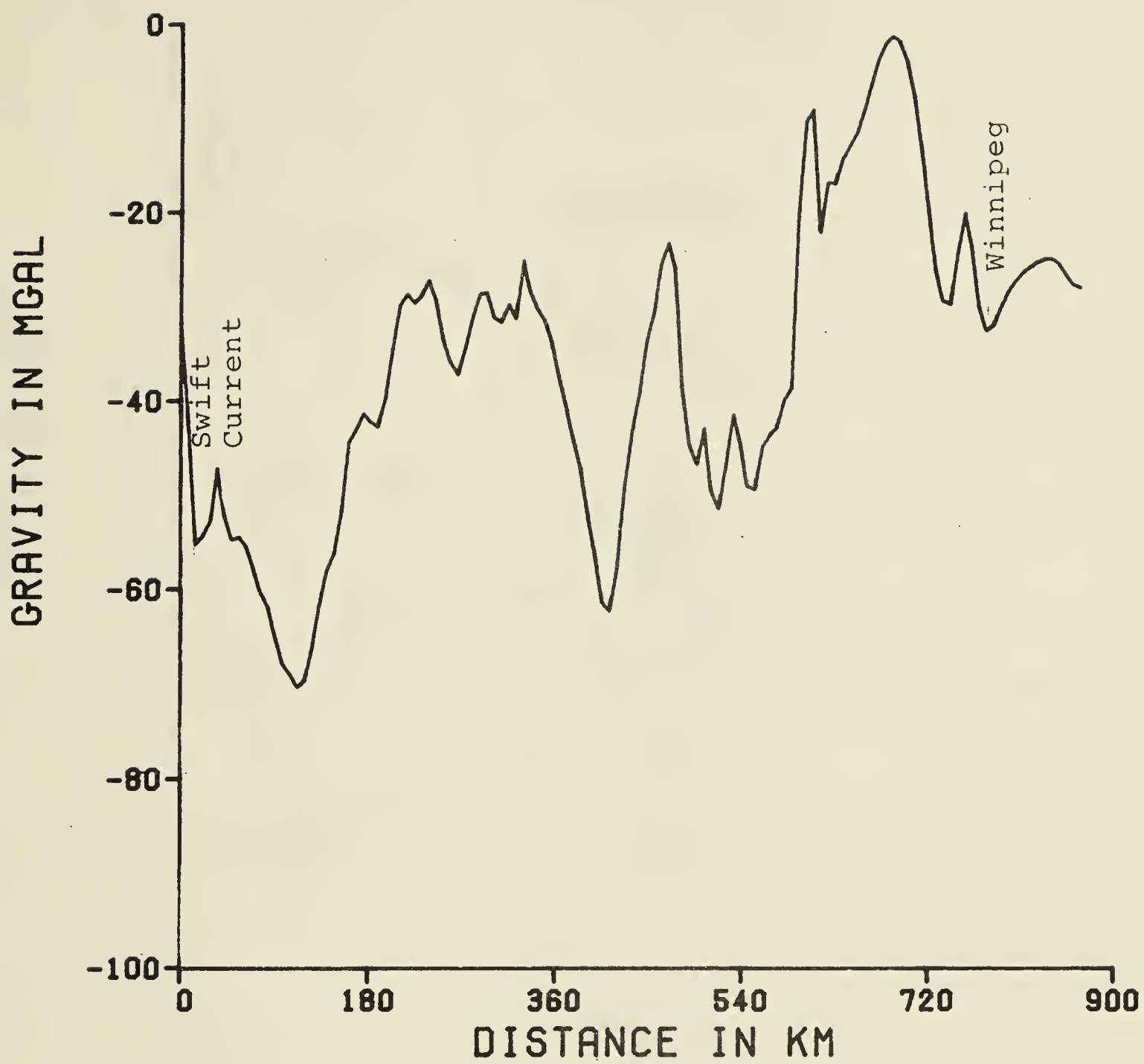


Figure 4.14: Reduced gravitational observation of the Swift Current-Winnipeg profile.

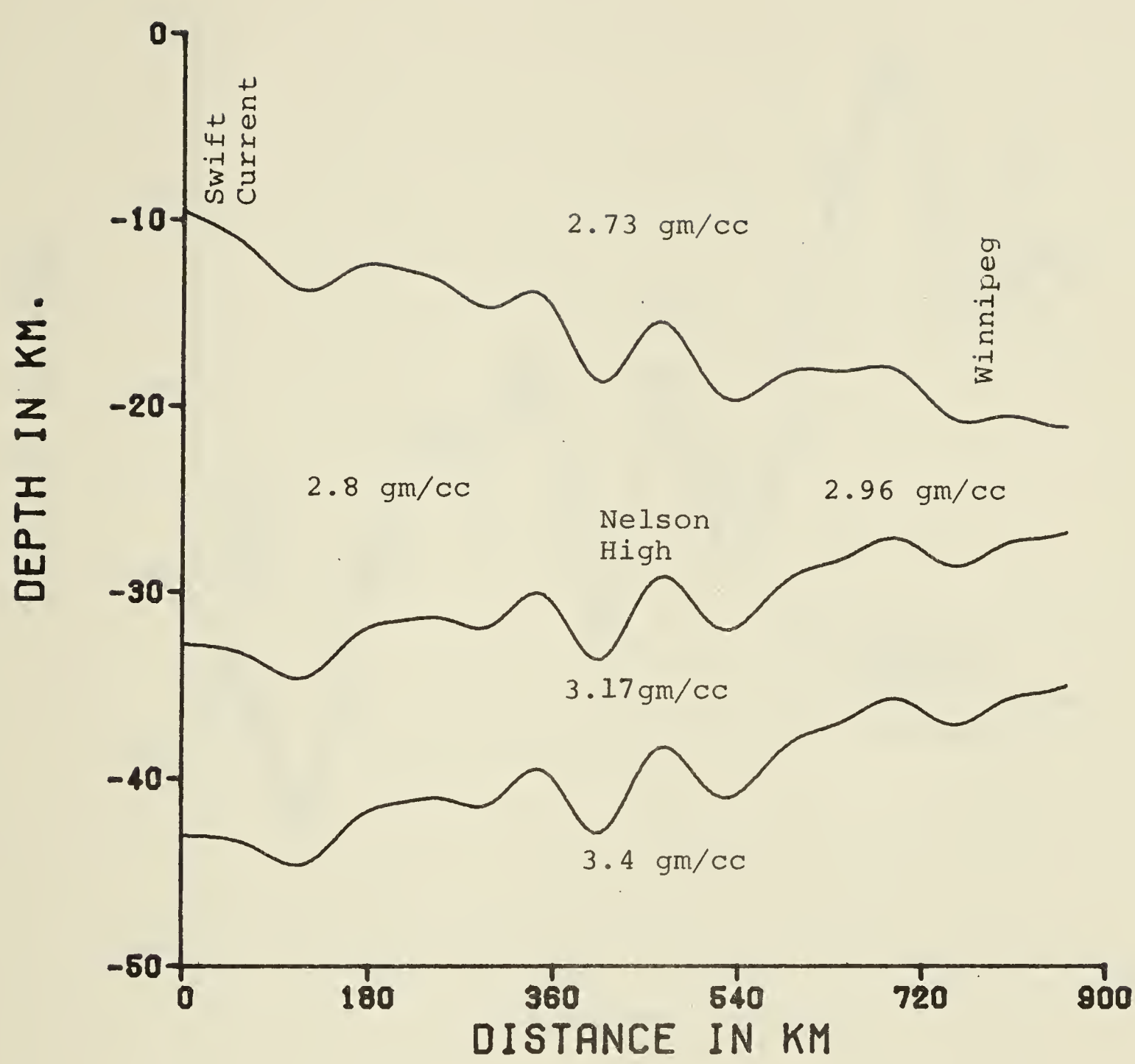


Figure 4.15: Inversion model of Swift Current-Winnipeg profile assuming crustal model I. Vertical exaggeration =18

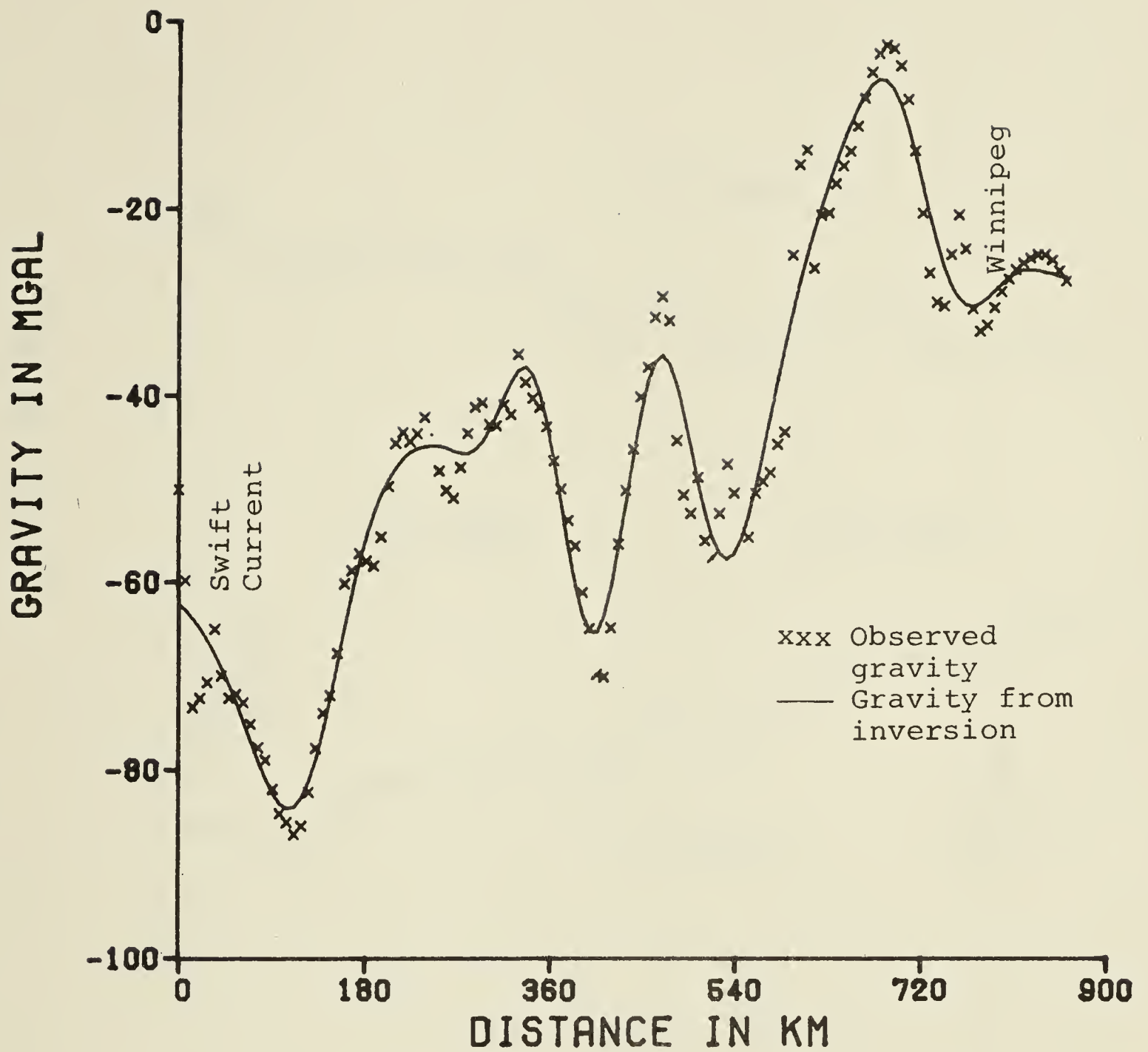


Figure 4.16: Comparison between observed gravity and gravity calculated from inversion model of Fig 4.15.

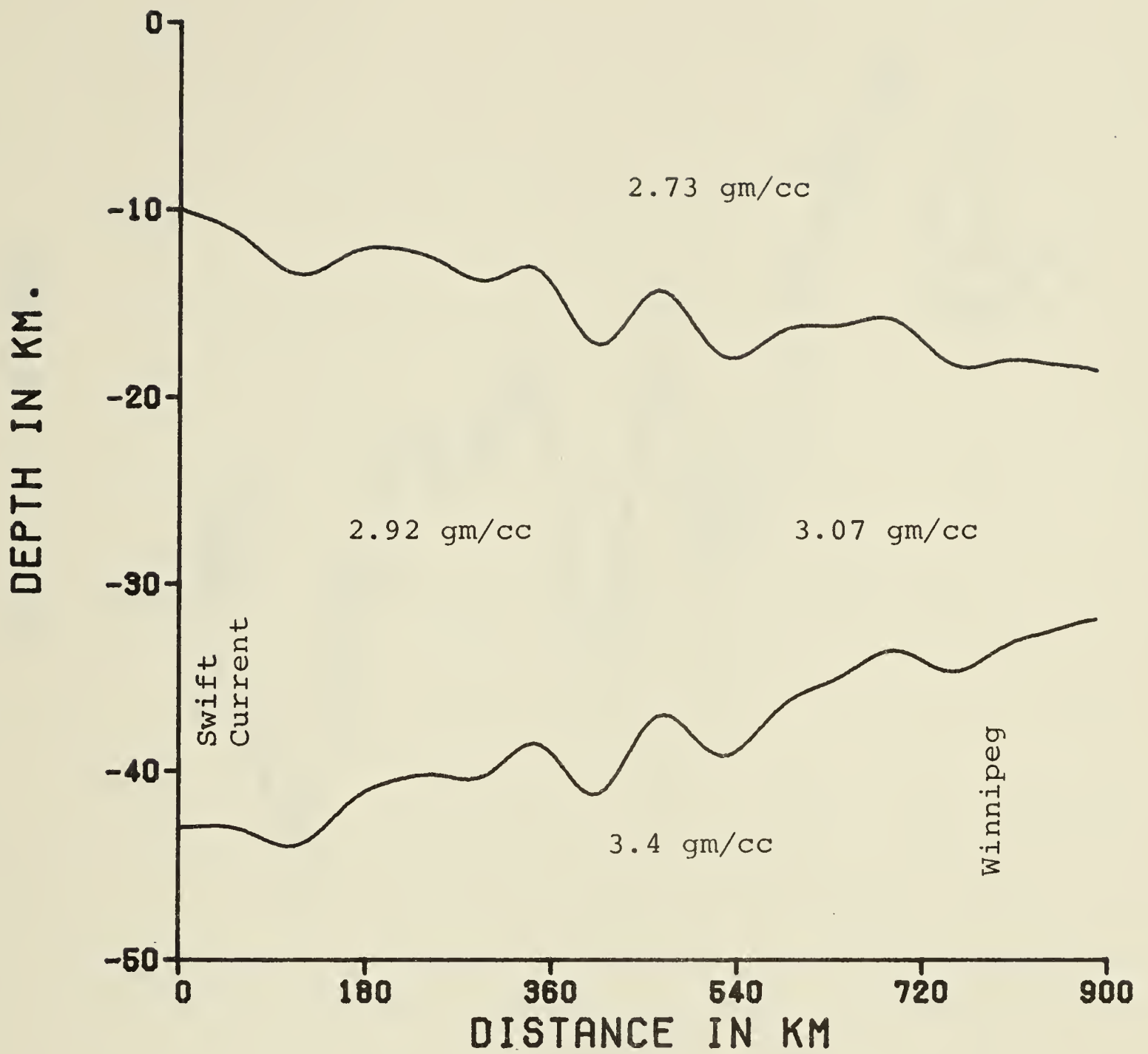


Figure 4.17: Inversion model of Swift Current-Winnipeg profile assuming crustal model II.

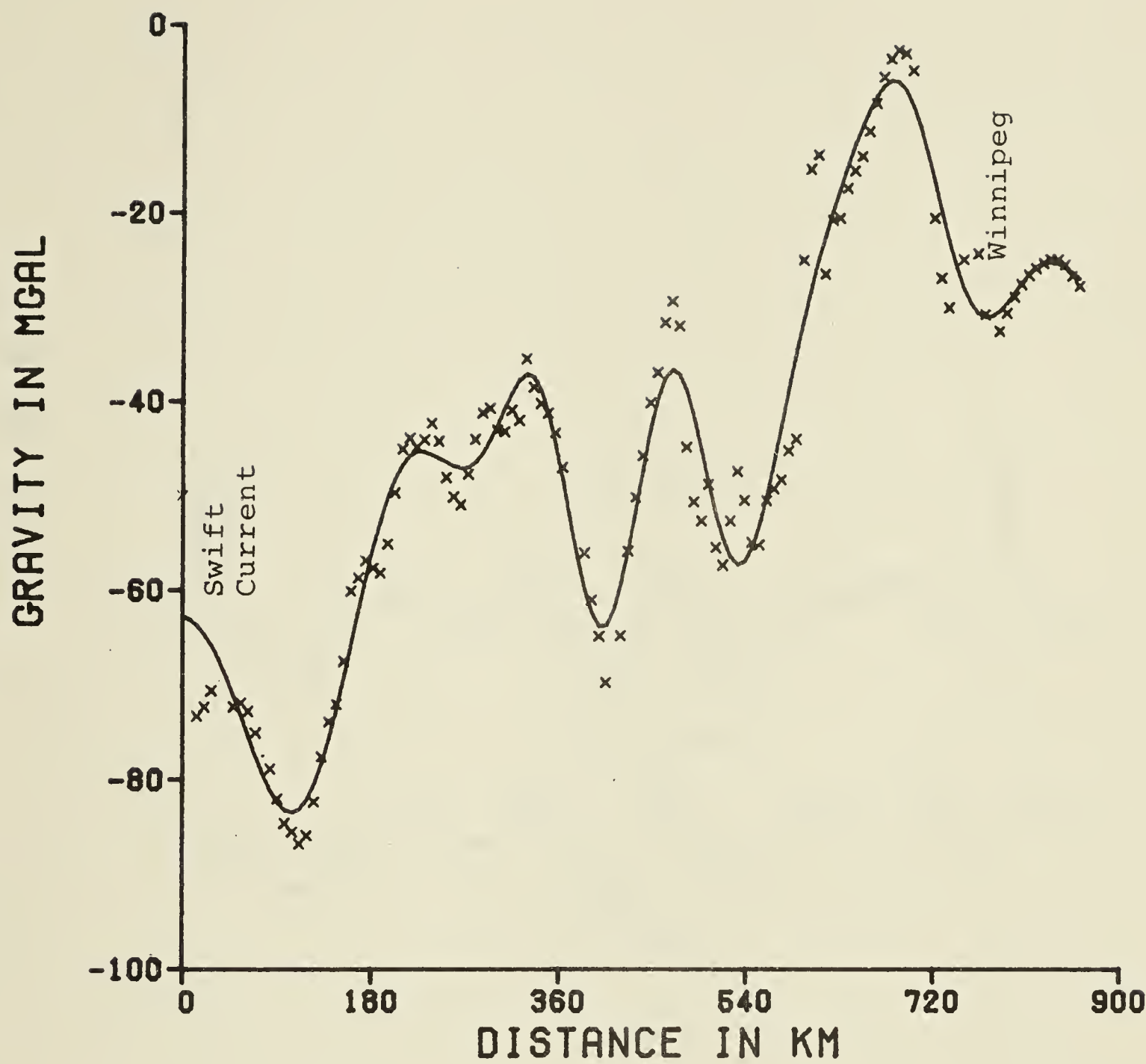


Figure 4.18: Comparison between observed gravity and gravity calculated from inversion model of Fig 4.17.

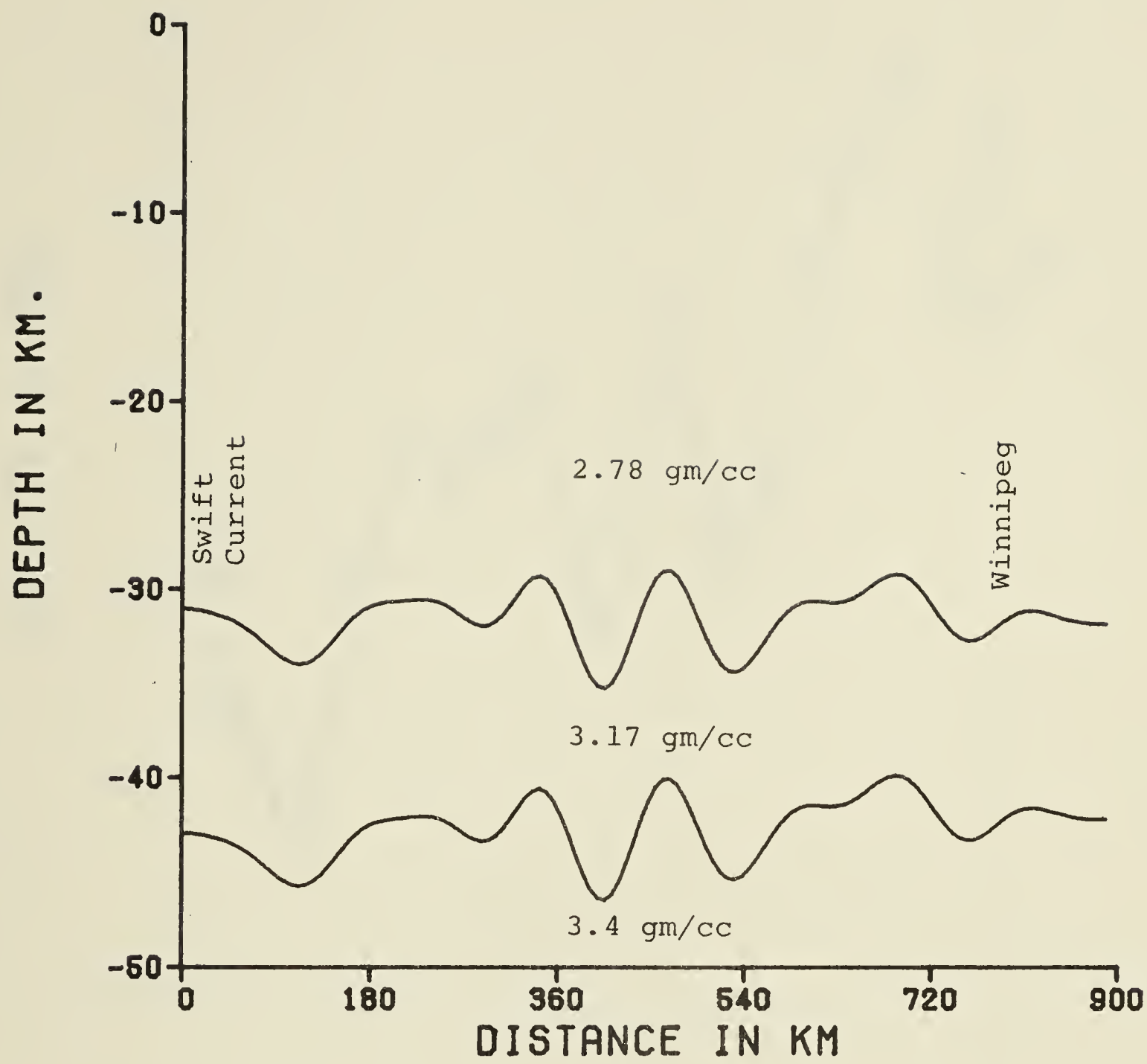


Figure 4.19: Inversion model of Swift Current-Winnipeg profile assuming crustal model III.

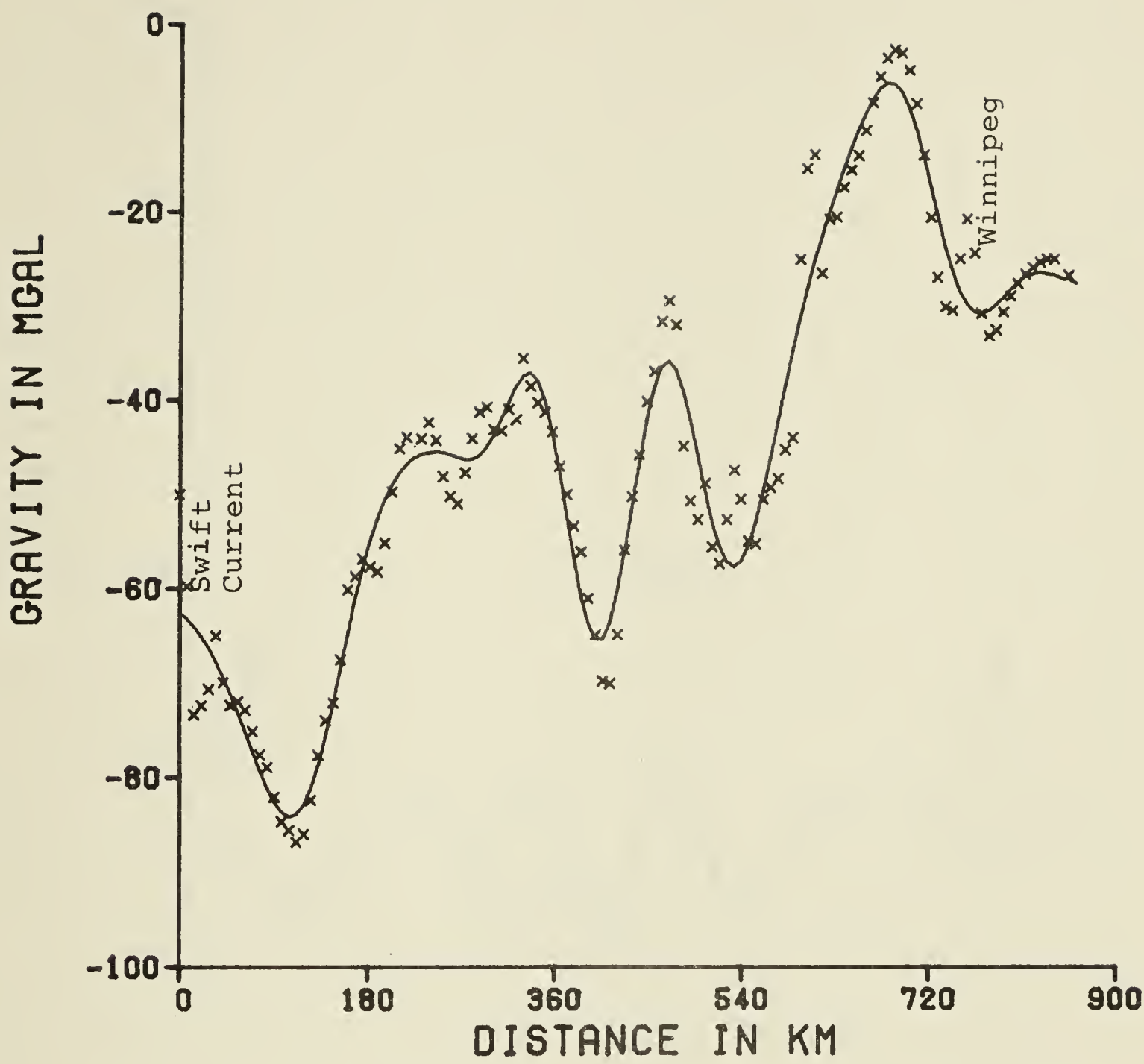


Figure 4.20: Comparson between observed gravity and gravity calculated from inversion model of Fig 4.19.

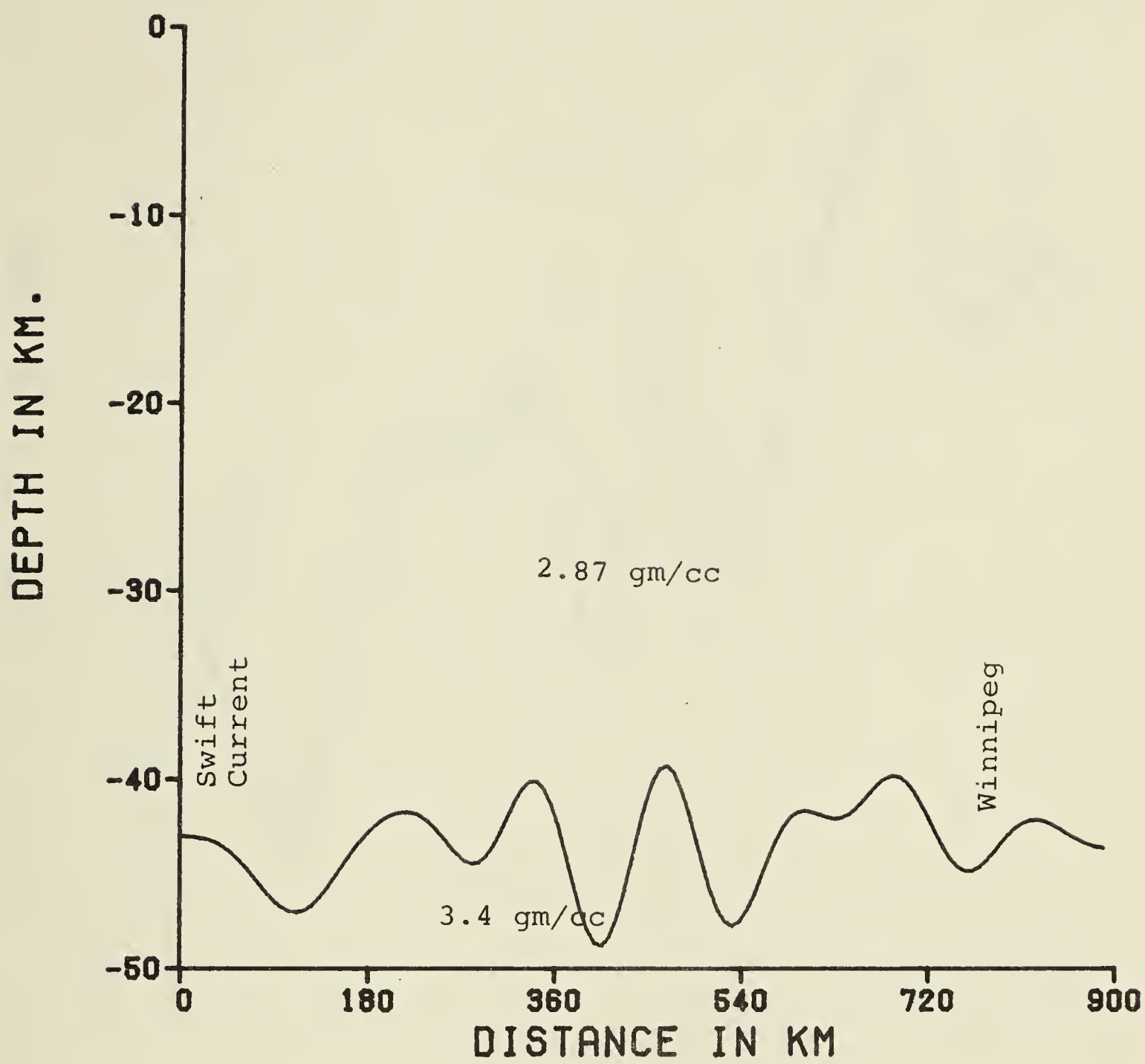


Figure 4.21: Inversion model of Swift Current-Winnipeg profile assuming crustal model IV.

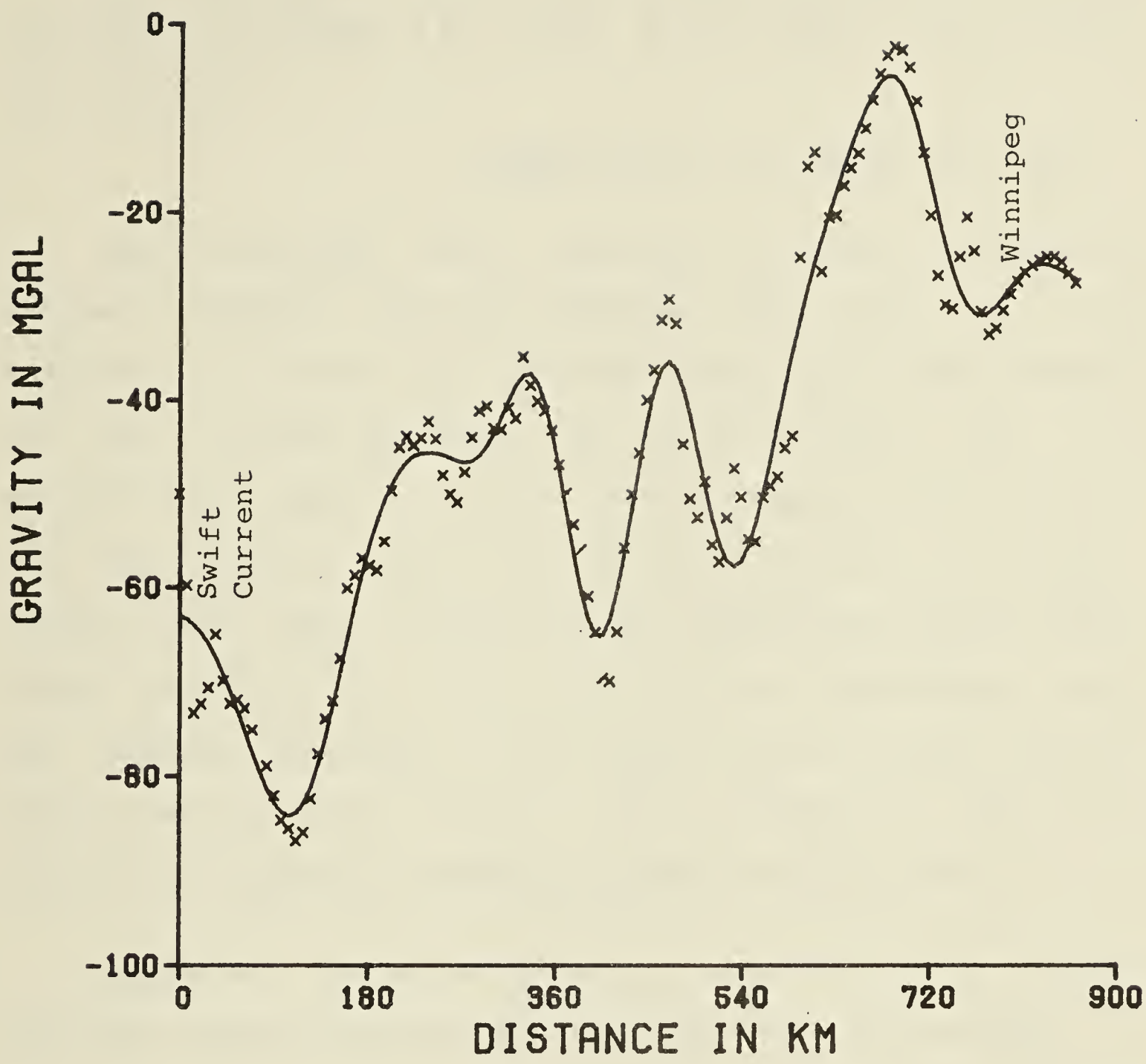


Figure 4.22: Comparison between observed gravity and gravity calculated from inversion model of Fig 4.21.

The inversion models and their gravitational profiles are shown in Figures 4.15, 4.16, 4.17, 4.18, 4.19, 4.20, 4.21 and 4.22.

Model I (Fig. 4.15 and Fig. 4.16)

This inversion model exhibits a gradual decrease in crustal thickness towards Winnipeg. The mean rate of thinning is (0.013). The inverted depths of the MRD and ARD and Moho around Winnipeg are 20.5, 28 and 36.5 km respectively; compared with the average depth of 18 ± 3 km for the MRD, 25.5 ± 3.5 km for the ARD and 34.0 ± 3 km for the Moho (Gurbuz 1969, 1970). The Moho shows considerable relief from 260 km to 540 km. The ridge around 470 km corresponds with the southern extension of the "Nelson River Bouguer gravity high". The east flank of this ridge corresponds with the Churchill - Superior boundary proposed by Bell (1971).

Figure 4.16 shows the gravity calculated from inversion fits the original gravitational observations rather well.

Model II (Fig. 4.17 and Fig. 4.18)

This model exhibits similar topographic relief as that obtained in Model I. The crustal-thinning trend which was indicated in Model I is also revealed in this model. However, the mean rate of crustal-thinning, which is 0.015, is greater in this model. The inverted depths of the MRD and Moho around Winnipeg are 18 and 34 km respectively. These values agree well with that obtained by seismic determination (Gurbuz 1967, 1970).

The agreement between the observed gravity and the anomalies calculated from the inversion model is shown in Figure 4.18.

Model III and IV (Fig. 4.19 to 4.22)

Even though the inverted topography of the Moho of these two models is of similar shape as that obtained in Model I and II, however, there are significant differences. Firstly, the structural relief is considerably stronger in these two models, a phenomenon which is consistent with that observed in Model III and IV of the Suffield - Swift Current profile. Secondly, though these two models still exhibit crustal-thinning towards Winnipeg, the rate of thinning is much lower than that in Model I and II. Thirdly, the inverted depths of the ARD of Model III, and the Moho of Model III and IV around Winnipeg fail to reach the average depths of these two interfaces determined by seismic data (Gurbuz 1967, 1970). Around Winnipeg the inverted depths of the ARD and Moho for model III are 32 km and 43 km respectively; compared with 25.5 ± 3.5 km for the ARD and 34.0 ± 3.0 km for the Moho (Gurbuz 1967, 1970). For Model IV the inverted depth of the Moho is 44 km which is about 10 km deeper than the average value determined by Gurbuz (1967, 1970).

Although the two gravitational waveforms (Fig 4.20 and 4.22) calculated from these two models fit the observed gravitational anomalies well, we do not consider these two

models acceptable because the inverted depths of the ARD and Moho around Winnipeg do not agree with that determined by seismic surveying (Gurbuz 1967, 1970).

4.4. Inversion of Profile (2)

This profile runs along latitude $51^{\circ}10.5'N$ and extends from longitude $107^{\circ}50'W$ to $96^{\circ}00'W$. It will be referred to as the "Elbow (longitude $106^{\circ}35'W$, latitude $51^{\circ}13'N$) - Lake Winnipeg" profile. Seismic data (Gurbuz 1969, 1970) indicated that depths of the MRD and Moho at latitude $51^{\circ}11'N$ and longitude $96^{\circ}23'W$ are 22.0 and 32.0 km respectively. These values are the assumed depths of these interfaces at 840 km. There is no seismic indication of the presence of the ARD in this area. To conform with the requirement of model I the ARD is assumed to be at a depth of 25.5 km which is the same as that used in the Swift Current-Winnipeg profile. The densities used for this profile are the same as the Swift Current - Winnipeg profile, and they are shown in Table IV. Other inversion parameters are shown in Table 4-3.

Elbow - Lake Winnipeg

The original observed gravitational anomalies is shown in Fig. 4.23, and the reduced gravitational profile is shown in Fig. 4.24. Sampling interval was 7 km and the data series contained 258 points.

Model I, II, III and IV (Fig. 4.25 to Fig.

4.32)

The inverted shape of the Moho of this profile differs significantly from that of the southern profile. Besides, it displays more relief. The crustal thinning trend which was exhibited by their southern counterparts is also displayed by all these 4 models. However, the mean rate of crustal-thinning is much lower for model III and IV; a phenomenon which is also observed in the Swift Current - Winnipeg profile. The mean rate of crustal-thinning for Model I is 0.014 while that of Model II is 0.016.

The inverted depth of the MRD, ARD and Moho at $107^{\circ}50'W$ latitude are 9.3, 32 and 42.2 km respectively; compared with 10.4 km for the MRD, 33.4 km for ARD and 43.2 km for the Moho at Swift Current. For Model II, the inverted depth of the Moho is 44.8 km while that of the MRD is 11.9 km. Like their counterparts in the Swift Current - Winnipeg profile the inverted depths of the ARD of Model III, and the Moho of Model III and IV at $107^{\circ}50'W$ latitude differ significantly from those determined at Swift Current.

Table V
MODEL I

INVERSION PARAMETERS		Z =32.3km k =0.087 k =0.057	FRACTION=0.3 OFFSET=-250.0 mgal ITER=14
LOCATION		ELBOW	LAKE WINNIPEG
Average	A	8.38	22.0
Thickness of	B	23.00	3.5
Layer (km)	C	9.80	6.5

MODEL II

INVERSION PARAMETERS		Z =35.1km k =0.087 k =0.057	FRACTION=0.3 OFFSET=-250.0 mgal ITER=6
LOCATION		ELBOW	LAKE WINNIPEG
Average Thickness	A	8.38	22.0
of Layer (km)	BC	32.80	10.0

MODEL III

INVERSION PARAMETERS		Z =24.6km k =0.087 k =0.057	FRACTION=0.3 OFFSET=-260.0 mgal ITER=5
LOCATION		ELBOW	LAKE WINNIPEG
Average Thickness	AB	31.38	25.5
of Layer (km)	C	9.80	6.5

MODEL IV

INVERSION PARAMETERS		Z =23.3km k =0.087 k =0.057	FRACTION=1.0 OFFSET=-240.0 mgal ITER=5
LOCATION		ELBOW	LAKE WINNIPEG
Average Thickness	ABC	41.18	32.0
of Layer (km)			

Table V. Inversion Parameters of Elbow - Lake Winnipeg profile.

OBSERVED GRAVITY

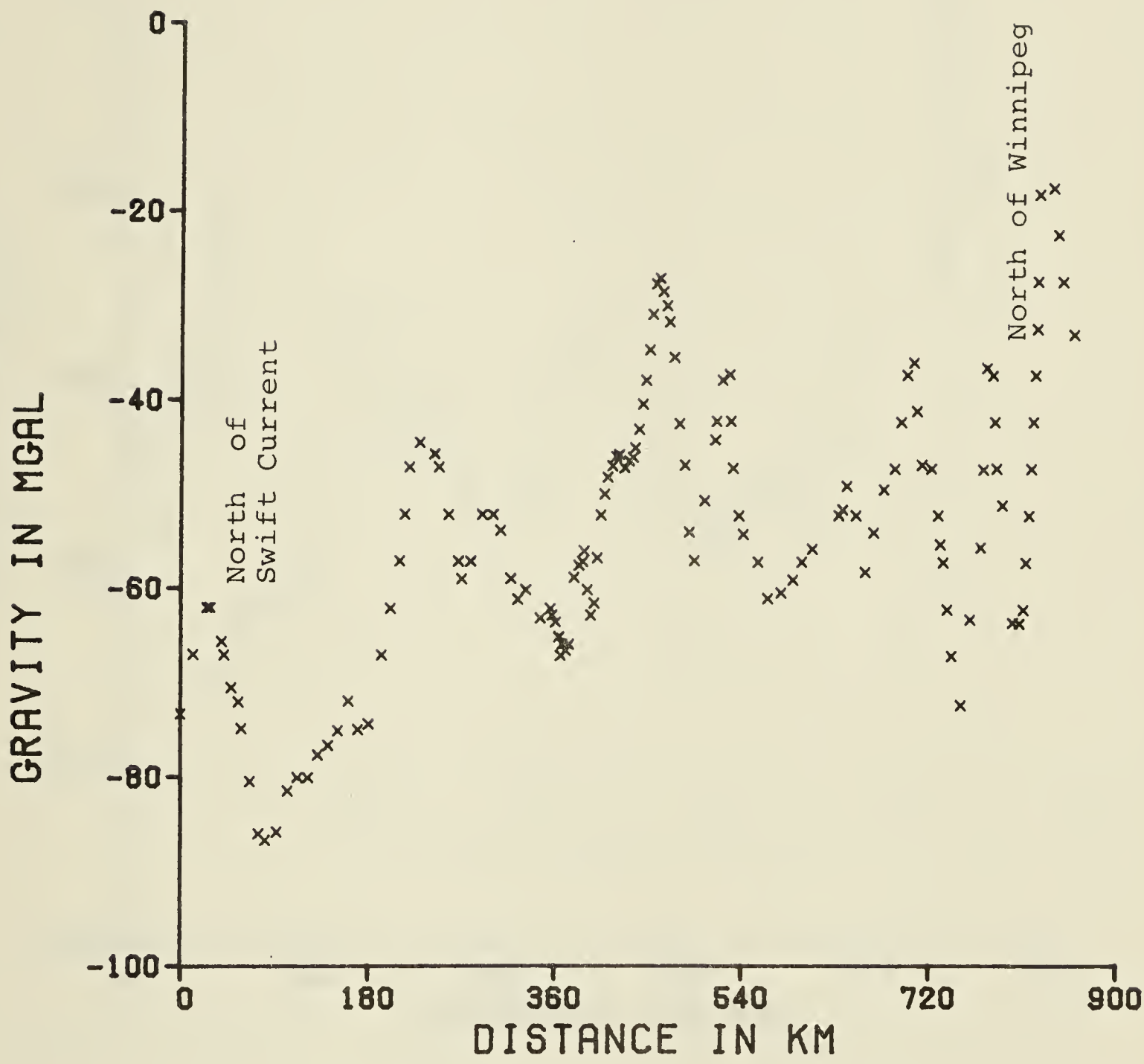


Figure 4.23: Gravitational observation of Elbow-Lake Winnipeg profile.

OBSERVED GRAVITY WITH SEDIMENT REMOVED

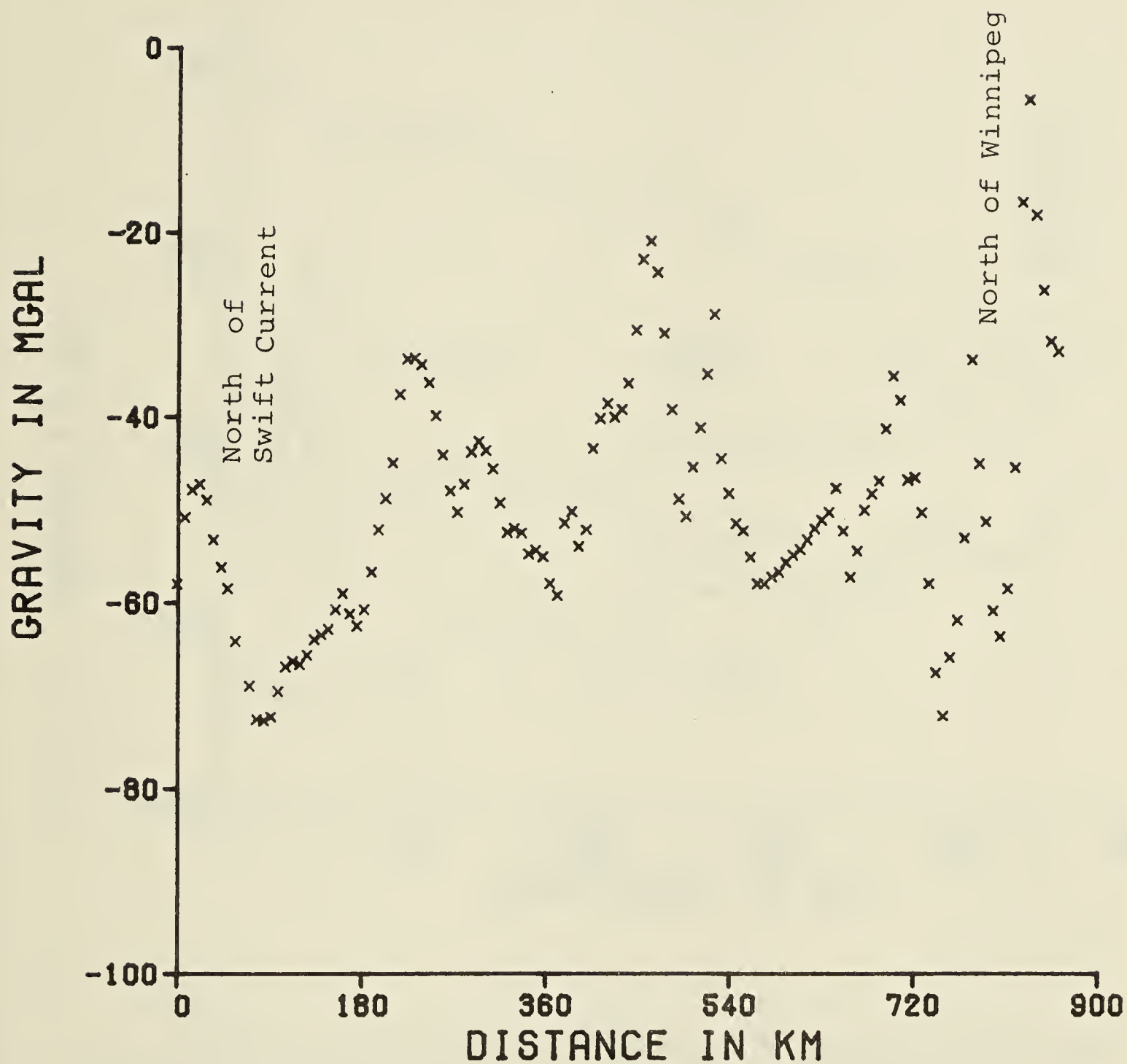


Figure 4.24: Reduced gravitational observation of the Elbow-Lake Winnipeg profile.

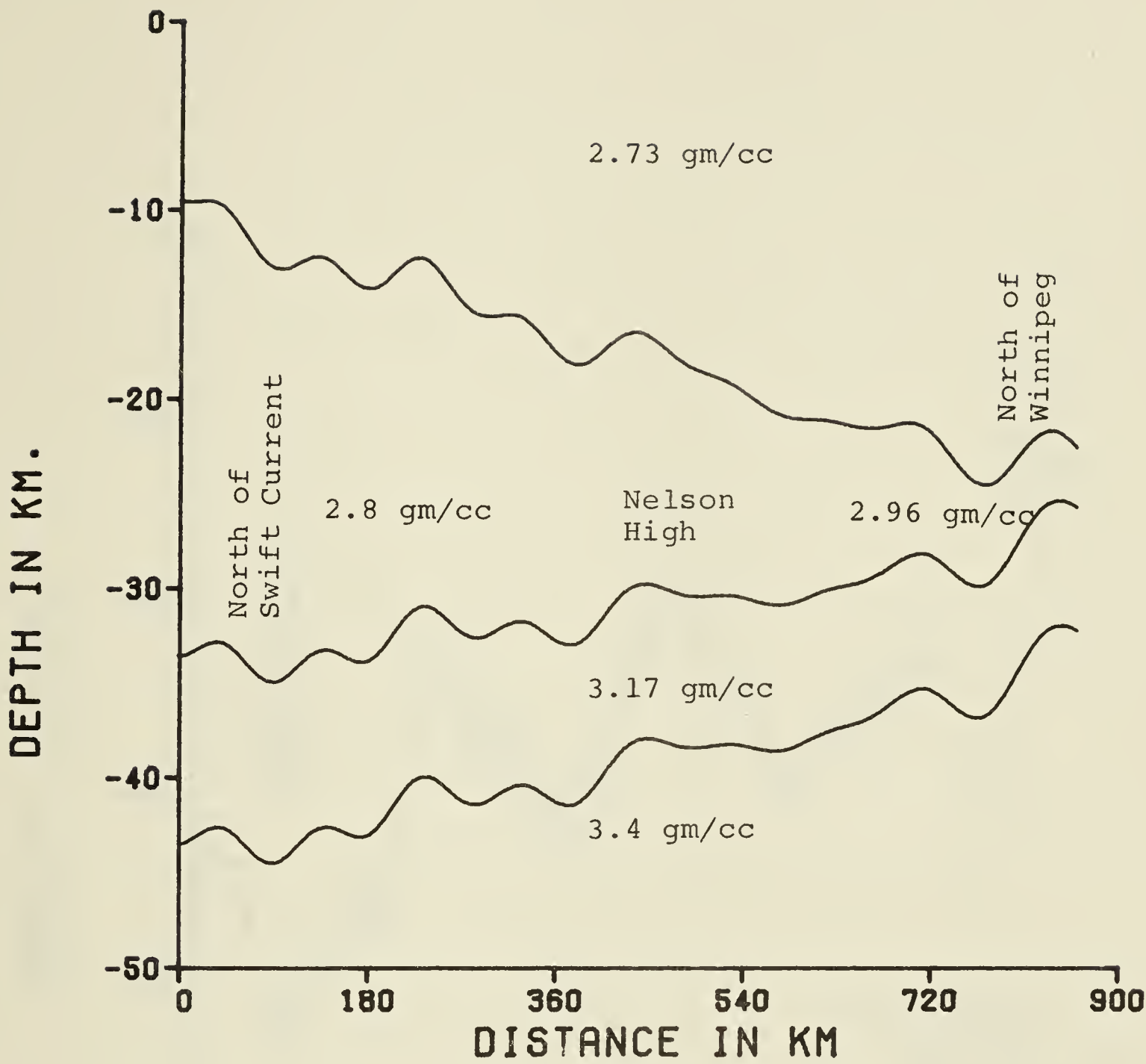


Figure 4.25: Inversion model of Elbow-Lake Winnipeg profile assuming model I. Vertical exaggeration =18.

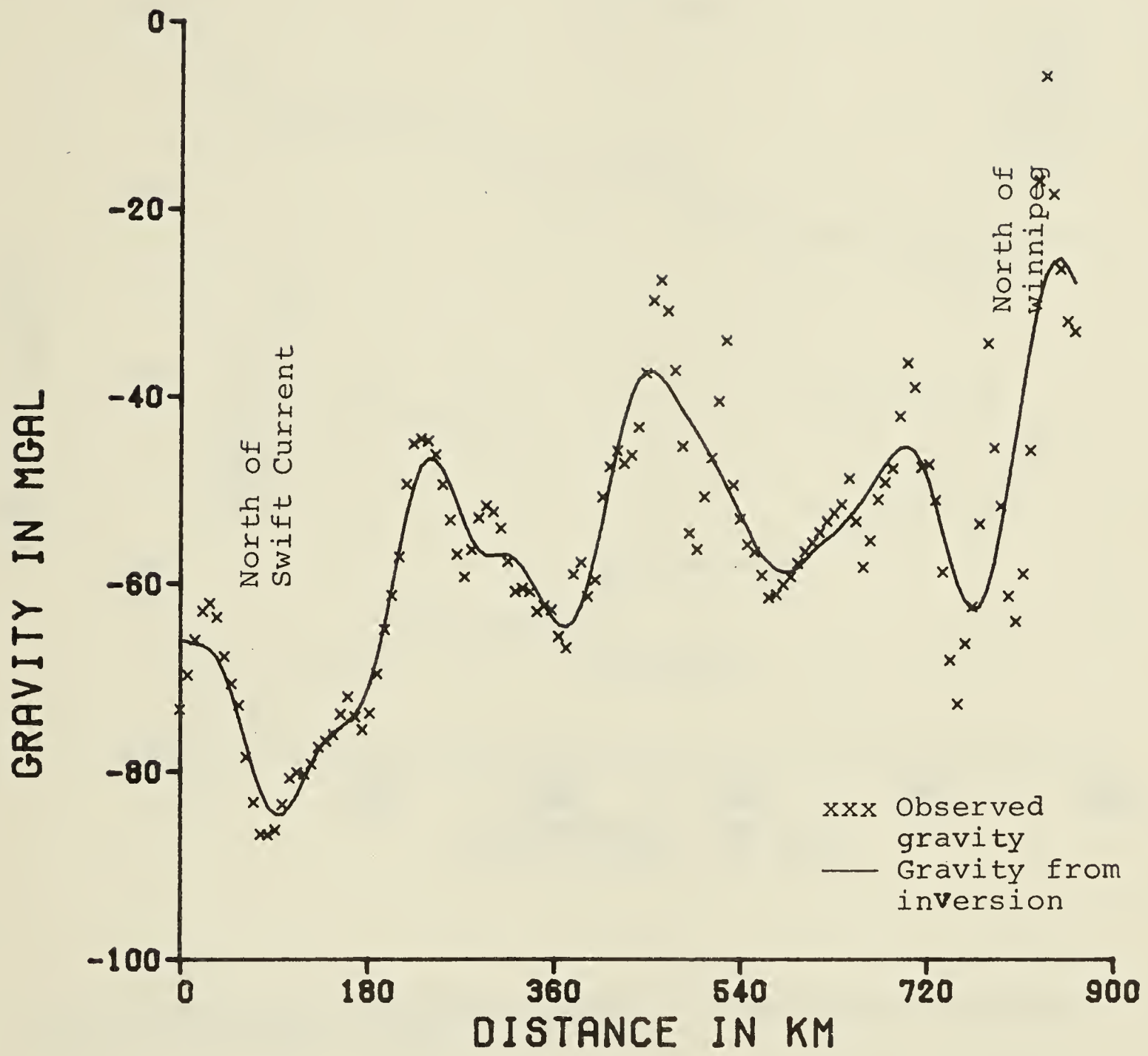


Figure 4.26: Comparison between observed gravity and gravity calculated from the inversion model of Fig 4.25.

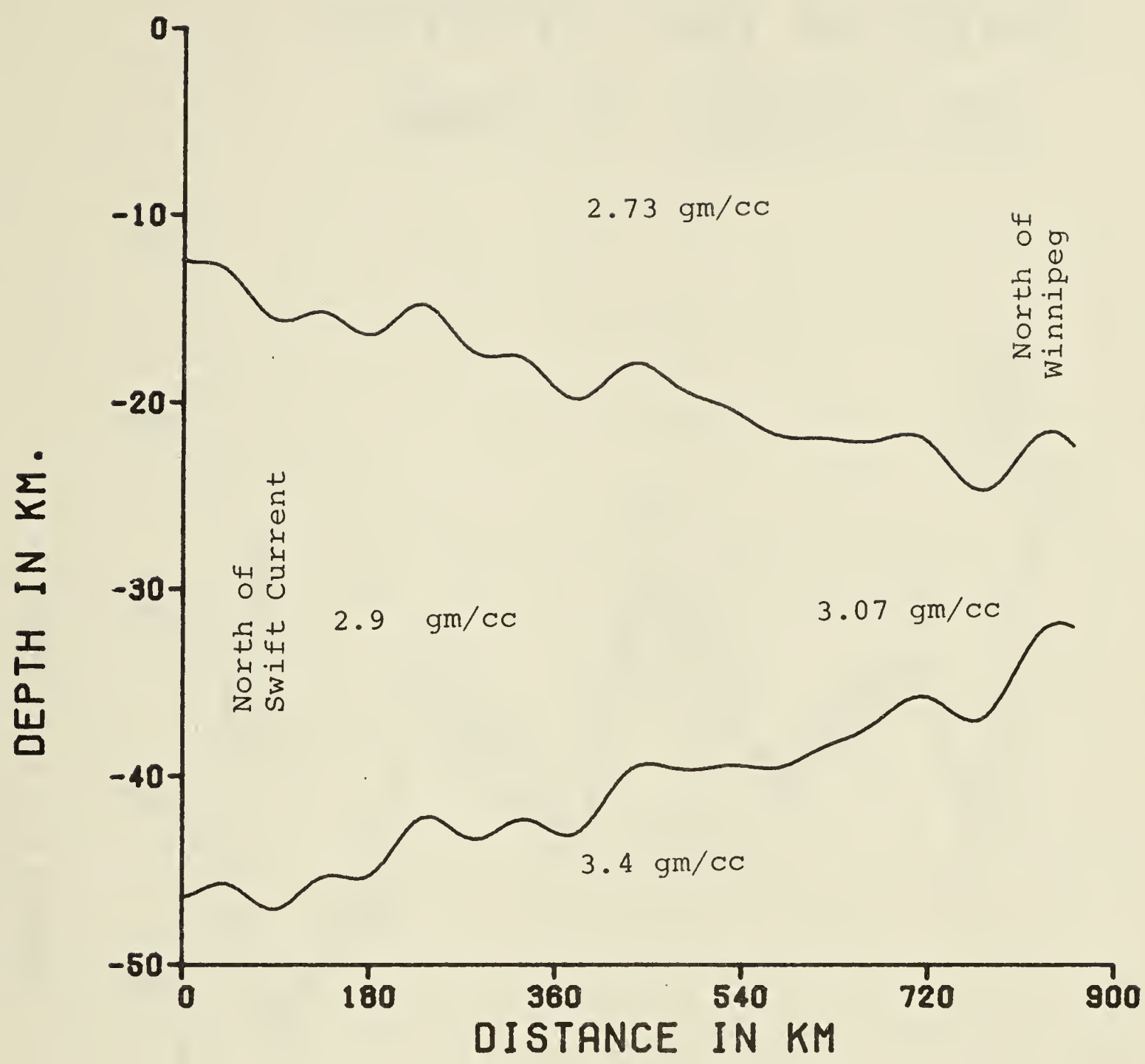


Figure 4.27: Inversion model of Elbow-Lake Winnipeg profile assuming crustal model II.

INVERTED AND ORIGINAL GRAVITY ANOMALIES

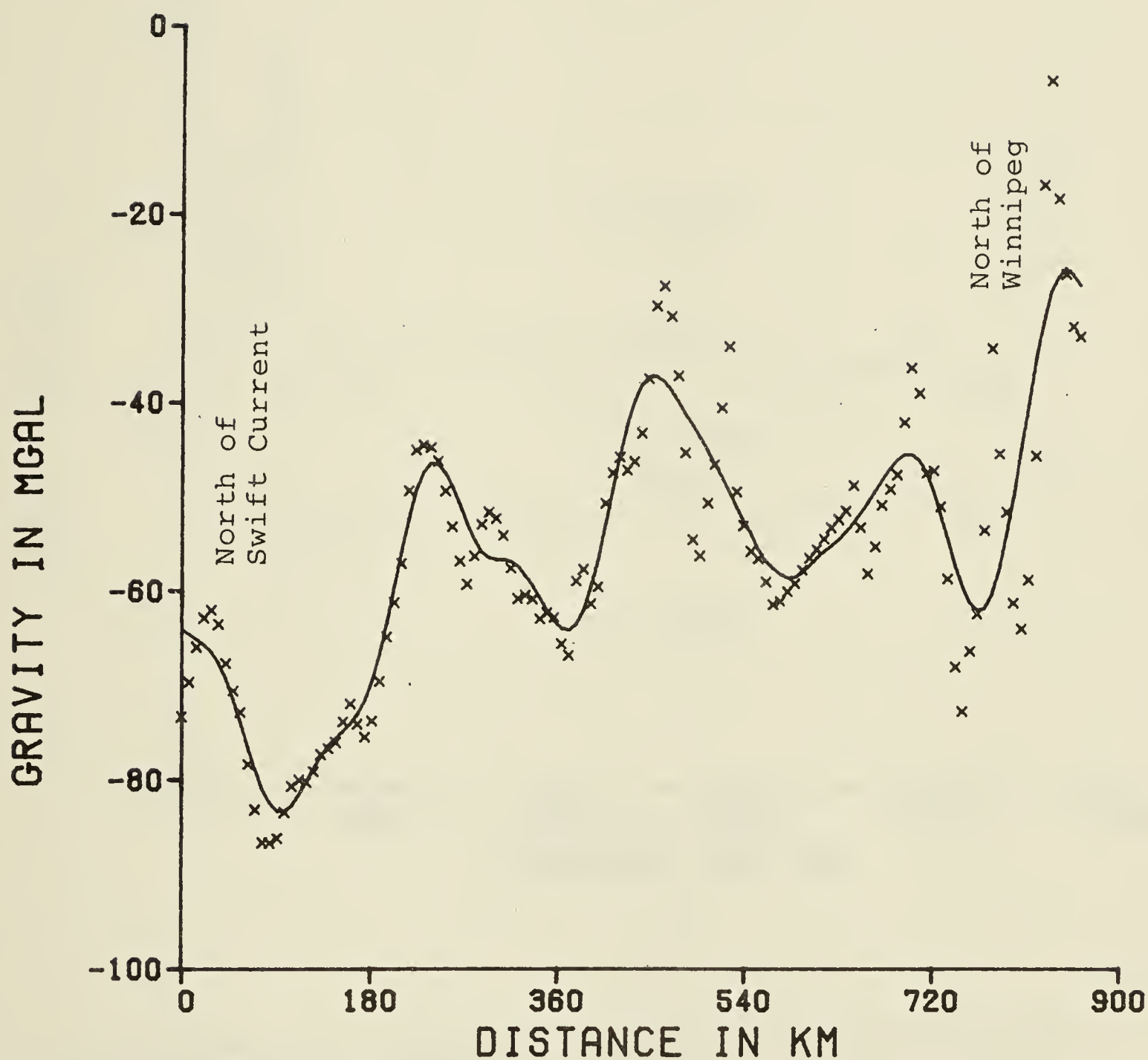


Figure 4.28: Comparison between observed gravity and gravity calculated from inversion model of Fig 4.27.

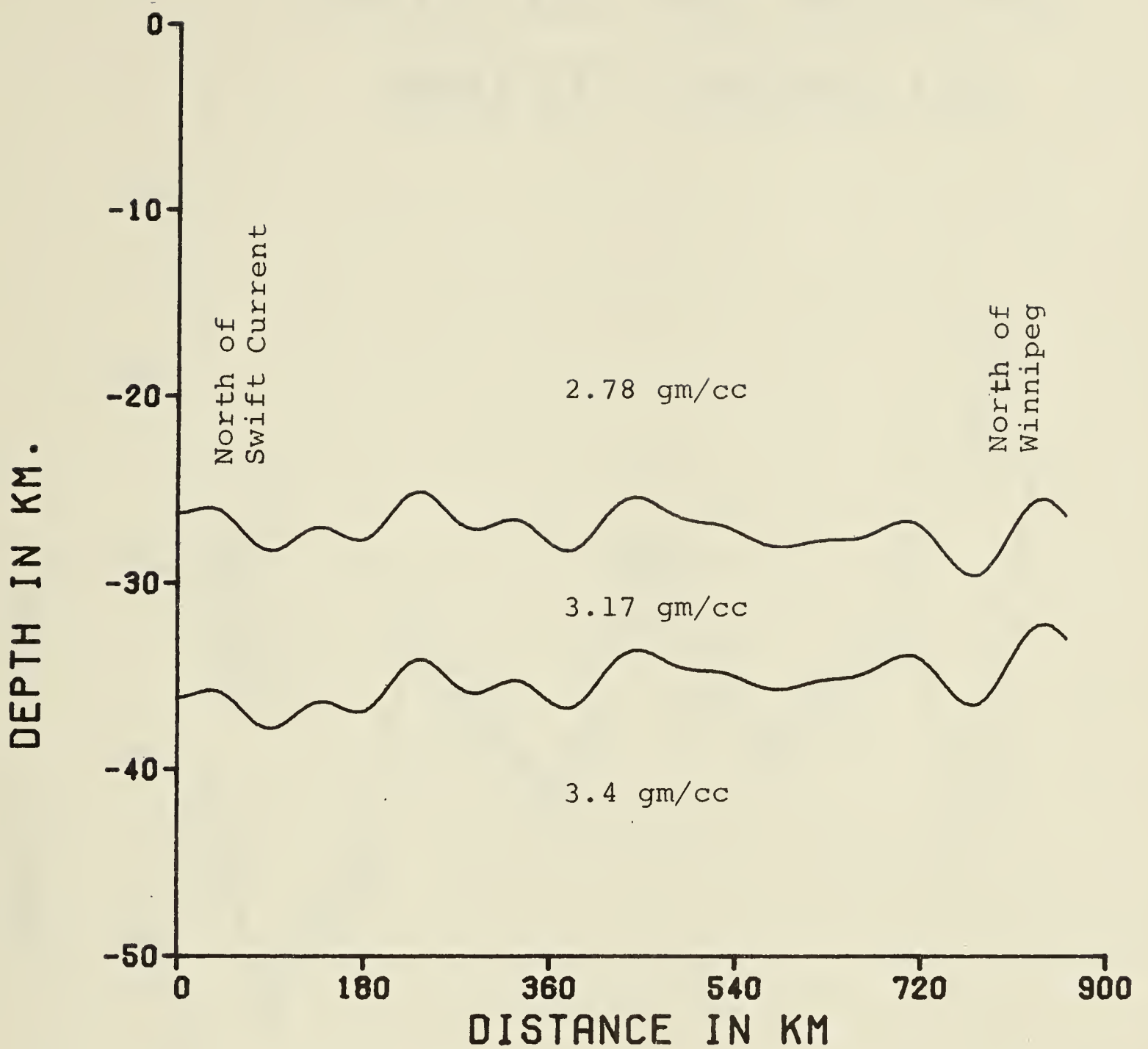


Figure 4.29: Inversion model of Elbow-Lake Winnipeg profile assuming crustal model III.

INVERTED AND ORIGINAL GRAVITY ANOMALIES

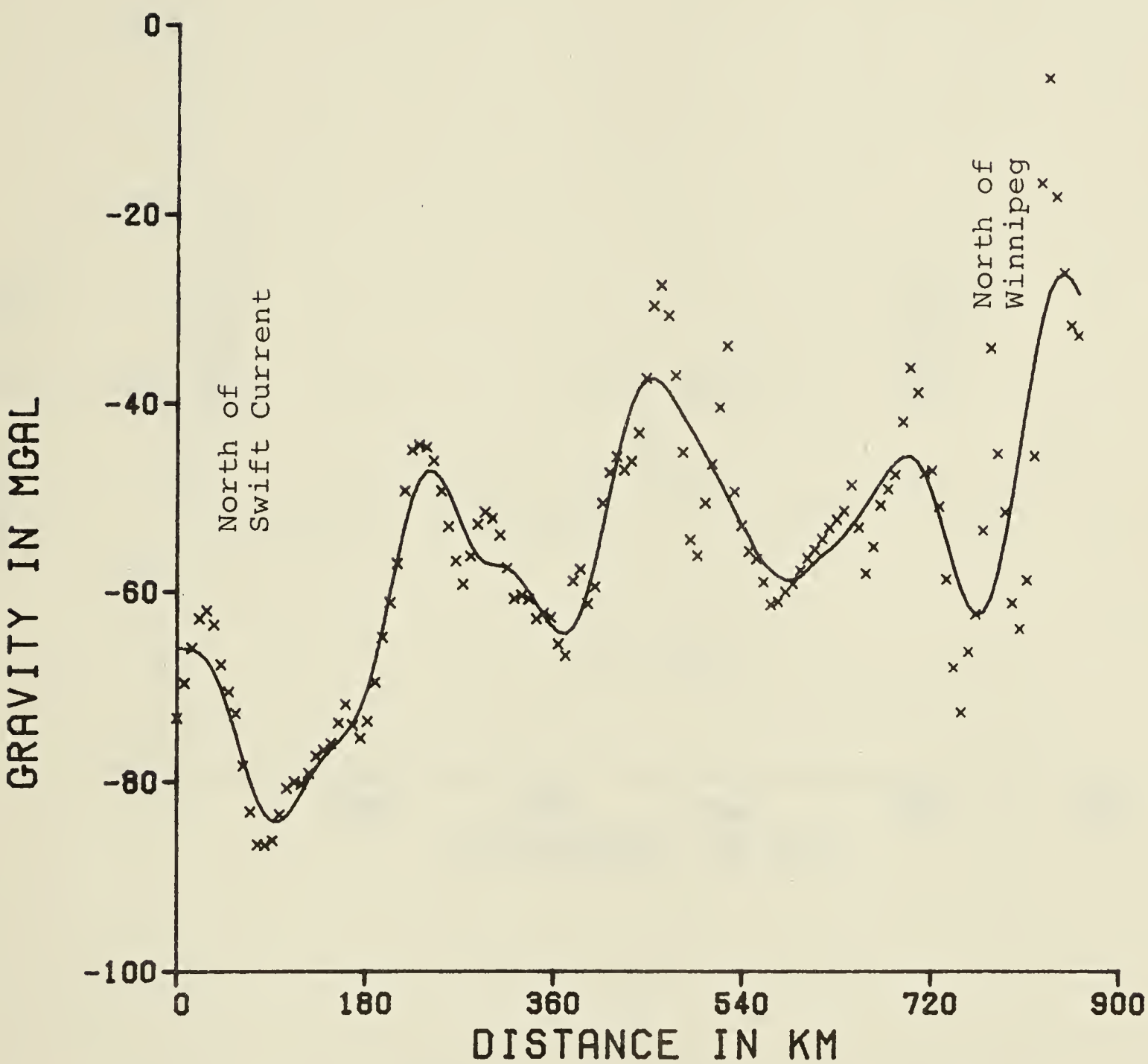


Figure 4.30: Comparision between observed gravity and gravity calculated from inversion model of Fig 4.31.

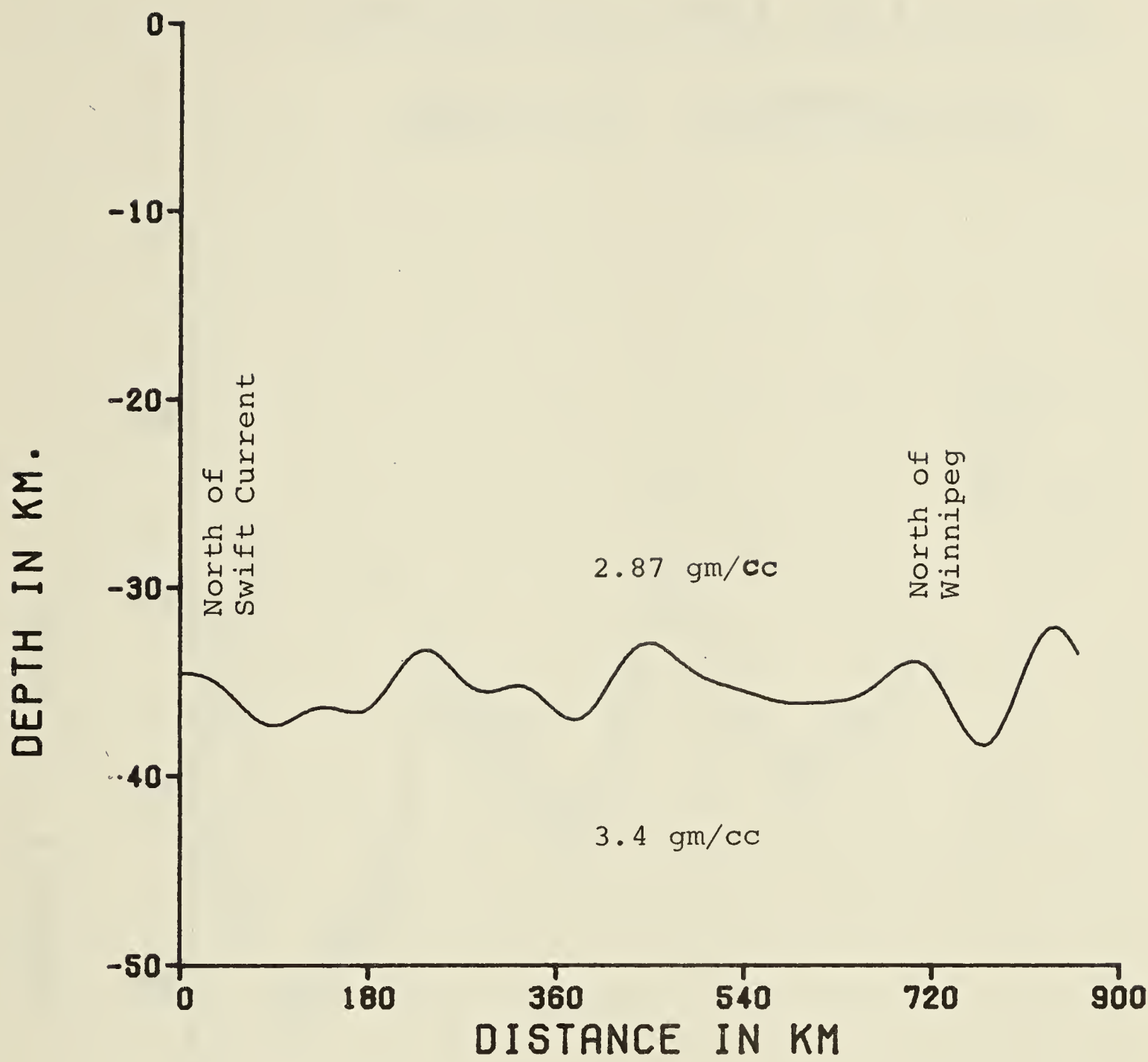


Figure 4.31: Inversion model of Elbow-Lake Winnipeg profile assuming crustal model IV.

INVERTED AND ORIGINAL GRAVITY ANOMALIES

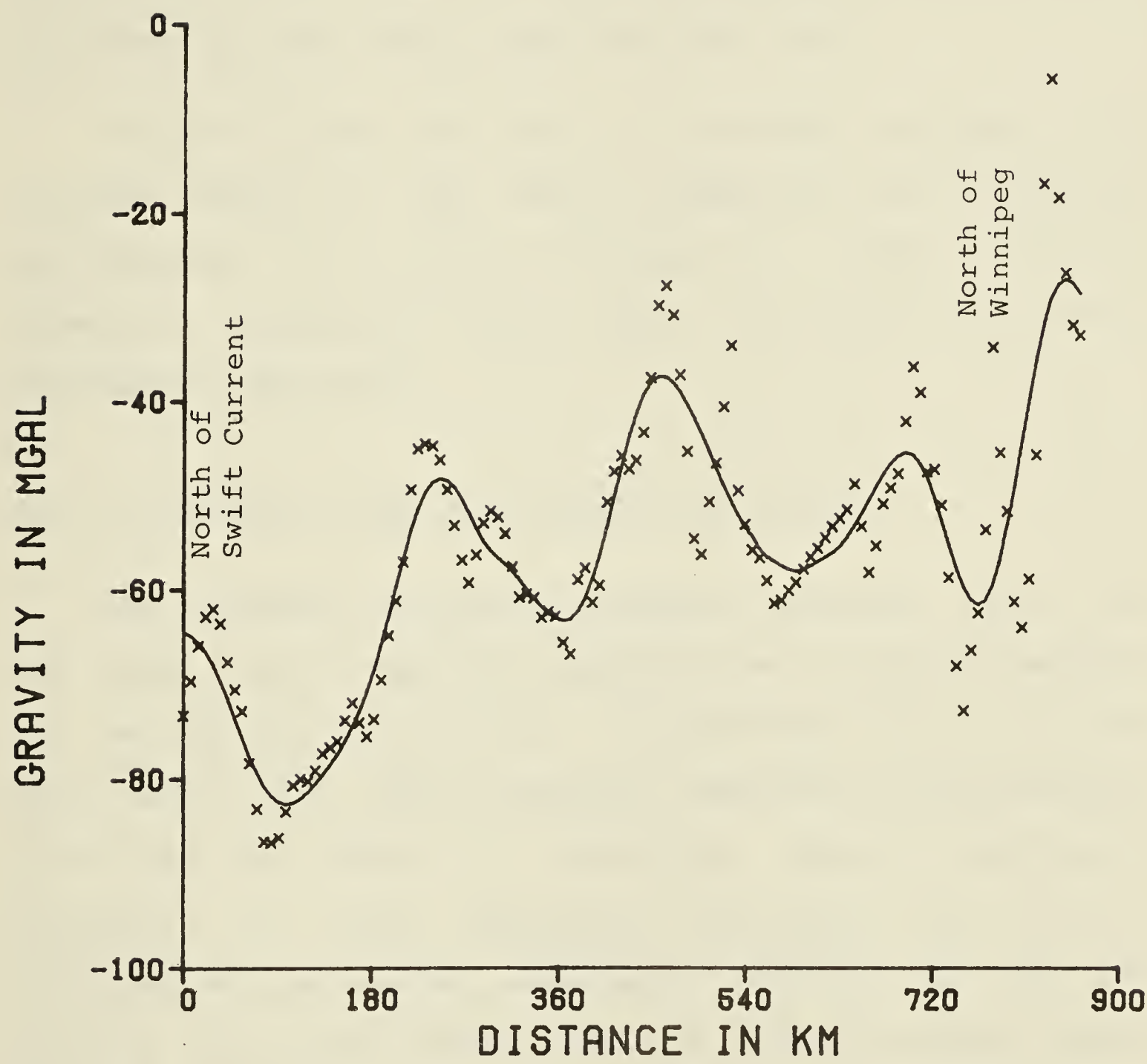


Figure 4.32: Comparison between observed gravity and gravity calculated from inversion model of Fig 4.31.

The southern extension of the "Nelson River Gravity High" corresponds with the ridge at 445 km

The gravitational anomalies computed from the 4 inversion models agree well with the observed gravitational observations (Fig. 4.26, 4.28, 4.30 and 4.32).

Because of the fact that at $107^{\circ}50'W$ latitude the inverted depths of the Moho of Model III and IV differs significantly from those determined at Swift Current (Cumming, Kanasewich 1966) Model III and IV are not considered acceptable.

4.5. Inversion of Residual Gravity for Density

The preceding geological examples indicated that, on the whole, the anomalies computed from the various models fit the regional gravitational observations well. It was also shown that short wavelength anomalies might probably arise from the effect of additional shallow geological features. If short wavelength components were solely generated by the shallow geological features how can we possibly gain some insight about the features causing these high wavenumber components? As gravity interpretation is often nonunique without any geological and geophysical constraints, there are many possible features that might explain the same gravity anomaly. This results from the fact that a given gravity distribution can be produced by a variety of mass distributions. For example, the gravity

anomaly that may be explained by an intrusive body of constant density but variable thickness can also be caused by a similar body of constant thickness but variable density. Thus, until the time when additional information is available, any explanation based on the gravity data alone is purely educated speculation.

In the following we investigate one of the several possible shallow features causing the short wavelength components. A two-dimensional slab of constant thickness is presumed to be the source of the high wavenumber components, and we assumed variation of density within the slab solely responsible for the distribution of the short wavelength components.

The Inversion Scheme

To invert the difference between the observed gravity and the gravity computed from the inversion model for density we revert to equation (11):

$$F[d(x)h(x)] = -(F[g(\text{res})]/2\pi G) \exp([K]Z) - \sum_{n=2}^{\infty} ([K]^{n-1}/n!) F[d(x)h^n(x)] \quad (11)$$

Where $g(\text{res})$ (residual gravity) is the difference between the observed gravity and the gravity computed from the inversion model. The procedure is very similar to that described on page 11 of Chapter 2, except in this case $h(x)$ is presumed to be known and the iterative scheme is used to give the density at various locations along the profile. There are other minor differences as well. Since the

densities obtained by inversion are of small magnitude, usually less than 2 gm/c.c. the convergence criterion (S_n/S_1) for the inversion scheme has to be considerably smaller than that used to calculate $h(x)$. In the following inversion S_n/S_2 is set $\leq 5 \times 10^{-5}$. The filter parameters are also adjusted to accommodate the short wavelength components which composed the major part of the profile. Convergence of this inversion scheme is not much affected by using larger $k(WH)$ or $k(SH)$ because the residual gravity is usually of small magnitude; besides, there is no power term for $d(x)$. Furthermore, no offset is needed.

In the following inversions the slab used for investigation is 5 km thick and the top of this slab is 3 km below the surface.

Profile (1): Swift Current - Winnipeg

The residual gravity, $g(\text{inverted}) - g(\text{observed})$ of Model I, and the density obtained from inversion is shown in Fig. 4.33. It can be seen from Fig. 4.33 that the residual gravity and the gravity calculated from the inverted density agrees with each other very well. The maximum density contrast is 0.12 gm/c.c. (at 596 km of Figure 4.33). Thus at 596 km, where the local density is 2.73 gm/c.c., in order to have the gravity calculated from the inversion model to agree with that of the observed gravity the local density has to be 2.85 gm/cc. It is interesting to note that most of the activity is centered around the southern extension of the "Nelson River Gravity High" (540 km in Fig. 4.33).

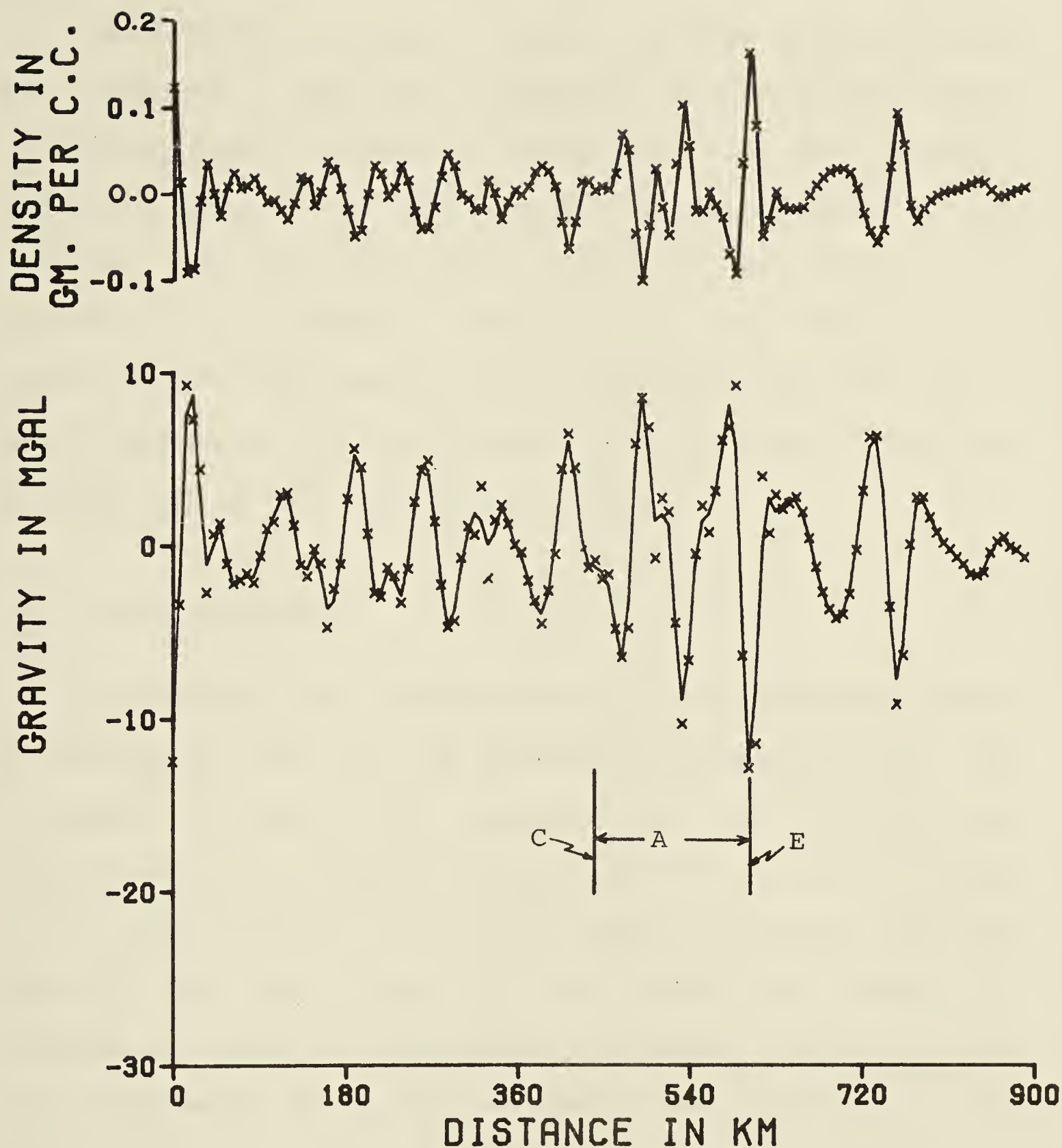


Figure 4.33: Density profile from inversion of residual gravity of the Swift Current-Winnipeg profile, and comparison of original residual gravity and gravity calculated from the inverted density profile.

Inversion parameters are shown in Figure 4.33.

Profile (2): Elbow - Lake Winnipeg (Fig 4.34)

The residual gravity of Model I of this profile is used for inversion. Like the preceding inversion the gravity calculated from the inverted densities fits the residual gravity very well. Two major density anomalies occur in this profile. The first one centres around 485 km, and is in the region of the southern extension of the "Nelson River Gravity High". The second one is around 800 km, just west of Lake Winnipeg. The significance of these density anomalies is discussed in the following section.

4.6. Interpretation

As seen from the cross sections of the inversion models of profile (1) and (2), the inverted topography of the Moho of Model I shows best agreement with that obtained from seismic data. The inverted topography of the Moho of Model II is very similar to that of Model I, however, the mean slope of the Moho tends to be greater for Model II. Structural relief is considerably stronger in Model III and IV; a phenomenon which is consistent in both profile (1) and (2).

Gravity analysis of the Swift Current - Winnipeg profile reveals that the thickness of the crust decreases eastward at a mean rate of 0.013. Other than the depression at the west end of the profile, the relief of the Moho in

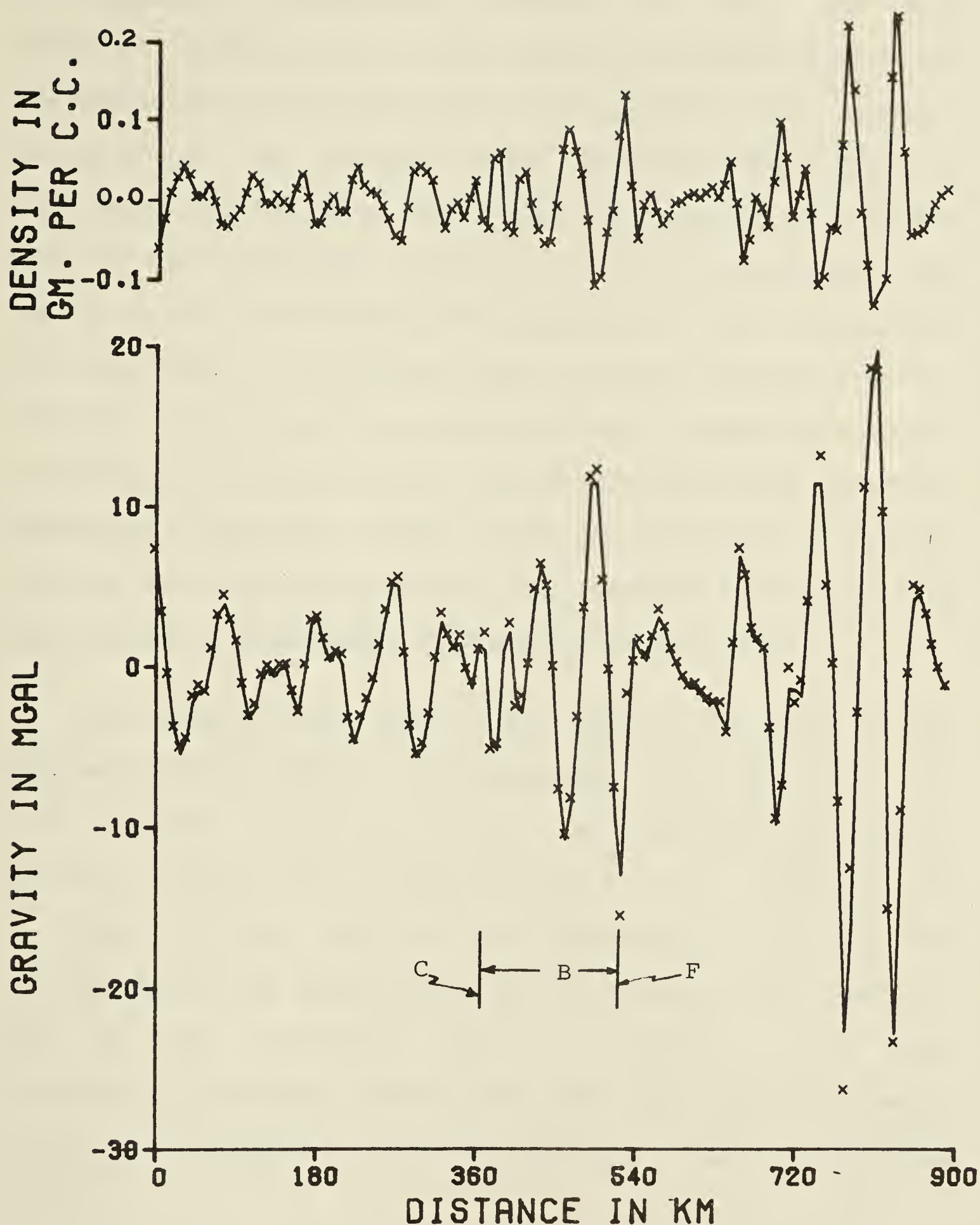


Figure 4.34: Density profile from inversion of residual gravity of the Elbow-Lake Winnipeg profile, and comparison of original residual gravity and gravity calculated from the inverted density profile.

the interior of the Churchill province is flat. The Moho exhibits little relief in the Superior province, except for the depression at the east end of the profile. The southern extension of the "Nelson River Bouguer gravity High" is inverted as a structural high. The depressions of either side of this structural high may be due to down buckling of the crust. The same might have happened for the depressions at either end of the profile. Bell (1971b) believed that the surfacing of the Pikwitonei province was probably due to the up-tilting of the continental plate which was made up of the Pikwitonei basement complex and the Archean supracrustal rocks of the Superior province. The inverted structural high seems to be in accordance with Bell's (1971b) idea.

The inverted topography of the Moho of the Elbow - Lake Winnipeg profile differs significantly from that of the Swift Current - Winnipeg profile. The structural high which occurs in profile (1) is also present in this profile; but of lesser relief. West of this topographic high, the Moho displays much more relief than that of profile (1). However, east of this structural high the relief of the Moho resembles its southern counterpart. The mean rate of crustal thinning is similar to that of the Swift Current - Winnipeg profile.

Looking at the inverted density waveform of the Swift Current - Winnipeg profile and the Elbow - Lake Winnipeg profile one can observe that all the high amplitude components occur in the eastern portion of both profiles.

This is especially obvious on profile (2). (Fig. 4.34) In fact both profiles can be roughly divided into two sections: the eastern section with the high amplitude density contrast, and the western section with the low amplitude density contrast. The dividing line for profile (1) (Fig. 4.33) is at 432 km, while that of profile (2) was chosen at 370 km. The range of density contrast of profile (1) is -0.09 gm/cc to +0.12 gm/cc, which gives a density range of 2.64 to 2.85 gm/cc. On the other hand, in profile (2) the range of density contrast is -0.13 to 0.23 gm/cc, and its density ranges from 2.6 gm/cc to 2.96 gm/cc. What possible information can be gathered from these observations? Do all these density anomalies arise from lithological contrast within the basement, or are they pseudo-density anomalies reflecting structural variation within the basement? Little information concerning basement geology and structure of the area is available, and it is not possible to state whether the gravity anomalies giving rise to the negative density contrasts are mainly due to low density rocks like schist (2.30-2.87 gm/c.c.), granulite (2.57-2.73 gm/c.c.), gneiss (2.59-3.0 gm/c.c.), or are mainly structural features (like faults, shear zones and grabens). If negative density contrasts were caused by low density rocks these density anomalies will have lithological significance, however, if they originated from faults and such like they will have structural significance. Likewise, it is difficult to say whether the positive density contrasts originated from dense rocks (gabbro, diorite, dykes, sills etc) or from structural

features (steps, horsts ect). It is most likely that lithological and structural contrasts within the basement are both responsible. In his delineation of the boundary between the Pikwitonei province and the Superior province Bell (1971b) used the distribution of mafic dyke swarms to substantiate his interpretation of the boundary. Several distinct dyke complexes were identified or inferred. The north-northeast gabbro-diabase dykes, called the Molson Dyke Swarm (Fabrig, et al., 1965, P289), occur in large numbers in the rocks at the west end of Cross Lake subprovince (S.W. of Pikwitonei province; belongs to the Superior province) and the granulites of the Pikwitonei province. However, none of these dykes are known to intrude any of the Churchill province² rock lying northwest and north of the Pikwitonei complex gneisses (Bell 1971b). This fact was utilized by Bell (1971b) to extend the Superior-Churchill boundary beneath the Paleozoic cover lying west of Lake Winnipeg. Bell (1971b) also pointed out the almost exact parallelism between the Churchill-Superior boundary and the 'Molson Dykes'.

Two distinct dyke complexes are also aligned with the Pikwitonei-Churchill boundary: Cuthbert and Nelson dykes (McDonald, 1960; Patterson, 1963, pp 27-29). They grade from peridotite to mafic gabbro, and intrude rocks of the Pikwitonei province and the Cross Lake subprovince (Bell

² Bell's Churchill province includes the Waboden subprovince.

1971b).

Bell (1971b) postulated that ultramafic dykes(?) are responsible for the coincidence of the southwestern extension of the 'Nelson River Bouguer Gravity High' with the aeromagnetic highs at longitude $100^{\circ}00'W$ and latitude $53^{\circ}30'N$. Bell (1971b) called it the Cedar Lake dyke(?). Bell (1971b) also postulated that the Pelican Lake dyke (?), which is 50 km to the southeast of the Cedar Lake dyke, is responsible for the chain of linear magnetic anomalies, which is fringed with a gravity high to the northwest. Bell (1971b) suggested the Pelican Lake dyke(?) is similar to the Fox River ultramafic sill or sills, and the Pelican Lake dyke is just west of the Churchill-Superior boundary.

As already indicated there are a number of high-amplitude-positive-density contrasts around the southern extension of the 'Nelson River Bouguer Gravity High'. These density anomalies probably correspond with dense rocks, dykes or sills. The density anomalies east of 600 km of both profiles most likely belong to the Superior province, because they are in an area with E-W trends; a trend typical of the Superior province. In area A of profile (1) and area (B) of profile (2) there are observable geophysical resemblances to that displayed by the Cedar Lake dyke(?) and the Pelican Lake dyke. Positive density anomalies of both areas A and B correspond with gravity highs which either have coincident magnetic highs or fringing magnetic highs. (Federal-Provincial aeromagnetic map coverage ends near

latitude 52°N and observation was made partly from the magnetic map in appendix C and partly from a confidential map of the Gulf Research and Development Company). If the western limit of the Superior province at latitude $52^{\circ}30'\text{N}$ and longitude 100°W is terminated by the Pelican Lake dyke(?) (Bell 1971b) point C and D of profile (1) and (2) respectively probably mark the western limit of the Superior province as well.

Like the magnetic and gravity anomalies of the Churchill province, which are small and low amplitude the density profile west of point E of profile (1) and F of profile (2) does not show the high amplitude density anomalies which are displayed in the eastern portions. It was indicated that dykes and sills are abundant in the Pikwitonei province, and also that some of the metasediments, metavolcanics, and migmatic gneisses of the Waboden subprovince are of lower to upper amphibolite facies. The high-amplitude-positive-density anomalies in area A of profile (1) and B of profile (2) afford the possibility of similar occurrence of these dense rocks.

The dividing line between the Churchill province and the boundary zone is postulated to be at point E of profile (1) and F for profile (2). For Superior province we postulate points C and D of profile (1) and (2) respectively to be the western limit of its existence.

4.7. Conclusions

The inversion scheme developed by Parker and Oldenburg (1974) has been extended to cover a multi-layered medium. Unlike other conventional gravity inversion methods this multilayer inversion scheme not only takes into account the gravitational effects of strata overlying the inversion interface but also allows for lateral variation of density and thickness within each layer. Interfaces overlying the inversion horizon are assumed to have the same shape as the inversion interface. It has been shown that if variation of density and thickness of beds overlying the inversion interface is only known at certain locations of the profile a linear interpolation of these parameters still gives satisfactory inversion models. Inversions based on various crustal models indicate that the inverted topography of the inversion interface of inversions models which take into account of the effect of overlying layers often shows lesser relief than that obtained from inversion models which attribute all gravitational variation to a single surface.

The nonuniqueness of the gravity inversion is characterised by two free parameters: d , the density contrast between adjacent layers, and Z , the level at which the inversion is made. Without additional information constraining these two parameters, the ambiguity in the gravity interpretation cannot be reduced.

The Parker-Oldenburg (1972, 1974) algorithm has been

rearranged to find the density distribution of a near surface slab in order to fit the difference between the original gravity and the gravity computed from the inverted topography. Together with other geological/geophysical controls the resultant density waveform provides a valuable tool for interpretation. However, in the absence of other information caution must be exercised in interpreting the resultant density profile. This is because a given gravity distribution can be produced by a variety of mass distributions.

The four-layered inversion model of the Swift Current - Suffield profile is in reasonable agreement with the crustal model proposed by Cumming and Kanasewich et al (1966). Gravity analysis of the Swift Current - Winnipeg profile and the Elbow - Lake Winnipeg profile reveals a crustal thinning towards the east. The southern extension of the "Nelson River Bouguer Gravity High" is inverted as a structural high which probably corresponds with the up-tilting of the Pikwitonei province (Bell 1971b).

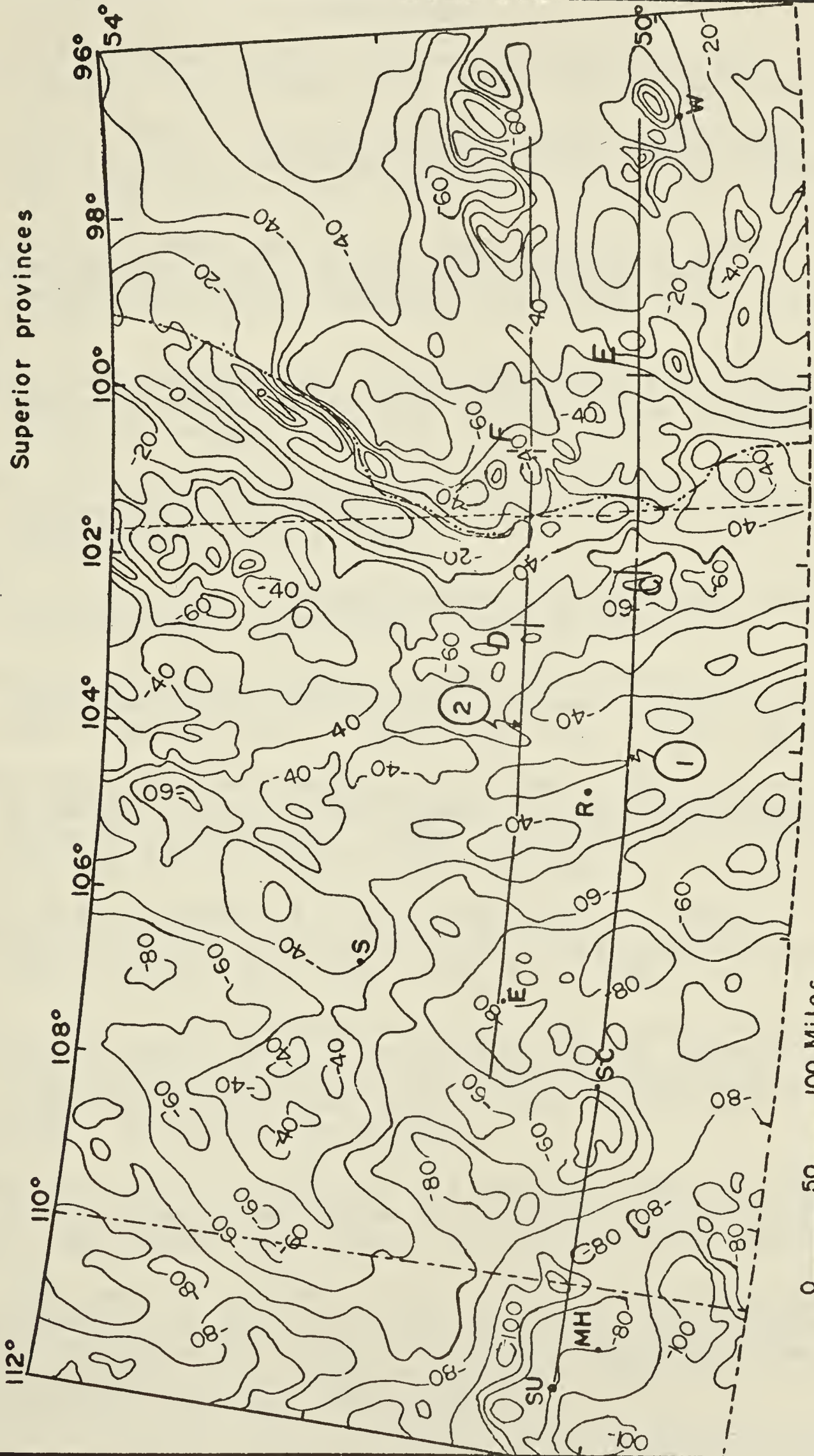
Density analysis of the residual gravity of the Swift Current - Winnipeg profile and the Elbow - Lake Winnipeg profile reveals several high amplitude anomalies in the central and eastern portions of both profiles. Some of the positive density anomalies around the location of the southern extension of the "Nelson River Bouguer Gravity High" probably correspond with dykes/sills which are so abundant in the Pikwitonei province, or with the amphibolite

facies of the Wabowden subprovince. For the Swift Current - Winnipeg profile the western and eastern limits of the boundary zone are tentatively set at $102^{\circ}15'W$ longitude $50^{\circ}20'N$ and $100^{\circ}00'$ longitude, $50^{\circ}20' N$ respectively. As for the Elbow - Lake Winnipeg profile the eastern limit of the Churchill province is set at longitude $102^{\circ}35'W$ lat. $51^{\circ}10.5'N$ and the western limit of the Superior province is set at longitude $101^{\circ}W$ latitude $51^{\circ}10.5'N$ (Figure 4.35).

Figure 4.35: Gravity map of the southern plains of Saskatchewan and Manitoba showing possible locations of the western limit of the Superior province and the eastern limit of the Churchill province.

E, F: postulated western limit of the Superior province
C, D: postulated eastern limit of the Churchill province

--- Bell's boundary between
the Churchill and
Superior provinces



Contour interval: 10 mgal

BIBLIOGRAPHY

- Bell, C.K., 1971a. History of the Churchill-Superior boundary. Geol. Assoc. Can. Spec. Pap. 9, pp. 5-10.
- Bell, C.K., 1971b. Boundary geology, upper Nelson River area, Manitoba and northwestern Ontario. Geol. Assoc. Can. Spec. Pap. 9, pp. 11-39.
- Bott, M.H.D., 1960, The use of rapid digital computer methods for direct gravity interpretation of sedimentary basins: Geophys. J., R. Astr. Soc., v. 3, p. 63-67.
- Burwash, R.A., Baadsgaard, H., and Peterman, Z.E., 1962, Precambrian K-Ar dates from western Canada sedimentary basin: J. Geophys. Research, v. 67, no. 4, p 1617-1625.
- Clowes, R.M., E.R. Kanasewich, and G.L. Cumming, 1968. Deep crustal seismic reflections at near vertical incidence. Geophysics 33, pp. 441-451.
- Corbato, C.E., 1965. A least-squares procedure for gravity interpretation. Geophysic, V. 30, pp. 228-233.
- Cranstone, D.A. and Turek, A., 1975. Geological and geochronological relationships of the Thompson nickel belt. Manitoba Can. J. Earth Sci. Vol. 13, pp. 1058.
- Cumming, G.L. and Kanasewich, E.R., 1966. Crustal structure in Western Canada. Final report for Air Force Cambridge Research Laboratories, Office of Aerospace Research, U.S. Air Force, Bedford, Massachusetts.
- Fahrig, W.F., Gaucher, E.H. and Larochelle, A. 1965, Paleomagnetism of diabase dykes of the Canadian Shield; Can. J. Earth Sci., vol. 2, No. 4, p. 278.
- Gurbuz, B.M., 1969. Structure of the earth's crust and upper Mantle under a portion of Canadian shield deduced from travel-times and spectral amplitudes of body waves using data from Project Early Rises, Unpublished Thesis, University of Manitoba.
- Gurbuz, B.M., 1970. A study of the earth's crust and upper mantle using travel times and spectrum characteristics of body waves, Bull. Seism. Soc. Am. 60, 1921-1935.
- Hall, D.H. and W.C. Brisbin, 1961. A study of Mohorovicic discontinuity near Flin Flon, Manitoba, Final Report for Geophysic Directorate, Air Force Cambridge Research Laboratories: U.S. Dept. of Commerce, Office of Technical Services, Washington, D.C.
- Hall, D.H. and W.C. Brisbin, 1965. Crustal structure from

- converted headwaves in Central Western Manitoba, Geophysics 31, pp. 1053-1067.
- Hall, D.H. and Z. Hajnal, 1969. Crustal structure of North Ontario. Refraction seismology, Can. J. Earth Sci. 6, pp. 81-99.
- Heiland, C.A., 1940, 1963. Geophysical Exploration Printice - Hall Inc., New York.
- Hinson, 1976. Gravity interpretation. Unpublished Master thesis. Texas A. and M. University.
- IEEE, 1967. Fast Fourier transform and its application to digital filtering and spectral analysis: Special issue, AU-15, pp. 43-117.
- Innes, M.J.S., 1960, Gravity and isostasy in northern Ontario and Manitoba: Canada Dominion Observatories Pub., v.21, no. 6, p263-338.
- Kanasewich, E.R., and Cumming, G.L., 1965. Near vertical-incidence seismic reflections from the 'Conrad' discontinuity: J. Geophys. Res., V. 70, pp. 3441-3446.
- Kornik, L.J., 1971. Magnetic subdivision of Precambrian rocks in Manitoba. Geol. Assoc. of Can. Special Pap. 9, pp. 51-60.
- Kornik, L.J. and A.S. MacLaren, 1966. Aeromagnetic study of the Churchill-Superior boundary in northern Manitoba, Can. J. Earth Sci., V. 3, pp. 547-557.
- McDonald, J.A., 1960. A petrological study of the Cuthbert Lake ultrabasic Dyke Swarm; a comparison of the Cuthbert Lake ultrabasis rocks to the Moak Lake serpentinites. Unpublished MSC Thesis, University of Manitoba, Winnipeg, Man., p. 174.
- Negi. J.G., and Garde, S.C., 1969, Symmetrical matrix method for gravity interpretation: J. Geophysics Res., v. 74, p 3804-3807.
- Oldenburg, D.G., 1974. The inversion and interpretation of gravity anomalies. Geophysics, vol. 39, No.4, pp. 526.
- Parker, R.L., 1972. The rapid calculation of potential anomalies: Geophys. J.R. Astr. Soci., V. 31, pp. 447-455.
- Paatterson, J.M. 1963, Geology of the Thompson-Moan Lake area; Mines Br., Manitoba, Publ. 60-4.
- Peterman, Z.E. and Hedge, C.E., 1964, Age of basement rocks from the Willison basin of North Dakota and adjacent

areas. Art. 141 in U.S. Geol. Survey Prof. Paper 475-D, pp D100-D104.

Talwani, M., Worzel, J.L., and Landisman, M., 1959. Rapid gravity computations for two-dimensional bodies with application to the Mendocino submarine fracture zone. J. of Geophys. Res., V. 64, No. 1, p. 49.

Tanner, J.G., 1967, An automated method of gravity interpretation: Geophys. J. R. Astr. Soc., v. 13, p. 339-347.

Vening Meinesz, F.A., J.H.F. Umbgrove, and PH.H. Kuenen, gravity expedition at sea, 1923-1932. V. 2, Pub. Netherl. Geod. Comm., 208 p. 1934.

Whittaker, E.T., and Watson, G.N., 1962. A course of modern analysis: Cambridge, Cambridge U. Press.

APPENDIX A

Derivation of Parker-Oldenberg Algorithms

In the following discussion we denote any three-dimensional position vector with a bar (e.g. $\bar{\mathbf{r}}$) and its projection on the X-Y plane by an arrow (e.g. $\vec{\mathbf{r}}$).

The upper and lower boundaries of a single layer of material, which is contained in a finite area D, is described by $Z=h(\bar{\mathbf{r}})$ and $Z=0$ (a flat surface) respectively. We further assume $h(\bar{\mathbf{r}})$ is bound and integrable. We also define the two-dimensional Fourier transform of any function $g(\vec{\mathbf{r}})$ and its inverse by:

$$F[g(\vec{\mathbf{r}})] = \int_{\mathbf{x}} dA \, g(\vec{\mathbf{r}}) \exp(i\vec{\mathbf{K}} \cdot \vec{\mathbf{r}})$$

$$g(\vec{\mathbf{r}}) = (1/4\pi^2) \int_{\mathbf{K}} d\mathbf{w} \, F[g(\vec{\mathbf{r}})] \exp(-i\vec{\mathbf{K}} \cdot \vec{\mathbf{r}})$$

respectively. \mathbf{x} indicates integration over the X-Y plane and \mathbf{K} integration over the K_x - K_y plane, $dA = dx dy$, and $d\mathbf{w} = dK_x dK_y$.

Consider a point on a horizontal plane which is everywhere above $h(\bar{\mathbf{r}})$ and is at a distance Z_0 above the origin, the potential field at a position $\bar{\mathbf{r}}_0$ from the origin is given by:

$$\begin{aligned}
 U(\vec{r}_0) &= Gd \int_V dV / |\vec{r}_0 - \vec{r}| \\
 &= Gd \int_D dA \int_{z=0}^{z=h(\vec{r})} dz / |\vec{r}_0 - \vec{r}|; \quad (A.1)
 \end{aligned}$$

where G is the Gravitation constant; d is the density of the layer, which is assumed constant; \vec{r} is the position vector from the origin to the source; and D is the finite area in the X - Y plane.

The two-dimensional Fourier transform of equation (A.1) is:

$$\begin{aligned}
 F[U(\vec{r}_0)] &= \int_{\mathbf{x}} dA_0 U(\vec{r}_0) \exp(i\vec{K} \cdot \vec{r}_0) \\
 &= Gd \int_{\mathbf{x}} dA_0 \exp(i\vec{K} \cdot \vec{r}_0) \int_D dA \int_{z=0}^{z=h(\vec{r})} dz / |\vec{r}_0 - \vec{r}|.
 \end{aligned}$$

Note: $\vec{K} \cdot \vec{r} = \vec{K} \cdot \vec{r}$.

Interchange the order of integration we obtain:

$$F[U] = Gd \int_D dA \int_0^z \int_{\mathbf{x}}^{h(\vec{r})} [dA_0 \exp(i\vec{K} \cdot \vec{r}_0)] / |\vec{r}_0 - \vec{r}|. \quad (A.2)$$

The last integral of equation (A.2) can be expressed as:

$$\begin{aligned}
 \int_{\mathbf{x}} [dA_0 \exp(i\vec{K} \cdot \vec{r}_0)] / |\vec{r}_0 - \vec{r}| &= \exp(i\vec{K} \cdot \vec{r}) \\
 \int_{\mathbf{x}} [dA_0 \exp(i|\vec{K}| |\vec{r}_0 - \vec{r}| \cos \theta)] / |\vec{r}_0 - \vec{r}| & \quad (A.3)
 \end{aligned}$$

because: $\vec{r}_0 = \vec{r}_0 - \hat{z}(\hat{z} \cdot \vec{r}_0)$
 $= \vec{r}_0 - (\hat{z} \cdot \hat{z}) \vec{r}_0.$

θ is the angle between the two vectors \vec{K} and $|\vec{r}_0 - \vec{r}|$ in the X-Y plane. Let $u = |\vec{r}_0 - \vec{r}|$ and transform (A.3) to polar coordinates we have:

$$\begin{aligned}
 &= \exp(i\vec{K} \cdot \vec{r}) \int_0^{2\pi} d\theta \int_0^\infty [u du \exp(i|\vec{K}|u \cos \theta)] / |\vec{r}_0 - \vec{r}| \\
 &= \exp(i\vec{K} \cdot \vec{r}) \int_0^{2\pi} d\theta \int_0^\infty [u du \exp(i|\vec{K}|u \cos \theta)] / [u^2 + (Z_0 - Z)]^{1/2}
 \end{aligned}$$

If we let $B = Z_0 - Z$, the integral becomes:

$$= \exp(i\vec{K} \cdot \vec{r}) \int_0^\infty u du / (u^2 + B^2)^{1/2} \int_0^{2\pi} [\exp(i|\vec{K}|u \cos \theta)] d\theta \quad (A.4)$$

Since $J_0(|\vec{K}|u)$, which is a Bessel Function, is:

$$= 1/2\pi \int_0^{2\pi} [\exp(i|\vec{K}|u \cos \theta)] d\theta,$$

(A.4) now becomes:

$$= 2\pi \exp(i\vec{K} \cdot \vec{r}) \int_0^\infty u du J_0(|\vec{K}|u) / (u^2 + B^2)^{1/2} \quad (A.5)$$

The integral of (A.5) can be found from standard integral tables, and is:

$$= [2\pi / |\vec{K}|] [\exp(i\vec{K} \cdot \vec{r} - |\vec{K}|(Z_0 - Z))] \quad (A.6)$$

Substituting (A.6) back into (A.2) we have:

$$F[U] = 2\pi G d \int_D dA \int_0^{h(\vec{r})} dZ [\exp(i\vec{K} \cdot \vec{r} - |\vec{K}|(Z_0 - Z))] / |\vec{K}| \quad (A.7)$$

Integrating over z from 0 to $h(\vec{r})$ equation (A.7) becomes:

$$F[U] = 2\pi G d \int_D dA [\exp(i\vec{K} \cdot \vec{r} - |\vec{K}| z_0)] [\exp(\vec{K} h(\vec{r}) - 1)] / |\vec{K}|^2 \quad (A.8)$$

Since $\exp(\vec{K} h(\vec{r}) - 1)$ can be expressed as $\sum_{n=1}^{\infty} [|\vec{K}|^{n-2} h^n(\vec{r})] / n!$ in Taylor series equation (A.8) can now be expressed as:

$$F[U] = 2\pi G d [\exp(-|\vec{K}| z_0)] \int_D dA \exp(i\vec{K} \cdot \vec{r}) \sum_{n=1}^{\infty} [|\vec{K}|^{n-2} h^n(\vec{r})] / n!$$

Since $|\vec{K}|$ is a constant with respect to dA :

$$F[U] = 2\pi G d [\exp(-|\vec{K}| z_0)] \sum_{n=1}^{\infty} |\vec{K}|^{n-2} / n! \int_D dA h^n(\vec{r}) \exp(i\vec{K} \cdot \vec{r})$$

Integrating, we obtain equation (A.9) which is:

$$F[U] = 2\pi G d \exp(-|\vec{K}| z_0) \sum_{n=1}^{\infty} |\vec{K}|^{n-2} / n! F[h^n(\vec{r})] \quad (A.9)$$

To find the vertical attraction of the perturbing mass, we note that for any observation datum above the masses $\nabla^2 U = 0$. This allows us to write:

$$U(\vec{r}_0) = 1/4\pi^2 \int d^2K U(\vec{K}) \exp(-i\vec{K} \cdot \vec{r}_0).$$

To upward continue the above expression to the observation datum we have to multiply it by $\exp(-|\vec{K}| \hat{z} \cdot \vec{r}_0)$.

$$U(\vec{r}_0) = 1/4\pi^2 \int d^2K U(\vec{K}) \exp(-i\vec{K} \cdot \vec{r}_0 - i|\vec{K}| \hat{z} \cdot \vec{r}_0)$$

Thus $F[U(\vec{r}_0)] = U(\vec{K}) \exp(-|\vec{K}| \hat{z} \cdot \vec{r}_0)$.

By definition, the vertical attraction, Δg , is:

$$\Delta g = + \partial U / \partial z.$$

$$= F[\Delta g] = -|\vec{K}| F[U]$$

$$= F[\Delta g] = -2\pi G d [\exp(-|\vec{K}| z_0)] \sum_{n=1}^{\infty} |\vec{K}|^{n-1} F[h^n(\vec{r})] / n!$$

which is Parker's algorithm.

APPENDIX B

Convergence of Parker-Oldenburg Algorithms

Parker (1972) Algorithm:

We revert to Parker's (1972) algorithm:

$$F[\Delta g(\vec{r})] = -2\pi G d \exp(-|\vec{K}| Z_0) \sum_{n=1}^{\infty} |\vec{K}|^{n-1} / n! F[h^n(\vec{r})]; \quad (B.1)$$

$h(\vec{r})$ is assumed to be bounded and integrable, and vanishes outside some finite domain D . Two-dimensional Fourier transform of $h(\vec{r})$ is:

$$F[h^n(\vec{r})] = \int_D dA h^n(\vec{r}) \exp(i\vec{K} \cdot \vec{r}), \text{ and:}$$

$$|F[h^n(\vec{r})]| \leq \int_D dA |h^n(\vec{r})| \cdot |\exp(i\vec{K} \cdot \vec{r})|$$

$$\leq \int_D dA |h^n(\vec{r})|$$

$$\leq A H^n$$

A = area of D

H = maximum value of $|h(\vec{r})|$

Substituting the bounds into equation (B.1) we have:

$$|F[\Delta g(\vec{r})]| \leq |-2\pi G d| / |\vec{K}| \sum_{n=1}^{\infty} (|\vec{K}| H)^n A / n!$$

$$|F[\Delta g(\vec{r})]| \leq 2\pi Gd A/|\vec{K}|[\exp(|\vec{K}|H)-1]; \quad (B.2)$$

Equation (B.2) is uniformly and absolutely convergent in any bounded domain of the K-plane (Whittaker and Watson, 1962, p581).

To show the rate of convergence can be optimised we let $S = \sum_{n=1}^{\infty} (K^n/n!) \exp(-KZ_0) F[h^n(\vec{r})]$ and write K for $|\vec{K}|$. Since $|F[h^n(\vec{r})]| \leq AH^n$ we have:

$$S' = A \exp(-KZ_0) \sum_{n=1}^{\infty} K^n H^n / n!,$$

and $|S| < S'$.

The preceeding result can be shown easily. If we take the nth term of both functions we have:

$$\begin{aligned} \frac{S_n}{S'_n} &= \frac{K^n/n! F[h^n(\vec{r})]}{A K^n/n! H^n} \\ \frac{S_n}{S'_n} &= \frac{F[h^n(\vec{r})]}{AH^n} \\ &\leq 1 \quad \because |F[h^n(\vec{r})]| \leq AH^n \end{aligned}$$

There is an upperbound for S' . The nth term of S' is:

$$\begin{aligned} S'_n &= [A (KH)^n / n!] / \exp(KZ_0) \\ &= [A (KH)^n / n!] / \sum_{i=0}^{\infty} (KZ_0)^i / i! \\ &< [A (KH)^n / n!] / [(KZ_0)^n / n!] \\ &< AH^n / Z_0^n \\ S'_n &< A (H/Z_0)^n \end{aligned}$$

Summing over all terms we have:

$$S' < \sum_{n=1}^{\infty} A (H/Z_0)^n$$

Therefore when $H < Z_0$ and $Z_0 > 0$ the serie for S' is uniformly convergent in the whole K -plane, as demonstrated by Weierstrass M-test (Whittaker and Watson, 1962, p49) and hence this is true for S . The smaller H/Z_0 can be made, the faster will be the rate of convergence.

It is not apparent that we have any control over H/Z_0 in a given calculation, but this is in fact not the case. In choosing our coordinate system, we chose $Z=0$ to be the bottom of the layer of material. It is an arbitrary choice, for we may choose any depth for an origin. Deplacing the origin does not affect the validity of equation (B.1) but it does change the numerical values of Z_0 and $h(\vec{r})$, and also H .

Oldenburg (1974) Algorithm:

Similar approach was used to derived at the convergence criterion of Oldenburg's inversion scheme.

We revert to Oldenburg's inverse formula:

$$F[h(x)] = -F[\Delta g(x)] \exp(|K|Z_0) / 2\pi Gd$$

$$- \sum_{n=2}^{\infty} (|K|^{n-1} / n!) F[h^n(x)]; \quad (B.3)$$

The one-dimensional Fourier transform of a function $h(x)$ by:

$$F[h^n(x)] = \int_D dx h^n(x) \exp(iKx)$$

and

$$|F[h^n(x)]| = \left| \int_D dx h^n(x) \exp(iKx) \right|$$

$$\leq \int_D |h^n(x)| dx$$

$$\leq L H^n$$

L is the length of D and $H = \max|h(x)|$. We also require that $h(x)$ be bounded and integrable and $h(x) = 0$ for x and D .

Inserting these bounds into the infinite sum in equation (B.3) we get:

$$\left| \sum_{n=2}^{\infty} (K^{n-1}/n!) F[h^n(x)] \right| \leq (L/K) \sum_{n=2}^{\infty} K^n H^n / n!$$

$$= (L/K) [\exp(KH) - 1 - KH]; \quad (B.4)$$

The right hand side of (B.4) is bounded for any finite value of K , hence, from the properties of the exponential function (Whittaker and Watson, 1962, p581) the sum of Fourier transforms is absolutely and uniformly convergent in any bounded domain of the K -plane.

The convergence criterion chosen by Oldenburg is that successive terms in the sum are computed until $S_n/S_2 < 5E-3$. For the forward algorithm, sufficient number of terms are evaluated until $R_n/R_1 < 10E-6$.

$$S_n = \max_{K} \text{ over all } | (|K|^{n-1}/n!) F[h^n(x)] |$$

and

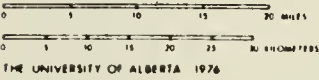
$$R_n = \max_{K} \text{ over all } | \exp(-|K|Z_0) |K|^{n-1}/n! F[h^n(x)] |$$

Though convergence of the infinite sum is assured, however, there is still no control over the convergence of the iterative procedure. Oldenburg was unable to establish analytical convergence criterion for the iterative procedure. He resorted to an empirical criterion which requires that the mean-root-square difference between two consecutive approximations of $h(x)$ be less than some arbitrary chosen small number. The mean-root-square error can be expressed mathematically as:

$$\text{Error} = \frac{1}{N} \sqrt{\sum_{i=1}^N [h_i(x) - h_{i+1}(x)]^2}$$

Magnetic map of southern Saskatchewan.

MAGNETIC ANOMALY MAP
CONTOUR INTERVAL 100 GAMMAS
MERCATOR PROJECTION



Computer program to do multilayer gravity inversion.

```

C *****
C   MULTILAYER GRAVITY INVERSION USING FOURIER TRANSFORMS
C   PROGRAM MODIFIED FROM OLDENBURG'S INVERSION PROGRAM
C   WRITEN BY J.S.K. LEE; UNIVERSITY OF ALBERTA, 1977.
C   PROGRAM TO CALCULATE THE GRAVITATINNAL ANOMALY AND DO THE
C   INVERSION OF MULTILAYER MODEL, WITH LATERAL LINEAR
C   VARIATION OF DENSITY AND BED THICKNESS.
C   INPUT TO THE PROGRAM SHOULD BE OF THE FOLLOWING FORMAT
C ** N2,NN,IG,NJJ,NLL,NKK,NLAY
C (# OF OBSERVED GRAVITY, # OF DIGITISED STATIONS TO BE PRODUCED,
C IG .NE. 1 FOR DATA NOT IN TENTH MGAL, # OF FILTERS TO BE USED,
C # OF DENSITY VALUES FOR INVERSION HORIZON, # OF Z, AND TOTAL
C # OF LAYERS.
C ** BTK (BEDTHICKNESS OF OVERLYING BEDS AT W END, FROM THE
C   INVERSION HORIZON UP, TOTAL INPUT SHOULD = NLAY-2 )
C ** BTK2 (SIMILAR TO BTK BUT AT THE E END)
C ** DERHO (DENSITY OF OVERLYING LAYERS AT W END, IN ASCENDING
C   ORDER FROM THE INVERSION HORIZON)
C ** DERHO2 (SIMILAR TO DERHO BUT AT E END)
C ** FRAC,UM (FRACTION OF INPUT GRAVITY TO BE USED FOR FIRST ITER
C   AND AMOUNT OF OFFSET TO BE USED TO FACILITATE CONVERGENCE)
C ** ZUP (INVERSION HORIZON, NKK TERMS)
C ** RHO (DENSITY CONTRAST OF INVERSION HORZ, NLL TERMS)
C ** RHOTWO (DENSITY CONTRAST OF INVSN HORZ AT E END, NLL TERMS)
C ** JPRINT (INDEX FOR PRINTING INTERMEDIATE RESULTS, 1=YES, 3=NO)
C ** X(J) (X CO-ORDINATE OF INPUT GRAVITY)
C ** GG(J) (OBSERVED GRAVITY)
C ** NR (# OF SEDI-ENT GRAVITY)
C ** GG(J) (SEDIMENT GRAVITY CALCULATED AT THE SAME LOCATIONS AS
C   OESERVED GRAVITY)
C ** WH,SH (LOW CUT-OFF AND HI CUT-OFF WAVENUMBERS, NJJ TERMS)
C *****
C   DIMENSION H1(512),H(512),X(512),GRAV(513),DG(512)
C   DIMENSION DG3(512),BTK(20),DG2(512),G1(512),G2(512)
C   DIMENSION RHO(20),BTK2(20),DERHO(20),DG4(512),ZZ(20)
C   DIMENSION RODIG1(512),RODIG2(512),F(512),H2(512),B(512)
C   DIMENSION DERHO2(20),RHOTWO(20)
C   DIMENSION AA(512),BB(512),CC(512),GG(512)
C   COMPLEX SUM(512),HTON(512),ANOM(512)
C   COMMON/BOUG/ACC,IPRINT
C   COMMON/HILLS/NN,DX,ZUP,GRHO,GRO
C   COMMON/INV/ITERMS,ITER,ISKIP,AC1,IZUP,JPRINT,FRAC,NLAY
C   DATA PI/3.1415926535/
C   DATA G/6.67/
C   READ(5,100) N2,NN,IG,NJJ,NLL,NKK,NLAY
100  FORMAT(7I4)
C   NBD=NLAY-2

```



```

      READ (5,101) (BTK(I),I=1,NBD)
      READ (5,101) (BTK2(I),I=1,NBD)
      READ (5,101) (DERHO(I),I=1,NBD)
      READ (5,101) (DERHO2(I),I=1,NBD)
101  FORMAT(10F8.3)
      READ (5,171) FRAC,UM
171  FORMAT(2E.3)
      READ (5,102) (ZZ(I),I=1,NKK)
      READ (5,102) (RHO(I),I=1,NLL)
      READ (5,102) (RHOTWO(I),I=1,NLL)
      READ (5,222) JPRINT
      IPRINT=JPRINT
222  FORMAT(I1)
102  FORMAT(5F8.3)
C    INPUT THE # OF TERMS TO BE USED IN POWER SERIES
      NTERMS=35
      READ (5,47) (X(J),J=1,N2)
47   FORMAT(10F8.3)
      READ (5,47) (GG(J),J=1,N2)
C    IF INPUT GRAVITY IS TENTH MILLIGAL CONVERT TO MILLIGAL
      IF (G.EQ.1) GO TO 99
      DO 1 I=1,N2
1     GG(I)=GG(I)*0.1
11    FORMAT(10F12.1)
99    WRITE (6,56) (X(J),GG(J),J=1,N2)
56    FORMAT (//////,40X,'INITIAL DISTANCE IN KM. AND GRAVITY ANOM
1     //,10(2F9.3,6X,2F9.3,6X,2F9.3,6X,2F9.3,6X,2F9.3,/) )
309   FORMAT(//////,30X,'SEDIMENT GRAVITY',//,10(10F12.
1     4,/) )
C    CALCULATE DIGITISING INTERVAL
      XMAX=X(N2)
      DX=XMAX/NN
C    *****
C    CALL SPLNCO TO PRODUCESPLINING COEFFICIENTS.
      CALL SPLNCO(1,N2,X,GG,AA,BB,CC)
      DO 23 J=1,NN
      H(J)=(J-1)*DX
      I1=0
C    CALL SPLNEV TO CALCULATE SPLINED VALUES AT EACH POINT.
C    SPLINED VALUES ARE STORED IN VECTOR G2.
      CALL SPLNEV(1,N2,X,GG,AA,BB,CC,H(J),G2(J),I1)
23   GRAV(J)=G2(J)
      WRITE (6,55) (H(J),GRAV(J),J=1,NN)
C    INPUT SEDIMENT GRAVITY AND DIGITISE
      READ (5,105) NR
105  FORMAT(I4)
      READ (5,47) (GG(J),J=1,NR)
      IF (JPRINT.LT.3) WRITE (6,309) (GG(J),J=1,NR)
      CALL SPLNCO(1,NR,X,GG,AA,BB,CC)
      DO 25 J=1,NN
      H(J)=(J-1)*DX
      I1=0
C    CALL SPLNEV TO CALCULATE SPLINED VALUES AT EACH POINT.

```



```

C      SPLINED VALUES ARE STORED IN VECTOR G1.
      CALL SPLNEV(1,NR,X,GG,AA,BB,CC,H(J),G1(J),I1)
25     GRAV(J)=GRAV(J)+G1(J)
      IF (JPRINT.GE.3) WRITE (6,905) (H(J),J=1,NN)
905    FORMAT(////////,30X,' DEGITISING INTERVAL',//,10(10F12.
1      4,/))
      IF (JPRINT.GE.3) WRITE (6,509) (GRAV(J),J=1,NN)
501    FORMAT (////////,40X,'DISTANCE IN KM. AND SYM. GRAVITY IN MILL
1,//,10(2F9.3,6X,2F9.3,6X,2F9.3,6X,2F9.3,6X,2F9.3,/) )
C      *****
C      TO GENERATE A SYMMETRICAL SERIES.
C      *****
      DO 71 J=1,NN
      GRAV(J+NN)=GRAV(NN-J+1)
71     H(NN+J)=H(NN)+DX*J
      NN=NN*2
      IF (JPRINT.LT.3) WRITE (6,509) (GRAV(J),J=1,NN)
509    FORMAT(////////,30X,' WITH SEDIMENT GRAVITY REMOVED',//,10(1
1      4,/))
      XMAX=H(NN)
      DX=XMAX/NN
C      OFFSET EACH SPLINED GRAVITY BY UM TO FACITATE CONVERGENCE
      DO 7 J=1,NN
7      GRAV(J)=GRAV(JUM
      IF (JPRINT.LT.3) WRITE (6,55) (H(J),GRAV(J),J=1,NN)
55     FORMAT (////////,40X,'DISTANCE IN KM. AND SPLINED GRAVITY IN M
1L',//,10(2F9.3,6X,2F9.3,6X,2F9.3,6X,2F9.3,6X,2F9.3,/) )
CC     COMPLETE THE INVERSION OF THE GRAVITATIONAL ANOMALY
C      INPUT THE MAX NUMBER OF TERMS IN THE SERIES TO BE TAKEN.
C      INPUT THE MAX NUMBER OF ITERATIONS TO BE USED.
C      THE DESIRED ACCURACY BETWEEN SUCCESSIVE TOPOGRAPHIC ITERAT
C      THE INDEX IZUP FOR ALTERING THE VALUE ZUP
C      FOR EACH ITERATION IZUP=0 IF THERE IS NO CHANGE FOR ZUP,
C      ELSE IZUP =1. CHANGING THE VALUE OF ZUP (BEING THE MEDIAN)
C      SPEED UP THE ITERATION PROCESS.
C      JPRINT=0 TO OUTPUT THE FOURIER AMPLITUDE, JPRINT>2 TO
C      OUTPUT THE LARGEST ABSOLUTE VALUE FOR THE FORWARD ITERATIO
      ITERMS=35
      ITER=15
      AC1=5.E-03
      ACC=1.E-03
      IZUP=0
      DO 34 JJ=1,NJJ
CC     CALCULATE A BANDPASS FILTER
      READ(5,35) WH,SH
35     FORMAT(2F8.4)
      CALL LOPASS(B,F,WH,SH,NN,1)
      WRITE(6,36) (WH,SH,(B(J),J=1,NN))
36     FORMAT(///,20X,23H LOW PASS FILTER      WH=,F6.4,10X,4H SH=,
1      F6.4,//,10(15F8.4,/) )
CC     CALCULATE THE LOW PASSED GRAVITY PROFILE
      DO 42 J=1,NN
42     ANOM(J)=CMPLX(GRAV(J),0.)

```



```

      CALL FFTWO(ANOM,NN)
      DO 43 J=1,NN
43      ANOM(J)=ANOM(J)*B(J)
      CALL FFTWO(ANOM,NN)
      CALL REORDR(ANOM,NN)
      DO 44 J=1,NN
44      DG(J)=REAL(ANOM(J))/NN
      WRITE(6,45) (DG(J),J=1,NN)
45      FORMAT(//////,30X,31H FILTERED GRAVITATIONAL ANOMALY,/,/,10(
1 4,/))

CC
CC
      DO 34 KK=1,NKK
      ZUP=ZZ(KK)

CC
      DO 34 LL=1,NLL
C      GRHO=6.67*RHO(LL)
      WRITE(6,39) RHO(LL),RHOTWO(LL)
39      FORMAT(//////////,20X,17H ASSUMED DENSITY=,2F8.2,/)
      DO 40 J=1,NN
      DG4(J)=0.0
      DG(J)=GRAV(J)
40      H1(J)=0.0
      ISKIP=0
      NTERMS=35
C      CALL INVERSION SBROUTINE TO DO INVERSIO-
      CALL RHOINV(DG3,DG2,H1,H2,H,DG,SUM,HTON,ANOM,B,SH,BTK2,
1BTK,DERHO,DERHO2,DG4,RHO(LL),RHOTWO(LL),RODIG1,RODIG2)
      NTERMS=35
C      REMOVE OFFSET AND ADD GRAVITY OF SEDIMENT
      NN=NN/2
      DO 98 M=1,NN
98      DG(M)=DG4(M)+UM-G1(M)

CC
      IF (JPRINT.LT.3) WRITE(6,51) (G2(J),DG(J),J=1,NN)
      IF (JPRINT.GE.3) WRITE(6,512) (G2(J),J=1,NN)
512      FORMAT(//////,30X,' ORIGINAL GRAVITY',/,/,10(10F12.
1 4,/))
      IF (JPRINT.GE.3) WRITE(6,511) (DG(J),J=1,NN)
511      FORMAT(//////,30X,' GRAVITY FROM INVERTED TOPOG',/,/,10(10F1
1 4,/))
51      FORMAT(//////,40X,48H OBSERVED AND CALCULATED GRAVITATIONAL
1IES,/,/, 10(2F9.3,6X, 2F9.3,6X, 2F9.3,6X, 2F9.3,6X, 2F9.
34      CONTINUE
      STOP
      END
      SUBROUTINE RHOB OG(H,DG,SUM,HTON,NTERMS,DELRO,
1DELRO2,RODIG2)
CC$$$$$ CALLS FFTWO
C      PROGRAM COMPUTES GRAVITY OF MODELS WITH LATERAL VARIATION
C      OF DENSITY.
C      DELRO IS DENSITY OF W END OF MODEL
C      DELRO2 IS DENSITY OF E END OF MODEL

```



```

C      RODIG2 STORES DIGITISED DENSITY
CC     COMPUTES 2-D BOUGUER ANOMALIES WITH FFT POWER METHOD
CC     'NTERMS' IS THE NUMBER OF TERMS IN POWER SERIES TO BE TAKEN.
CC     PARAMETERS COME THROUGH COMMON /HILLS/ - 'NN' NUMBER OF TERMS
CC     'DX' SPACING IN X DOMAIN, 'ZUP' VERTICAL DISTANCE ABOVE Y=0 OF
CC     'GRHO' BIG G TIMES RHO, 'H' ARRAY WITH 'NN' ELEMENTS CONTAININ
      COMMON/HILLS/NN,DX,ZUP,GRHO,GRO
      DIMENSION RODIG2(1),H(1),DG(1)
      COMPLEX SUM(1),HTON(1),HC
      COMMON/BOUG/ACC,IPRINT
      DATA TWOPI/6.283185307/
      DATA G/6.67/
      GRO=DELRO*G
      IF (DELRO.EQ.DELRO2) GOTO 77
      ND=NN/2
      ROIN=(DELRO-DELRO2)/(ND-1)
      DO 303 I=1,ND
      RODIG2(I)=DELRO-ROIN*(I-1)
      RODIG2(I+ND)=DELRO-ROIN*(ND-I)
303   CONTINUE
      IF (IPRINT.LE.2) WRITE(6,123) (RODIG2(I),I=1,NN)
123   FORMAT(///,'DIGITISED DENSITY',//,10(10F12.3,/) )
77    WRITE(6,55) DELRO,DELRO2
55    FORMAT(//,35X,'DENSITY = ',2F8.4)
C
      WRITE(6,20) ACC
20    FORMAT(///,30X,29H ACCURACY LEVEL IN BOUGER IS=,E12.3,/)
CC     SETS VARIOUS CONSTANTS AND ZEROS 'SUM' READY TO RECEIVE SERIE
      NNBY2=NN/2
      N2PLUS=NNBY2+1
      DK=TWOPI/(DX*NN)
      DO 110 I=1,NN
110   SUM(I)=(0.0,0.0)
      FAC=1.0
      BIGM1=10.
C
CC     'N' COUNTS NUMBER OF TERMS IN SERIES.
      DO 2500 N=1,NTERMS
      FAC=N*FAC
CC     COPIES N-TH POWER OF TOPOGRAPHY INTO COMPLEX 'HTON'
      BIG=0.0
      IF (DELRO.EQ.DELRO2) GOTO 211
      DO 233 J=1,NN
233   HTON(J)=CMPLX(RODIG2(J)*H(J)**N,0.0)
      GOTO 234
211   DO 210 I=1,NN
210   HTON(I)=CMPLX(H(I)**N,0.0)
&
234   CALL FFTTWO(HTON,NN)
C
CC     FILTERS FOURIER COEFFS AND ADDS THEM INTO 'SUM'
CC     FEWER THAN NTERMS IN THE SUM MAY BE TAKEN IF AN ABSOLUTE CON
CC     CRITERION IS MET.

```



```

CC  ALSO PERFORM THE UPWARD CONTINUATION AT THIS STAGE
      TERM=TWOPI*G/NN
      IF (DELRO.EQ.DELRO2) TERM=TERM*DELRO
      DEXP=EXP(-DK*ZUP)
      IF(N.EQ.1) SUM(1)=HTON(1)*TERM
      DO 2200 K=2,N2PLUS
      TERM=TERM*DEXP
      CAYN=((K-1)*DK)**(N-1)/FAC
      CAYN=CAYN*TERM
      IF(K.EQ.N2PLUS) GO TO 40
      HC=HTON(K)*CAYN
      B=CABS(HC)
      IF(B.GT.BIG) BIG=B
      SUM(K)=SUM(K)+HC
40    MINUS=NN-K+2
      HC=HTON(MINUS)*CAYN
      B=CABS(HC)
      IF(B.GT.BIG) BIG=B
2200  SUM(MINUS)=SUM(MINUS)+HC
      IF(N.EQ.1) FIRS/=BIG
      IF(IPRINT.LE.5) WRITE(6,42) N,BIG
42    FORMAT(30X,3H N=,I4 10X,51H LARGEST ABSOLUTE VALUE OF TERM
1WARD PROBLEM=,E15.4)
      BB=AMAX1(BIG,BIGM1)
      IF( BB/FIRST .LT. ACC ) GO TO 43
      BIGM1=BIG
2500  CONTINUE
      WRITE(6,44) FIRST,BB
44    FORMAT(////,51H ***** THE FORWARD PROBLEM HAS NOT CONVERGE
1 ,10X,7H FIRST=,E12.3,10X,5H BIG=,E12.3)
43    CALL FFTTWO(SUM,NN)
      CALL REORDR(SUM,NN)
      DO 70 I=1,NN
70    DG(I)=REAL(SUM(I))
      RETURN
      END

      SUBROUTINE RHOINV(DG3,DG2,H1,H2,H,DG,SUM,HTON,
1ANOM,FIL,SH,BTK2,BTK,DERHO,DERHO2,DG4,RHO1,
1RHO2,RODIG1,RODIG2)
C *****
C  ROUTINE COMPUTES THE TOPOGRAPHY FROM A GRAVITATIONAL ANOMALY
C  OF A MULTILAYER MODEL, WITH LATERAL VARIATION OF DENSITIES
C  BEDTHICKNESS.
CC  H1 CONTAINS THE INITIAL GUESSED TOPOGRAPHY MEASURED WITH RES
CC  REFERENCE LINE ZUP.
CC  IN THE PERTURBATION EXPANSION WE SUM FROM 2 TO NTERMS.
CC  ITER IS THE TOTAL NUMBER OF ITERATIONS TAKEN TO FIND THE TOP
CC  IF ISKIP=0 THEN THE PERTURBATION TERM IS NOT ADDED.
CC  IF THE MEAN ROOT SQUARE DEVIATION OF TWO SUCCESSIVE TOPOGRAP
CC  CALCULATION IS LESS THAN ACC THE PROCEDURE IS TERMINATED.
C  H1 IS THE INITIAL GUESSED TOPOGRAPHY WHICH CAN BE INITIALISE
C  =0.0 IF THERE IS NO KNOWN OR GUESSED VALUES.
C  H IS A DUMMY VARIABLE FOR THE INVERSION OF TOPOGRAPHY.

```



```

C      DG IS THE OBSERVED GRAVITY.
C      SUM IS THE SUMMATION OF THE FFT OF GRAVITY AND TOPO TERMS.
C      HTON IS A DUMMY COMPLEX VARIABLE FOR THE TOPOGRAPHY H(X), WH
C      FOR FFT OF TOPOGRAPHY.
C      ANOM IS A DUMMY VARIABLE FOR COMPLEXING THE OBSERVED GRAVITY
C      FOR FFT OF DRAVITY DATA.
C      FIL IS THE FILTER COEFFICIENTS SUPPLY BY LOPASS SUBROUTINE.
C      SH IS THE CUT OFF FREQUENCY.
C      THIS PROGRAM EXPECTS VALUES FOR NTERMS, ITER, ISKIP, ACC, IZUP,
C      NN, DX, ZUP, AND GRHO FROM THE COMMON STATEMENT.
C      IPRINT IS THE INDEX FOR PRINTING THE VALUES OF SUM FOR CHECK
C      ISKIP IS THE INDEX FOR SKIPPING THE PERTURBATION TERMS IF TH
C      TOPO IS 0. ISKIP = 0 FOR TOPO =0 ELSE ISKIP =1
C      IZUP IS THE INDEX FOR CHANGING THE VALVE OF ZUP IF THE INITI
C      S NOT THE MEDIAN OF THE TOPO. UNLESS THE ZUP VALUE IS IS OB
C      MEDIAN IZUP PRETTY WELL HAS TO BE =1
C      *****
C      GRAVITY OF EACH OVERLYING LAYER IS REMOVED BEFORE EACH ITERA
C      LINEAR VARIATION OF BEDTHICKNESS AND DENSITIES IS ASSUMED
C      IF DENSITIES AT OPPOSITE ENDS OF EACH LAYER IS SAME DIGITISI
C      PROCESS IS SKIPPED. SAME IS TRUE FOR BEDTHICKNESS.
C      *****
C      COMMON/HILLS/NN,DX,ZUP,GRHO,GRO
C      COMMON/INV/NTERMS,ITER,ISKIP,ACC,IZUP,IPRINT,FRAC,NLAY
C      *****
C      DIMENSION DG3(1),H2(1),DG2(1),H1(1),H(1),DG(1),FIL(1)
C      DIMENSION RODIG1(1),RODIG2(1),DERHO2(1),BTK(1),BTK2(1),DERH
C      DIMENSION DG4(1)
C      *****
C      COMPLEX SUM(1),HTON(1),ANOM(1)
C      COMPLEX HC
C      DATA PI/3.1415926535/,G/6.67/
CC
C      TWOPI=2*PI
C      NND2=NN/2
C      N2PLUS=NND2+1
C      DK=TWPPI/(DX*NN)
CC
CC      CALCULATE CONTEIBUTIONS BELOW THE CUTOFF FREQUENCY
C      NFINAL=NN*SH +2
C      IF(NFINAL .GT. N2PLUS) NFINAL=N2PLUS
C      STORE INPUT GRAVITY IN DG2 TO FIND RESIDUE GRAVITY
C      A FRACTION OF INPUT GRAVITY IS USED FOR FIRST ITERATION
C      DG3 STORE GRAVITY TO FIND THE AVERAGE OF TWO ADJ ITERATIONS
C      DO 9 I=1,NN
C      DG2(I)=DG(I)
C      DG(I)=DG(I)*FRAC
9      DG3(I)=DG(I)
C      IF (IPRINT.LE.2) WRITE (6,8) (DG(I),I=1,NN)
8      FORMAT (//,20X,'GRAVITY USED FOR FIRST INVERSION',
1//,10(10F12.3,/) )
C      DO 10 J=1,NN
C      SUM(J)=CMPLX(0., 0.)

```



```

10      ANOM(J)=CMPLX(DG(J),0.)
6      FORMAT(//,'OFFSET GRAVITY FOR INVERSION',F10.5,/,/,
110(10F12.3,/))
C
      CALL FFTTWO(ANOM,NN)
C
      SOLD=1.E05
C      *****
      DO 50 JJ=1,ITER
C
CC      CONVERGENCE IS MOST RAPID IF THE TOPOGRAPHY IS EQUALLY POSIT
CC      WITH RESPECT TO ZUP.  FIND THE LARGERS AND SMALLEST VALUES O
C
      BIG=-1.E09
      SMALL=1.E09
      DO 12 J=1,NN
      IF(H1(J).GT.BIG) BIG=H1(J)
      IF(H1(J).LT.SMALL) SMALL=H1(J)
12      CONTINUE
      DELZUP=-(BIG+SMALL)/2
C      COMPUTE ELEVATION OF TOP HORIZON
      WRITE(6,13) JJ,BIG,SMALL,ZUP,DELZUP
13      FORMAT(//,5X,6H ITER=,I4,5X,10H MAX ELEV=,F10.4,5X,10H MIN
1      F10.4,5X,5H ZUP=,F8.4,5X,8H DELZUP=,F8.4)
      IF(IZUP.EQ.0) GO TO 31
      ZUP=ZUP+DBLZUP
      DO 14 J=1,NN
14      H1(J)=H1(J)+DELZUP
C
CC      INITIALIZE SUM
C      *****
31      DEXP=EXP(DK*ZUP)
      TERM=1./(TWOPI*G)
C      IF DENSITIES AT OPPOSITE ENDS ARE SAME USE CONSTANT DENSITY
      IF(RHO1.EQ.RHO2) TERM=TERM/RHO1
      SUM(1)=ANOM(1)*TERM
      DO 15 K=2,NFINAL
      TERM=TERM*DEXP
      IF(K.NE.N2PLUS) SUM(K)=ANOM(K)*TERM
      MINUS=NN-K+2
15      SUM(MINUS)=ANOM(MINUS)*TERM
C      *****
C
      IF(IPRINT.EQ.0) WRITE(6,55) (SUM(J),J=1,NN)
55      FORMAT(////,19H FOURIER AMPLITUDES,/,/, 10(10E12.3,/))
C      DIGITISE DENSITY
      IF(RHO1.EQ.RHO2) GOTO 621
      ND2=NN/2
      ROIN=(RHO1-RHO2)/(ND2-1)
      DO 303 I=1,ND2
      RODIG1(I)=RHO1-ROIN*(I-1)
      RODIG1(I+ND2)=RHO1-ROIN*(ND2-I)
303      CONTINUE

```



```

C *****
      IF (IPRINT.LE.2) WRITE(6,373) (RODIG1(I),I=1,NN)
373  FORMAT(///,10X,' DIGITISED DENSITY=',
1    //, 10(10F12.4,/))
C  IF THE INITIAL TOPOGRAPHY IS ZERO THEN DO NOT CALCULATE THE
621  IF (ISKIP.EQ.0) GO TO 20
      FAC=1.0
      DO 16 N=2, NTERMS
      FAC=N*FAC
CC  COPY THE NTH POWER OF THE TOPOGRAPHY INTO COMPLEX HTON
      IF (RHO1.EQ.RHO2) GOTO 217
      DO 724 J=1, NN
724  HTON(J)=CMPLX(RODIG1(J)*H1(J)**N,0.0)
      GOTO 127
217  DO 17 J=1, NN
17   HTON(J)=CMPLX(H1(J)**N,0.)
C
127  CALL FFTTWO(HTON,NN)
C
C
CC  FIND THE LARGEST VALUE OF THE PERTURBATION TERM
      BIG=0.0
      DO 18 K=2, NFINAL
      CAYN=((K-1)*DK)**(N-1)/FAC
      IF (K.EQ.N2PLUS) GO TO 40
      HC=HTON(K)*CAYN
      B=CABS(HC)
      IF (B.GT.BIG) BIG=B
      SUM(K)=SUM(K-HC
40  MINUS=NN-K+2
      HC=HTON(MINUS)*CAYN
      B=CABS(HC)
      IF (B.GT.BIG) BIG=B
18  SUM(MINUS)=SUM(MINUS) - HC
      IF (N.EQ.2) FIRST=BIG
      IF (IPRINT.LE.2) WRITE(6,41) N,BIG
41  FORMAT(30X,3H N=,I4,10X,51H LARGEST ABSOLUTE VALUE OF TERM
1WARD PROBLEM=, E15.4)
      IF (BIG/FIRST .LT. 5.E-03) GO TO 20
16  CONTINUE
      WRITE(6,56)
56  FORMAT(20X,34H THE FORWARD SUM HAS NOT CONVERGED)
C
CC  APPLY THE LOWPASS FILTER
20  IF (IPRINT.EQ.0) WRITE(6,55) (SUM(J),J=1,NN)
      IF (RHO1.EQ.RHO2) GOTO 521
C  *****
C  INVERSE TRANSFORM TO GET TOPOG, DIVIDE BY CORRESPONDING
C  DENSITY, TRANSFORM AND FILTER AND COMPARE EACH ADJACENT
C  ITERATION.
      CALL FFTTWO(SUM,NN)
      CALL REORDR(SUM,NN)
      DO 272 J=1, NN

```



```

272  H(J)=REAL(SUM(J))/(NN*RODIG1(J))
      DO 299 J=1,NN
299  SUM(J)=CMPLX(H(J),0.0)
      CALL FFTTWO(SUM,NN)
      DO 37 K=1,NN
37   SUM(K)=SUM(K)*FIL(K)
      CALL FFTTWO(SUM,NN)
      CALL REORDR(SUM,NN)
      S1=0.0
      DO 263 I=1,NN
      H(I)=REAL(SUM(I))/NN
      H2(I)=H(I)
263  S1=S1+(H(I)-H1(I))**2
C    *****
      GOTO 727
521  DO 32 J=1,NN
32   SUM(J)=SUM(J)*FIL(J)
      IF(IPRINT.EQ.0) WRITE(6,55) (SUM(J),J=1,NN)
C
CC   CALCULATE THE TOPOGRAPHY BY TAKING THE FOURER TRANSFORM
      CALL FFTTWO(SUM,NN)
      CALL REORDR(SUM,NN)
C
      S1=0.0
      DO 22 J=1,NN
      H(J)=REAL(SUM(J))/NN
      H2(J)=H(J)
22   S1=S1+(H(J)-H1(J))**2
C    *****
727  S1=SQRT(S1)/NN
      WRITE(6,23) JJ,S1
23   FORMAT(//,40X,11H ITERATION=,I5,10X,7H ERROR=,E12.4)
      IF(IPRINT.LE.2) WRITE(6,24) ZUP,(H(J),J=1,NN)
24   FORMAT(///,10X,41H THE TOPOGRAPHY MEASURED RELATIVE TO ZUP
1     F8.4,/,10(10F12.4,/))
C
CC   CHECK TO SEE IF ITERATION IS STARTING TO DIVERGE
      XX=(S1-SOLD)/SOLD
C
C   DO NOT CHECK FOR DIVERGENCE OF SECOND ITERATION BECAUSE
C   FIRST ITERATION USE VERY DIFFERNT GRAVITY
      IF(JJ.EQ.2) GOTO 42
      IF(XX.LT..01) GO TO 42
      WRITE(6,43)
43   FORMAT(///,20X,57H **** THE ITERATION PROCEDURE IS STARTIN
1     VERGE ****,///)
C
C   USE THE TOPOGRAPHY FROM THE LAST ITERATION
      DO 44 J=1,NN
      H2(J)=H1(J)
44   H(J)=H1(J)
      GO TO 30
C *****

```



```

42      IF (S1.LE.ACC) GO TO 30
        IF (JJ.EQ.ITER) GOTO 381
        SOLD=S1
C      *****
C      IF ANY OVERLYING LAYER HAS ZERO BEDTHICKNESS (I.E.) TWO LAYER
C      DO NOT COMPUTE GRAVITY OF OVERLYING LAYERS.
        DO 711 K=1,NN
711     DG4 (K)=0.0
        DZUP=ZUP
        NND2=NN/2
        NBD=NLAY-2
C      IF BED IS OF SAME THICKNESS DO NOT CALCULATE VARIATION
        DO 909 I=1,NBD
        IF (BTK(I).EQ.BTK2(I).AND.BTK(I).EQ.0.0) GOTO 742
        IF (BTK(I).EQ.BTK2(I)) GOTO 623
        DBTK=BTK(I)-BTK2(I)
        BTKIN=DBTK/(NND2-1)
        DO 99 L=1,NND2
        H2(L)=H2(L-BTKIN*(L-1))
99     H2(NND2+L)=H2(NND2+L-BTKIN*(NND2-L))
C      READJUST HORZN RESPONSIBLE FOR CORRESPONDING BED
623     ZUP=ZUP-BTK(I)
        IF (IPRINT.LE.2) WRITE(6,75) ZUP, (H2(J),J=1,NN)
75     FORMAT(///,10X,41H THE TOPOGRAPHY MEASURED RELATIVE TO ZUP
1      F8.4,///, 10(10F12.4,/))
C      COMPUTE GRAVITY OF OVERLYING LAYER
        CALL RHOBGG(H2,DG,SUM,HTON,NTERMS,DERHO(I),DERHO2(I),RODIG2
        IF (IPRINT.LE.2) WRITE(6,74) ZUP, (DG(J),J=1,NN)
        DO 919 K=1,NN
919     DG4 (K)=DG4 (K)+DG (K)
909     CONTINUE
C      *****
74     FORMAT(///,10X,' THE GRAVITY CALCULATED RELATIVE TO ZUP=',
1      F8.4,///, 10(10F12.0,/))
C      USING THE AVG OF THE GRAVITY USED IN THE LAST ITERATION AN
C      THE DIFFERENCE OF THE INPUT GRAVITY AND THE GRAVITY OF
C      OVERLYING LAYER
C      COMPUTE THE RESIDUAL GRAVITY
        DO 88 M=1,NN
        DG (M)=(DG2 (M)-DG4 (M)+DG3 (M))/2.0
88     DG3 (M)=DG (M)
        IF (IPRINT.LE.2) WRITE(6,76) DZUP, (DG(J),J=1,NN)
76     FORMAT(///,10X,' THE RESIDUE GRAVITY CALCULATED RELATIVE T
1      ,F8.4,///, 10(10F12.4,/))
C      RESTORE ZUP TO ITS STARTING VALUE
        ZUP=DZUP
        DO 77 J=1,NN
        SUM (J)=CMPLX(0.,0.)
77     ANOM (J)=CMPLX(DG (J),0.)
        CALL FFTTWO(ANOM,NN)
CC     TRANSFER THE TOPOGRAPHY BACK TO H1
742     DO 25 J=1,NN
25     H1 (J)=H (J)

```



```

50      ISKIP=1
C
381     WRITE(6,26) S1,ACC,ITER
26      FORMAT(///,44H ***** CONVERGENCE HAS NOT BEEN OBTAINED
1 10X,7H ERROR=,E12.3,10X,18H DESIRED ACCURACY=,E12.3,10X,
1 22H NUMBER OF ITERATIONS=,I5)
C      COMPUTE FINAL INVERTED GRAVITY OF INVERTED TOPOG.
30      MN=NN/2
        ZUP=DZUP
        IF (IPRINT.GT.2) WRITE(6,24) ZUP, (H(J),J=1,MN)
        CALL RHOBG(H2,DG,SUM,HTON,NTERMS,RHO1,RHO2,RODIG2)
        DO 633 N=1,MN
          DG4(N)=0.0
633     DG4(N)=DG(N)
          IF (IPRINT.LT.2) WRITE(6,74) ZUP, (DG(J),J=1,MN)
          DO 809 I=1,NBD
C      IF ANY OVERLYING LAYER HAS ZERO BEDTHICKNESS(I.E.) TWO LAYER
C      DO NOT COMPUTE GRAVITY OF OVERLYING LAYERS.
          IF (BTK(I).EQ.BTK2(I).AND.BTK(I).EQ.0.0) GOTO 809
          IF (BTK(I).EQ.BTK2(I)) GOTO 624
          DBTK=BTK(I)-BTK2(I)
          BTKIN=DBTK/(NND2-1)
          DO 701 L=1,NND2
            H2(L)=H2(L-BTKIN*(L-1))
701     H2(NND2+L)=H2(NND2+L-BTKIN*(NND2-L))
624     ZUP=ZUP-BTK(I)
          IF (IPRINT.GT.2) WRITE(6,24) ZUP, (H2(J),J=1,MN)
          CALL RHOBG(H2,DG,SUM,HTON,NTERMS,DERHO(I),DERHO2(I),RODIG2)
          IF (IPRINT.LT.2) WRITE(6,74) ZUP, (DG(J),J=1,MN)
          DO 929 K=1,MN
929     DG4(K)=DG(K)+DG4(K)
809     CONTINUE
        RETURN
        END
        SUBROUTINE LOPASS (B,F,WH,SH,N,II)
C
C      CALCULATE A HIGH PASS FILTER USING A COSINE TAPER BETWEEN WH
C      AT FREQUENCIES LESS THAN WH THE FILTER IS EQUAL TO UNITY, AND
C      GREATER THAN SH THE FILTER IS ZERO.
C      IF II=1 A FULL TWO SIDED FILTER COMPATIVLE WITH FOURERR TRANS
C
        DIMENSION B(1),F(1)
        DATA PI/3.1415926535/
        NN=N/2+1
        DO 11 J=1,NN
C      1.4 IS MULTIPLIED BECAUSE DIFF SAMPLING INTERVALS WERE USED
C      5 KM. AND 7 KM. WERE USED IN TWO SEPARATE PROFILES.
11      F(J)=(J-1)*1.4/(N*1.0)
        DO 10 J=1,NN
          IF (F(J-WH) 20,20,21
20      B(J)=1.0
          GO TO 10
21      IF (F(J-SH) 24,24,25

```



```

24      B(J) = (1. - COS(PI*(F(J-SH)/(WH-SH)))/2.
      GO TO 10
25      B(J) = 0.0
10      CONTINUE
C
      IF(II.NE.1) RETURN
C      CALCULATE A TWO SIDED FILTER SERIES
      NN=N/2-1
      DO 30 J=1,NN
30      B(N+1-J)=B(J+1)
      RETURN
      END
      SUBROUTINE SPLNCO (N1,N2,X,Y,B,C,D)
C      COMPUTATION OF THE COEFFICIENTS OF A CUBIC SPLINE
C      INTERPOLATING BETWEEN GIVEN DATA POINTS.
C      INPUT.
C      N1,N2  NUMBER OF FIRST AND LAST DATA POINT(0.LT.N1.LT.N2)
C      X(I),Y(I),I=N1,N1+1,...,N2 ARRAYS WITH X(1) AND Y(1) AS ABS
C      AND ORDINATE OF I-TH DATA POINT. THE COMPONENTS OF THE
C      ARRAY X MUST BE EITHER STRICTLY MONOTONIC INCREASING
C      OR DECREASING.
C      OUTPUT.
C      B(I),C(I),D(I),I=N1,N1+1,...,N2 ARRAYS COLLECTING THE COEFFI
C      THE CUBIC SPLINE F(XX). IF XX LIES BETWEEN X(I) AND X(
C      THEN F(XX) = ((D(I)*H+C(I))*H+B(I))*H+Y(I),
C      WHERE H=XX-X(I).
C      FURTHERMORE,C(N2)=0 WHILE B(N2) AND D(N2) ARE LEFT
C      UNDEFINED.
      DIMENSION X(1),Y(1),B(1),C(1),D(1)
      M1=N1+1
      M2=N2-1
      S=0.
      M3=M1+M2
      DO 1 K=N1,M2
      D(K)=X(K+1)-X(K)
      R=(Y(K+1)-Y(K))/D(K)
      C(K)=R-S
1      S=R
      C(N2)=0
      C(N1)=0
      S=0
      R=0
      DO 2 K=M1,M2
      C(K)=C(K)+R*C(K-1)
      B(K)=(X(K-1)-X(K+1))*2.-R*S
      S=D(K)
2      R=S/B(K)
      DO 3 K=M1,M2
      L=M3-K
3      C(L)=(D(L)*C(L+1)-C(L))/B(L)
      DO 4 K=N1,M2
      B(K)=(Y(K+1)-Y(K))/D(K)-(C(K)+C(K)+C(K+1))*D(K)
      D(K)=(C(K+1)-C(K))/D(K)

```



```

4      C(K)=3.*C(K)
      RETURN
      END
      SUBROUTINE SPLNEV (N1,N2,X,Y,B,C,D,XINT,YINT,I)
C      EVALUATION OF A CUBIC SPLINE AT ABSCISSA XINT.
C      INPUT DATA.
C      N1,N2          NUMBER OF FIRST AND LAST DATA POINT(0.LT.N1.LT.N2
C      X(K),Y(K),K=N1,N1+1,N2 ARRAYS WITH X(K) AND Y(K) AS ABSCISS
C      AND ORDINATE OF THE K-TH DATA POINT. THE COMPONENTS
C      OF X MUST BE EITHER STRICTLY MONOTONIC INCREASING OR
C      DECREASING.
C      B(K),C(K),D(K),K=N1,N1+1,...,N2 SPECIFY THE SPLINE FUNCTION
C      TO BE EVALUATED. IF XX LIES BETWEEN X(K) AND X(K+1),
C      (I.E. WITHIN THE K-TH INTERVAL), THEN
C      F(XX)=((D(I)*H+C(I))*H+B(I))*H+Y(I)
C      WHERE H=XX-X(I)..
C      XINT ABSCISSA, FOR WHICH YINT=F(XINT) HAS TO BE EVALUATED.
C      I IF ON ENTRY I=0, THEN THE NUMBER OF THE INTERVAL, IN WHI
C      XINT LIES, IS NOT KNOWN (ERROR MESSAGE, IF XINT LIES
C      NOT BETWEEN X(N1) AND X(N2)).
C      ON LEAVING THE ROUTINE, I IS EQUAL TO THIS INTERVAL
C      NUMBER.
C      IF ON ENTRY I.NE.0, THEN I SPECIFIES THE NUMBER OF THE
C      INTERVAL, WHERE XINT IS LOCATED (ERROR MESSAGE IF
C      I.LT.0, 0.LT.I.LT.N1 OR N2.LT. I. UPON EXIT, I IS NOT
C      OUTPUT DATA.
C      I (SEE ABOVE)
C      YINT = F(XINT).
C
      DIMENSION X(1),Y(1),B(1),C(1),D(1)
      IF(I) 16,1,11
11     IF(I.LT.N1.OR.I.GE.N2) GO TO 16
      GO TO 12
1     IS=1
      IF(X(N1)-X(N2)) 2,3,3
3     IS=-IS
2     IF((XINT-X(N1))*IS) 10,14,4
14    YINT=Y(N1)
      RETURN
4     IF((X(N2)-XINT)*IS) 10,15,9
15    YINT=Y(N2)
      RETURN
9     I=N1
      I2=N2
5     IF(I2-I-1) 12,12,6
6     I3=(I+I2+.1)*.5
      IF((XINT-X(I3))*IS) 7,13,8
7     I2=I3
      GO TO 5
8     I=I3
      GO TO 5
13    YINT=Y(I3)
      RETURN

```



```

12      H=XINT-X(I)
        YINT=( (D(I)*H+C(I))*H+B(I))*H+Y(I)
        RETURN
10      PRINT 101,XINT
101     FORMAT(8H XINT = E18.9,32H, OUT OF RANGE FOR INTERPOLATION)
        RETURN
16      PRINT 102,I
102     FORMAT(5H I = I5,32H, OUT OF RANGE FOR INTERPOLATION)
        RETURN
        END
        SUBROUTINE FFTTWO(A,N)
C
CC      ROUTINE FOR FINDING DISCRETE FOURIER TRANSFORM OF A COMPLEX
CC      MODIFIED FROM COOLEY ET AL IEEE TRANS OF EDUCATION 12 NO 1 (
CC      ARGUMENT LIST
CC      A IS A COMPLEX ARRAY CONTAINING THE SERIES TO BE TRANSFORMED
CC      RESULTS ARE RETURNED IN A OVER-WRITEING THE ORIGINAL SERIES
CC      N IS THE NUMBER OF TERMS IN THE SERIES. IT MUST BE A POWER
CC      THE ROUTINE WILL PRINT A MESSAGE AND RETURN WITHOUT DOING AN
CC      FINDS FOR M=0,N-1 SUM,A(K+1)*EXP(2*PI*(0,1)*(K+1)*M+1)), WIT
CC      K=0,N-1.
CC      NOTE INDIECES ARE DISPLACED WITH RESPECT OF FREQUENCY, EG. Z
CC      FREQUENCY IS HELD IN A(1).
C
        DIMENSION A(N)
        COMPLEX A,U,W,T
        DATA PI/3.1415926535/
        M=ALOG(FLOAT(N))/0.693147
        IF(N.NE.2**M) GO TO 1000
        NV2=N/2
        NM1=N-1
        J=1
        DO 7 I=1,NM1
        IF(I.GE.J) GO TO 5
        T=A(J)
        A(J)=A(I)
        A(I)=T
5       K=NV2
6       IF(K.GE.J) GO TO 7
        J=J-K
        K=K/2
        GO TO 6
7       J=J+K
        LE=1
        DO 20 L=1,M
        LE1=LE
        LE=2*LE
        U=(1.,0.)
        B=PI/FLOAT(LE1)
        W=CMPLX(COS(B),SIN(B))
        DO 20 J=1,LE1
        DO 10 I=J,N,LE
        IP=I+LE1

```



```

      T=A(IP)*U
      A(IP)=A(I-T
10    A(I)=A(I)+T
20    U=U*W
      RETURN
1000  PRINT 100,N
100   FORMAT(5(4H ***),I6,70H IS NOT A POWER OF 2.  FFTWO CANNO
1FORM A SERIES OF THIS LENGTH  )
      RETURN
      END
      SUBROUTINE REORDR(A,N)
      COMPLEX A(1),DUM
CC    ROUTINE REORDERS THE OUTPUT FROM A FOURERR TRANSFORM ROUTINE
      ND2=N/2
      DO 10 J=2,ND2
      DUM=A(J)
      A(J)=A(N+2-J)
10    A(N+2-J)=DUM
      RETURN
      END

```


Program to invert residual gravity to obtain density.

```

C      THIS PROGRAM INVERTS RESIDUAL GRAVITY TO OBTAIN A DENSITY
C      -CONTRAST PROFILE.
C      WRITTEN BY JOSEPH S.K. LEE, UNIVERSITY OF ALBERTA, 1977.
C      THIS PROGRAM CALLS SUBROUTINE DENSTY AND DENBOU, AND
C      ASSUMES INPUT RESIDUAL GRAVITY TO BE EQUALLY SPACED.
C      IT IS TO BE NOTED THAT THIS PROGRAM WAS MODIFIED FROM THE
C      MULTILAYER INVERSION SCHEME, AND NO TIME WAS SPENT TO CHANG
C      THE VARIABLES TO MEANINGFUL VARIABLES.
C      INPUT TO THE MAIN PROGRAM SHOULD BE OF THE FOLLOWING FORMAT
C **   NJJ,NLL,NKK,NN,IG,ITOP,JPRINT. (# OF FILTERS, # OF SLABS,
C      # OF HORIZONS Z, TOTAL NUMBER OF RESIDUAL GRAVITY STATIONS
C      FOR GAVITY IN TENTH OF MGAL IG .NE. 1,IF H(X) ALONG PROFIL
C      IS GIVEN ITOP.EQ. 1 ELSE ITOP .NE. 1
C      JPRINT .EQ. 3 FOR NO OUTPUT OF INTERMEDIATE RESULTS.
C **   DX (SAMPLING INTERVAL OF RESIDUAL GRAVITY)
C **   RHO (THKNES OF SLAB AT W END OF PROFL FOR ITOP.NE.1; NLL TERM
C **   RHOTWO (SIMILAR TO RHO, BUT AT THE E END; NLL TERMS)
C **   RODIG1 (DIGITISED H(X) ALONG PROFL, FOR ITOP.EQ.1, NN TERMS)
C **   GG (RESIDUAL GRAVITY, NN TERMS)
C **   WH,SH (FILTER PARAMETERS, NJJ TERMS)
C *****
C      DIMENSION H1(512),H(512),DG(512),RHO(512),RHOTWO(512)
C      DIMENSION RODIG1(512),F(512),ZZ(512),B(512)
C      DIMENSION AA(512),BB(512),CC(512),GG(512)
C      COMPLEX SUM(512),HTON(512),ANOM(512)
C      COMMON/BOUG/ACC,IPRINT
C      COMMON/HILLS/NN,DX,ZUP,GRHO,GRO
C      COMMON/INV/ITERMS,ITER,ISKIP,AC1,IZUP,JPRINT,FRAC,NLAY
C      DATA PI/3.1415926535/
C      DATA G/6.67/
C      READ(5,100) NJJ,NLL,NKK,NN,IG,ITOP,JPRINT
C      READ(5,171) DX
100  FORMAT(10I4)
101  FORMAT(10F10.3)
171  FORMAT(2F8.3)
C      READ(5,102) (ZZ(I),I=1,NKK)
C      IF (ITOP .NE. 1) READ(5,102) (RHO(I),I=1,NLL)
C      IF (ITOP .NE. 1) READ(5,102) (RHOTWO(I),I=1,NLL)
C      IF (ITOP .EQ. 1) READ (5,47) (RODIG1(J),J=1,NN)
C      IPRINT=JPRINT
102  FORMAT(5F8.3)
C      INPUT THE # OF TERMS TO BE USED IN POWER SERIES
C      NTERMS=35
47   FORMAT(10F12.3)
C      READ(5,47) (GG(J),J=1,NN)
C      NBY2=NN
C      NN=NN*2

```



```

C   GENERATE MIRROR IMAGE.
      DO 37 I=1,NBY2
37  GG(NN-I+1)=GG(I)
      IF(ITOP.NE.1) GO TO 55
      DO 49 J=1,NBY2
49  RODIG1(NN-J+1)=RODIG1(J)
C   IF INPUT GRAVITY IS TENTH MILLIGAL CONVERT TO MILLIGAL
55  IF (IG.EQ.1) GO TO 99
      DO 1 I=1,NN
1    GG(I)=GG(I)*0.1
11   FORMAT(10F12.1)
99   IF (JPRINT.LT.3) WRITE (6,56) (GG(J),J=1,NN)
      IF (ITOP.EQ.1) WRITE (6,65) (RODIG1(J),J=1,NN)
65   FORMAT (////////,40X,' INITIAL TOPOG',
1     //,10(10F9.3,/))
56   FORMAT (////////,40X,' INITIAL GRAVITY ANOMALY',
1     //,10(10F9.3,/))
CC  COMPLETE THE INVERSION OF THE GRAVITATIONAL ANOMALY
C   INPUT THE MAX NUMBER OF TERMS IN THE SERIES TO BE TAKEN.
C   INPUT THE MAX NUMBER OF ITERATIONS TO BE USED.
C   THE DESIRED ACCURACY BETWEEN SUCCESSIVE TOPOGRAPHIC ITERAT
C   DISREGARD STAMENTS CONCERNING IZUP AND ZUP, THEY HAVE NO CONC
C   THIS PROGRAM.
C   THE INDEX IZUP FOR ALTERING THE VALUE ZUP
C   FOR EACH ITERATION IZUP=0 IF THERE IS NO CHANGE FOR ZUP,
C   ELSE IZUP =1. CHANGING THE VALUE OF ZUP (BEING THE MEDIAN)
C   SPEED UP THE ITERATION PROCESS.
C   JPRINT=0 TO OUTPUT THE FOURIER AMPLITUDE, JPRINT>2 TO
C   OUTPUT THE LARGEST ABSOLUTE VALUE FOR THE FORWARD ITERATIO
      ITERMS=35
      ITER=15
      AC1=5.E-05
      ACC=1.E-03
      DO 34 JJ=1,NJJ
CC  CALCULATE A BANDPASS FILTER
      READ(5,35) WH,SH
35   FORMAT(2F8.4)
      CALL LOPASS(B,F,WH,SH,NN,1)
      IF (JPRINT.LT.3) WRITE(6,36) WH,SH,(B(J),J=1,NN)
36   FORMAT(///,20X,23H LOW PASS FILTER      WH=,F6.4,10X,4H SH=,
1     F6.4,///,10(15F8.4,/))
CC  CALCULATE THE LOW PASSED GRAVITY PROFILE
      DO 42 J=1,NN
42   ANOM(J)=CMPLX(GG(J),0.)
      CALL FFTTWO(ANOM,NN)
      DO 43 J=1,NN
43   ANOM(J)=ANOM(J)*B(J)
      CALL FFTTWO(ANOM,NN)
      CALL REORDR(ANOM,NN)
      DO 44 J=1,NN
44   DG(J)=REAL(ANOM(J))/NN
      IF (JPRINT.LT.3) WRITE(6,45) (DG(J),J=1,NN)
45   FORMAT(////////,30X,31H FILTERED GRAVITATIONAL ANOMALY,///,10(

```



```

1 4,/) )
CC
CC
DO 34 KK=1,NKK
ZUP=ZZ(KK)
CC
DO 34 LL=1,NLL
IF (ITOP .NE. 1) WRITE (6,39) RHO(LL),RHOTWO(LL)
39  FORMAT(////////,20X,'BED THICKNESS AT EITHER OF PROFILE=',2F
DO 40 J=1,NN
40  H1(J)=0.0
ISKIP=0
NTERMS=35
C  CALL INVERSION SBROUTINE TO DO INVERSION
CALL DENSTY(ITOP,RODIG1,RHO(LL),RHOTWO(LL),GG,H1,H,
1SUM,ANOM,HTON,B,SH)
IF (JPRINT .LT. 3) WRITE (6,65) (RODIG1(J),J=1,NN)
NTERMS=35
ND=NN/2
C  COMPUTE GRAVITY FROM INVERTED DENSITY PROFILE.
CALL DENBOU(DG,RODIG1,H,SUM,HTON,NTERMS)
IF (JPRINT.LT.3) WRITE(6,51) (GG(J),DG(J),J=1,NN)
IF (JPRINT.GE.3) WRITE(6,512) (GG(J),J=1,ND)
512  FORMAT(////////,30X,' ORIGINAL GRAVITY',//,10(10F12.
1 4,/) )
IF (JPRINT.GE.3) WRITE(6,511) (DG(J),J=1,ND)
511  FORMAT(////////,30X,' GRAVITY FROM INVERTED TOPOG',//,10(10F1
1 4,/) )
51  FORMAT(////////,40X,48H OBSERVED AND CALCULATED GRAVITATIONAL
1IES,//, 10(2F9.3,6X, 2F9.3,6X, 2F9.3,6X, 2F9.3,6X, 2F9.
34  CONTINUE
STOP
END
SUBROUTINE DENSTY(ITOP,RODIG1,RHO1,RHO2,GG,H1,
1H,SUM,ANOM,HTON,FIL,SH)
C  *****
C  ROUTINE COMPUTES THE DENSITY FROM RESIDUAL GRAVITY PROFILE.
C  ** ITOP .EQ. 1 IF H(X) AT EITHER ENDS OF PROFILE IS GIVEN, ELSE
C  ** RODIG1 VECTOR FOR DIGITISED H(X)
C  ** RHO1 H(X) AT W END OF PROFILE.
C  ** RHO2 H(X) AT E END OF PROFILE.
C  ** GG RESIDUAL GRAVITY.
C  ** H1 VECTOR CONTAINS INITIAL GUESSED VALUES OF DENSITY .
C  ** H VECTOR CONTAINS INTERMEDIATE AND FINAL COMPUTED VALUES OF
C  ** SUM IS THE SUMMATION OF THE FFT OF GRAVITY AND DENSITY TERMS
C  ** HTON IS A DUMMY COMPLEX VARIABLE FOR THE DENSITY D(X), WHICH
C  FOR FFT OF DENSITY.
C  ** ANOM IS A DUMMY VARIABLE FOR CIMPLEXING THE RESIDUAL GRAVITY
C  USED FOR FFT OF GRAVITY DATA.
C  ** FIL IS THE FILTER COEFF SUPPLY BY LOPASS SUBROUTINE.
C  ** SH IS THE CUT OFF FREQUENCY.
C  *****
COMMON/HILLS/NN,DX,ZUP,GRHO,GRO

```



```

COMMON/INV/NTERMS,ITER,ISKIP,ACC,IZUP,IPRINT,FRAC,NLAY
C *****
DIMENSION RODIG1(1),H1(1),H(1),GG(1),FIL(1)
C *****
COMPLEX SUM(1),HTON(1),ANOM(1)
COMPLEX HC
DATA PI/3.1415926535/,G/6.67/

CC
TWOPI=2*PI
NND2=NN/2
N2PLUS=NND2+1
DK=TWOPI/(DX*NN)

CC
CC CALCULATE CONTEIBUTIONS BELOW THE CUTOFF FREQUENCY
NFINAL=NN*SH +2
IF(NFINAL.GT.N2PLUS) NFINAL=N2PLUS
DO 10 J=1,NN
SUM(J)=CMPLX(0.,0.)
10 ANOM(J)=CMPLX(GG(J),0.)
C
CALL FFTTWO(ANOM,NN)
C
SOLD=1.E05
C IF H(X) ALONG PROFILE IS NOT KNOWN ASSUME LINEAR VARIATION OF
IF (ITOP.EQ. 1) GOTO 621
ND2=NN/2
ROIN=(RHO1-RHO2)/(ND2-1)
DO 303 I=1,ND2
RODIG1(I)=RHO1-ROIN*(I-1)
RODIG1(I+ND2)=RHO1-ROIN*(ND2-I)
303 CONTINUE
C *****
IF (IPRINT.LE.2) WRITE(6,373) (RODIG1(I),I=1,NN)
C *****
621 DO 50 JJ=1,ITER
C
C
BIG=-1.E09
SMALL=1.E09
DO 12 J=1,NN
IF(H1(J).GT.BIG) BIG=H1(J)
IF(H1(J).LT.SMALL) SMALL=H1(J)
12 CONTINUE
WRITE(6,13) JJ,BIG,SMALL
13 FORMAT(/,5X,6H ITER=,I4,5X,13H MAX DENSITY=,F13.4,5X
1 ,13H MIN DENSITY=,F10.4)
CC INITIALIZE SUM
C *****
31 DEXP=EXP(DK*ZUP)
TERM=1./(TWOPI*G)
SUM(1)=ANOM(1)*TERM
DO 15 K=2,NFINAL
TERM=TERM*DEXP

```



```

      IF (K.NE.N2PLUS) SUM(K) = ANOM(K) *TERM
      MINUS=NN-K+2
15      SUM(MINUS) = ANOM(MINUS) *TERM
C      *****
C
      IF (IPRINT.EQ.0) WRITE (6,55) (SUM(J),J=1,NN)
55      FORMAT(////,19H FOURIER AMPLITUDES,/, 10(10E12.3,/))
C      DIGITISE DENSITY
373      FORMAT(///,10X,' DIGITISED TOPOG=',
1        //, 10(10F12.4,/))
C      IF THE INITIAL DENSITY IS ZERO THEN DO NOT CALCULATE THE PER
      IF (ISKIP.EQ.0) GO TO 20
      FAC=1.0
      DO 16 N=2, NTERMS
      FAC=N*FAC
CC      COPY THE NTH POWER OF THE TOPOGRAPHY INTO COMPLEX HTON
      DO 724 J=1, NN
724      HTON(J)=CMPLX(H1(J)*RODIG1(J)**N,0.0)
127      CALL FFTTWO(HTON,NN)
C
C
CC      FIND THE LARGEST VALUE OF THE PERTURBATION TERM
      BIG=0.0
      DO 18 K=2, NFINAL
      CAYN= ((K-1)*DK)**(N-1)/FAC
      IF (K.EQ.N2PLUS) GO TO 40
      HC=HTON(K)*CAYN
      B=CABS(HC)
      IF (B.GT.BIG) BIG=B
      SUM(K)=SUM(K-HC
40      MINUS=NN-K+2
      HC=HTON(MINUS)*CAYN
      B=CABS(HC)
      IF (B.GT.BIG) BIG=B
18      SUM(MINUS)=SUM(MINUS) - HC
      IF (N.EQ.2) FIRST=BIG
      IF (IPRINT.LE.2) WRITE (6,41) N,BIG
41      FORMAT(30X,3H N=,I4,10X,51H LARGEST ABSOLUTE VALUE OF TERM
1WARD PROBLEM=, E15.4)
      IF (BIG/FIRST .LT. 5.E-03) GO TO 20
16      CONTINUE
      WRITE (6,56)
56      FORMAT(20X,34H THE FORWARD SUM HAS NOT CONVERGED)
C
CC      APPLY THE LOWPASS FILTER
20      IF (IPRINT.EQ.0) WRITE (6,55) (SUM(J),J=1,NN)
C      *****
C      INVERSE TRANSFORM TO GET TOPOG, DIVIDE BY CORRESPONDING
C      TOPOG, TRANSFORM AND FILTER AND COMPARE EACH ADJACENT
C      ITERATION.
      CALL FFTTWO(SUM,NN)
      CALL REORDR(SUM,NN)
      DO 272 J=1, NN

```



```

272  H(J)=REAL(SUM(J))/(NN*RODIG1(J))
      DO 299 J=1,NN
299  SUM(J)=CMPLX(H(J),0.0)
      CALL FFTTWO(SUM,NN)
      DO 37 K=1,NN
37   SUM(K)=SUM(K)*FIL(K)
      CALL FFTTWO(SUM,NN)
      CALL REORDR(SUM,NN)
      S1=0.0
      DO 263 I=1,NN
      H(I)=REAL(SUM(I))/NN
263  S1=S1+(H(I)-H1(I))**2
C    *****
727  S1=SQRT(S1)/NN
      WRITE(6,23) JJ,S1
23   FORMAT(//,40X,11H ITERATION=,I5,10X,7H ERROR=,E12.4)
      IF(IPRINT.LE.2) WRITE(6,24) ZUP,(H(J),J=1,NN)
24   FORMAT(///,10X,41H THE DENSITY MEASURED RELATIVE TO ZUP=,
1     F8.4,///,10(10F12.4,/))
C
CC   CHECK TO SEE IF ITERATION IS STARTING TO DIVERGE
      XX=(S1-SOLD)/SOLD
C
      IF(XX.LT..01) GO TO 42
      WRITE(6,43)
43   FORMAT(///,20X,57H **** THE ITERATION PROCEDURE IS STARTIN
1     VERGE ****,///)
C
C   USE THE DENSITY FROM THE LAST ITERATION
      DO 44 J=1,NN
44   H(J)=H1(J)
      GO TO 381
C *****
42   IF(S1.LE.ACC) GO TO 30
      SOLD=S1
C *****
742  DO 25 J=1,NN
25   H1(J)=H(J)
50   ISKIP=1
C
381  WRITE(6,26) S1,ACC,ITER
26   FORMAT(///,44H ***** CONVERGENCE HAS NOT BEEN OBTAINED
1     10X,7H ERROR=,E12.3,10X,18H DESIRED ACCURACY=,E12.3,10X,
1     22H NUMBER OF ITERATIONS=,I5)
30   IF(IPRINT.GT.2) WRITE(6,24) ZUP,(H(J),J=1,NND2)
      RETURN
      END
      SUBROUTINE DENBOU(DG,RODIG1,H,SUM,HTON,NTERMS)
CC$$$$$ CALLS FFTWO
C   PROGRAM COMPUTES GRAVITY FROM INVERTED DENSITY PROFILE.
C   DG CONTAINS COMPUTED FINAL GRAVITY FROM INVERTD DENSITY PRO
C   RODIG1 CONTAINS DIGITISED H(X) ALONG THE PROFILE.
C   H CONTAINS DIGTISED DENSITY VALUES ALONG PROFILE.

```



```

C      SUM AND HTON ARE THE SAME AS THOSE OF DENSTY SUBROUTINE.
CC     COMPUTES 2-D BOUGUER ANOMALIES WITH FFT POWER METHOD
CC     'NTERMS' IS THE NUMBER OF TERMS IN POWER SERIES TO BE TAKEN.
CC     PARAMETERS COME THROUGH COMMON /HILLS/ - 'NN' NUMBER OF TERMS
CC     'DX' SPACING IN X DOMAIN, 'ZUP' VERTICAL DISTANCE ABOVE Y=0 OF
CC     'GRHO' BIG G TIMES RHO, 'H' ARRAY WITH 'NN' ELEMENTS CONTAININ
      COMMON/HILLS/NN,DX,ZUP,GRHO,GRO
      DIMENSION RODIG1(1),H(1),DG(1)
      COMPLEX SUM(1),HTON(1),HC
      COMMON/BOUG/ACC,IPRINT
      DATA TWOPI/6.283185307/
      DATA G/6.67/
      WRITE(6,20) ACC
20     FORMAT(///,30X,29H ACCURACY LEVEL IN BOUGER IS=,E12.3,/)
CC     SETS VARIOUS CONSTANTS AND ZEROS 'SUM' READY TO RECEIVE SERIE
      NNBY2=NN/2
      N2PLUS=NNBY2+1
      DK=TWOPI/(DX*NN)
      DO 110 I=1,NN
110    SUM(I)=(0.0,0.0)
      FAC=1.0
      BIGM1=10.

C
CC     'N' COUNTS NUMBER OF TERMS IN SERIES.
      DO 2500 N=1,NTERMS
      FAC=N*FAC
CC     COPIES N-TH POWER OF TOPOGRAPHY INTO COMPLEX 'HTON'
      BIG=0.0
      DO 233 J=1,NN
233    HTON(J)=CMPLX(H(J)*RODIG1(J)**N,0.0)

C
234    CALL FFTTWO(HTON,NN)

C
CC     FILTERS FOURIER COEFFS AND ADDS THEM INTO 'SUM'
CC     FEWER THAN NTERMS IN THE SUM MAY BE TAKEN IF AN ABSOLUTE CON
CC     CRITERION IS MET.
CC     ALSO PERFORM THE UPWARD CONTINUATION AT THIS STAGE
      TERM=TWOPI*G/NN
      DEXP=EXP(-DK*ZUP)
      IF(N.EQ.1) SUM(1)=HTON(1)*TERM
      DO 2200 K=2,N2PLUS
      TERM=TERM*DEXP
      CAYN=((K-1)*DK)**(N-1)/FAC
      CAYN=CAYN*TERM
      IF(K.EQ.N2PLUS) GO TO 40
      HC=HTON(K)*CAYN
      B=CABS(HC)
      IF(B.GT.BIG) BIG=B
      SUM(K)=SUM(K)+HC
40    MINUS=NN-K+2
      HC=HTON(MINUS)*CAYN
      B=CABS(HC)
      IF(B.GT.BIG) BIG=B

```



```

2200  SUM(MINUS)=SUM(MINUS)+HC
      IF(N.EQ.1) FIRST=BIG
      IF(IPRINT.LE.5) WRITE(6,42) N,BIG
42    FORMAT(30X,3H N=,I4,10X,51H LARGEST ABSOLUTE VALUE OF TERM
1WARD PROBLEM=,E15.4)
      BB=AMAX1(BIG,BIGM1)
      IF( BB/FIRST .LT. ACC      ) GO TO 43
      BIGM1=BIG
2500  CONTINUE
      WRITE(6,44) FIRST,BB
44    FORMAT(////,51H ***** THE FORWARD PROBLEM HAS NOT CONVERGE
1    ,10X,7H FIRST=,E12.3,10X,5H BIG=,E12.3)
43    CALL FFTTWO(SUM,NN)
      CALL REORDR(SUM,NN)
      DO 70 I=1,NN
70    DG(I)=REAL(SUM(I))
      RETURN
      END

```


B30185